Retinotectal projections influence optic tectum growth in zebrafish

Hannah Rouse

Department of Cell and Developmental Biology
University College London

A thesis submitted in partial fulfilment of the degree of
Doctor of Philosophy
University College London

April 2015

Declaration

I, Hannah Rouse confirm that the work presented in this thesis is my own. Where information has been derived from other sources, I confirm that this has been indicated in the thesis.

Abstract

In the zebrafish visual system, the retina and optic tectum grow in register throughout life. Both regions add new neurons from proliferation zones at their margins, with newly differentiated retinal ganglion cells projecting to, and making new synapses in the tectum. Retinal ganglion cell axon innervation appears to regulate size of the target tissue, because the contralateral tectum is reduced in size when an eye is removed. The mechanisms by which the retina affects cell proliferation and/or survival in the optic tectum remain to be elucidated.

In this thesis I use the *atoh7* mutant, *lakritz*, and unilateral eye enucleations to investigate the effect of lack of retinal input on growth of the optic tectum. Without retinal ganglion cell innervation, tectal cell proliferation and survival is reduced, yet proliferating cells in non-innervated tectal lobes still migrate away from the germinal margins and differentiate as occurs in innervated tecta. A candidate approach of innervated versus non-innervated brains suggests that retinal ganglion cell axons activate *axin2* expression in the tectum. In addition, a novel transgenic approach to silence retinal ganglion cell activity was designed to test the effect of neuronal activity from retinal ganglion cell axons but, as yet, has failed to provide conclusive results. Together, these results show that retinal afferents into the optic tectum regulate tectal cell proliferation and survival..

Acknowledgement

This thesis would not be possible without a number of people who have helped me (and put up with me) over the past five years. First and foremost, I wish to thank Steve Wilson, for letting me join his lab and giving me his time and support. I have really enjoyed being a part of the Wilson lab.

Thank you to Kara Cerveny, for suggesting this amazing project, teaching me the ropes and continuing to offer advice and support even after leaving the country and academia! Your enthusiasm for science is infectious and kept me going through the difficult times.

Thank you to Maté Varga, for your generosity and support. I would not have made it on time without you.

Thanks also to the Wilson lab members. Especially to Ana and Leo for stepping in last minute when I needed help, and to Diz for her continual support over the years.

Finally, thank you to my family, who will probably only read this page, but I love them anyway.

For my parents

Table of Contents

List of figures, tables and graphs

Chapter 1. Introduction

Chapter 3. Results I.

Chapter 4. Results II.

Chapter 5. Results III.

Appendix

Chapter 1. Introduction

1. The visual system

1.1 Design of the visual system

Conservation in the design of insect and vertebrate visual systems was first noted in the early 20th century by Ramon y Cajal and since this time, the visual system has regularly been used as a model with which to study neuronal circuitry and cellular behaviour. From insects to mammals, flow of information through the visual system is organised in the same way: photoreceptors in the retina convert photons into changes in membrane potential, with subsequent action potentials relayed through multiple cellular layers to the brain. Each cellular layer consists of a regular array of neurons, enabling the physical relationships between neurons to be preserved from layer to layer. This preservation maintains the visuotopic register such that a two-dimensional surface of the retina is constructed in most retino-recipient regions of the brain so that appropriate behavioural outputs can be generated. However, there are obvious differences in the composition of the visual system between species. Most notably, the insect retina is made up of about 800 ommatidia, each containing eight photoreceptors arranged in a trapezoid pattern and twelve accessory cells (Ready et al., 1976). In contrast, the vertebrate retina is structurally and functionally organised into laminae, with the cell bodies of six principal cell types arranged in three nuclear layers, separated by two plexiform layers containing their neuronal synapses (Sanes and Zipursky, 2010).

Amongst the six principal cell types of the vertebrate retina, a huge number of distinct subclasses add complexity and allow for the processing of distinct types of visual information from the photoreceptors in the outer layer to the ganglion cells (RGCs) in the inner layer. For example, direction-selectivity is encoded through most of the layers of the visual system. Microelectrode recordings in ganglion cells identified cells that respond to movements in a particular direction that do not fire when a stimulus is moved in the opposite direction (Barlow et al., 1964).

RGCs are the sole output neurons of the vertebrate retina. Recordings from optic-tract fibres led to the identification of two or three major types of RGC. In frogs, three classes where initially identified: cells that respond to either ON or OFF light and cells that respond to both ON and OFF light (Hartline, 1938). However, in cats only two classes were identified: ON-centred with an OFF surround and the converse (Kuffler, 1952; Enroth-Cugell and Robson, 1966). In mammals, there are now thought to be upwards of 20 different RGCs, with variations in morphology, physiology and connectivity distinguishing the subtypes. This diversity is thought to reflect distinct physiological functions (Masland, 2001; Rockhill et al., 2002; Völgyi et al., 2009).

Glutamate is the principle neurotransmitter in RGCs, with RGCs exhibiting glutamate immunoreactivity in humans (Crooks and Kolb, 1992), cats (Jojich and Pourcho, 1996) and chicks (Sun and Crossland, 2000). In zebrafish, RGC synaptic responses are completely blocked by addition of glutamate receptor antagonists, but not by addition of GABA receptor antagonists, which suggests that RGCs are exclusively glutamateric (Smear et al., 2007). This is despite evidence that RGCs are immunoreactive for GABA in *Bufo marinus* (Gabriel et al., 1992) and *Rana pipiens* (Li and Fite, 1998).

1.2 The mammalian visual system

Not only does the proportion of retinal subtypes vary among mammals, but cell topography also varies. For example, in nocturnal prey species, such as the rabbit, there is a horizontal band of high density ganglion cells termed the ‘visual streak’ (Hughes, 1971). In predators and primates there is a concentrated area of photoreceptors and RGCs termed the ‘area centralis’ and in more visually specialized primates, this area is further specialized and termed the ‘fovea centralis’ (reviewed by Provis et al., 2013). In many mammals, the primary RGC target is the superior colliculus in the dorsal midbrain, which controls saccadic eye movement and co-ordination of sensory information. RGC axons also project to the lateral geniculate nucleus (LGN), which relays signals to the primary visual cortex. A small number of RGC projections also innervate other retino-recipient regions of the brain (Hofbauer and Drager, 1985). However, in cats, 50% of RGCs project to the superior colliculus (Wassle and Illing, 1980) and in primates, no more than 10% project to the superior colliculus, with the majority of RGCs targeting the LGN (Perry and Cowey, 1984). Targeting the LGN over

the superior colliculus seems to have evolved in animals that rely heavily on cortical processing of visual information (Isbell, 2006).

The proportion of RGC axons that project to the ipsilateral or contralateral superior colliculus depends on the position of the eyes and therefore the amount of binocular overlap. In species such as rodents with side-positioned eyes, there are only a small number of ipsilateral projections, whereas in species with forward facing eyes, there are considerably more ipsilateral projections to the superior colliculus. Autoradiographic studies on the retinal projection to the superior colliculus were the first to show that contralateral and ipsilateral axon terminals segregate into patches and, to an extent, different laminae (Pollack and Hickey, 1979; Tigges and Tigges, 1981).

1.3 The visual system in anurans

Non-mammalian vertebrates do not have an exactly equivalent structure to the mammalian LGN. Instead, in fish and amphibians, the majority of RGC axons project to the optic tectum, the non-mammalian equivalent of the superior colliculus. The optic tectum is a multiprocessing centre, where visual and somatosensory inputs are organised into "maps" of the external world so that appropriate behavioural outputs can be generated. Investigations into visuomotor behaviour have often focussed on amphibians, because the optic tectum is easily accessible and because amphibians display a relatively simple, sequential response to prey: toads orient, approach, fixate and then snap towards prey (reviewed by Ewert, 1987; Ewert et al., 2001). Assays for visually guided behaviours in zebrafish have been developed more recently, with the larval zebrafish response to prey starting with eye convergence, followed by prey-tracking and capture swim phases (Bianco et al., 2011).

As with mammals, the extent of binocular overlap depends on lateral eye position. Prior to metamorphosis in *Xenopus laevis*, a larvae's eyes are laterally placed and all RGCs cross at the optic chiasm, projecting contralaterally. However, during metamorphosis, a larvae's eyes migrate frontally and dorsally to become forward-facing and generate overlapping visual fields. Not only do the eyes shift during metamorphosis, but also some RGC axons innervate the ipsilateral thalamus (Hoskins and Grobstein, 1985) In

addition, the isthmotectal map develops, whereby the nucleus isthmi relays information from the contralateral tectum to the ipsilateral tectum, to generate a representation of the binocular field in both tecta (Udin and Fisher, 1985).

1.4 The visual system in zebrafish

Unlike most vertebrates, the zebrafish visual system develops fairly rapidly, and larvae start to exhibit an optokinetic reflex to visual stimuli between 73 and 80 hpf (hours post fertilisation; Burrill and Easter, 1994). Rapid visual system development, along with larval transparency and external fertilization are just some of the reasons why zebrafish is used as a model for visual system studies. Although early histological studies focussed on the goldfish (*Carassius auratus*) visual system, the development of zebrafish as a genetic tool in the 1990's has allowed researchers to dissect how various components of the visual system develop. For example, mutant screens have identified zebrafish with genetic defects in retinotectal pathfinding (Karlstrom et al., 1996) and visual behaviours (Neuhauss et al., 1999). The recent development of tools to specifically manipulate the genome with TALENs (Transcription activator-like effector nucleases; Zu et al., 2013) and CRISPRs (Clustered regularly interspaced short palindromic repeats; Hwang et al., 2013) will undoubtedly advance the use of this species as a model with which to study processes *in vivo*.

In fish, RGC axons target ten locations along the optic tract, termed arborization fields (AFs; Stuermer, 1988; Burrill and Easter, 1994). The largest of these, and the target for the vast majority of RGC axons, is AF-10, the optic tectum in the dorsal midbrain. As fish have monocular vision, with laterally positioned eyes, each eye projects solely to the contralateral tectum. There are no ipsilateral connections and this is the same for each of the other arborization fields, except AF-1 (the suprachiasmatic nucleus in the hypothalamus), which has contralateral and ipsilateral retinal afferents (Burrill and Easter, 1994). Little is known about the functions of AF-1 through to AF-9, although brainstem lesions in lampreys suggest that different nuclei mediate different visual behaviours (Ullén et al., 1997).

1.5 The optic tectum

The optic tectum (or superior colliculus) is composed of a series of layers, with variations between species in their size and number. In chickens, there are 16 laminae, of which only three contain RGC arbors. In zebrafish, there are six tectal laminae (illustrated in *Figure 1*.): the stratum marginale is the most peripheral, followed by the stratum opticum (SO), stratum fibrosum et griseum superficiale (SFGS), stratum griseum centrale (SGC), stratum album centrale (SAC) and the deepest layer where most of the cell bodies reside, the stratum periventriculare (SPV). The main tectal afferents are RGC axons that project from the ganglion cell layer of the retina to the SFGS, SO, SGC and the boundary between the SAC and SPV (Meek, 1983). RGC axons enter the tectum superficially, segregate into specific layers and remain in those layers as they project to their target. Multi-day imagining has revealed that initial targeting of lamina by RGC axons is precise and does not go through a period of refinement (Robles et al., 2013). These same authors also show that different combinations of RGC axons innervate different sublamina, which results in superficial sublaminae that predominantly respond to ON inputs, and deep sublaminae that predominantly respond to OFF inputs. In addition, studies on RGC direction selectivity and orientation selectivity found that direction-selective RGCs target the superficial layer of the SFGS (Nikolaou et al., 2012), whilst orientation-selective RGCs exhibit a bilaminar distribution, with the majority of orientation-selective responses in the mid SFGS and the remainder in a deeper region of the SFGS (Lowe et al., 2013). Direction-selective and orientation-selective RGCs also map to distinct topographic regions of the tectum (Nikolaou et al., 2012). Tectal cells may also target their dendritic arbors to specific sublaminae. A study on direction selectivity in tectal cells, found that two types of tectal cell with different preferred directions arborize in distinct retinorecipient laminae (Gabriel et al., 2012). This segregation of subtypes of RGC afferents and tectal dendritic arbors could help in the connectivity between distinct RGCs and tectal neurons, thus aiding downstream processing of visual information, leading to different behaviours to visual stimuli.

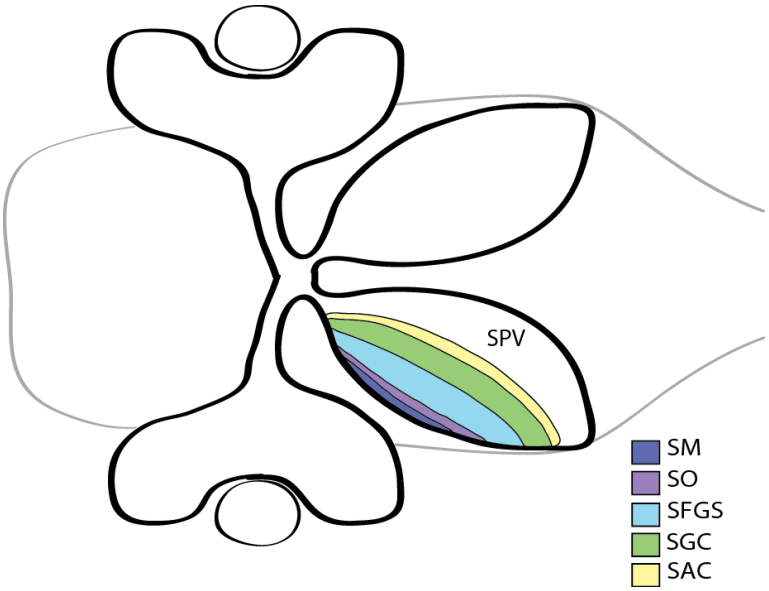

Figure 1. Lamination in the optic tectum A cartoon dorsal view of the zebrafish optic tectum, depicting the six tectal laminae: the stratum marginale (SM), stratum opticum (SO), stratum fibrosum et griseum superficiale (SFGS), stratum griseum centrale (SGC) and stratum album centrale (SAC) of the neuropil region and the deepest layer, the stratum periventriculare (SPV).

Lamination is not restricted to the optic tectum, but is also evident in other CNS regions such as the hippocampus, and it is possible that similar molecules are employed to control targeting of axons to specific laminae (reviewed by Sanes and Yamagata, 1999). In the optic tectum, several guidance molecules, such as N-cadherin and Ephrin B (Inoue and Sanes, 1997; Braisted et al., 1997) appear to be involved in controlling lamina specificity. A genetic screen by Xiao et al. (2005) also identified a zebrafish mutant with RGC axons that travel between the SFGS and SO. Subsequent work identified a mutation in the *collagen type* $IV_{\alpha 5}$ gene, and found that removing collagen or heparan sulfate proteoglycans (HSPGs) by intra-tectal injections of collagenase or heparitinase disrupted RGC axon targeting (Xiao and Baier, 2007). Guidance cues in the tectum also direct RGC axons to the appropriate terminal position, to generate retinotopic organisation. The dominant model for the development of the visual map is the chemoaffinity hypothesis proposed by Sperry (1963) and matched gradients of ephrinA/ephA and ephrinB/ephB molecules were found in the retina and tectum in support of this (Drescher et al., 1997; Mann et al., 2002). However, retinotectal mapping may also be influenced by competition for target space in the tectum (Prestige and Wilshaw, 1975) and by neuronal activity (Hua et al., 2005). Although injections of tetrodotoxin (TTX) into zebrafish retinae silence RGC action potentials, retinotopic maps still form in the tectum (Meyer, 1983), albeit with enlarged RGC axonal arbors. Axonal arbors are also enlarged in situations where zebrafish larvae have only a single RGC projection to the contralateral tectum (Gosse et al., 2008). These studies suggest that neuronal activity and axon-axon interactions are involved in the refinement of the visual map rather than initial retinotectal map formation.

The development of RGC axonal arbors in the optic tectum and superior colliculus differs among species. Anterograde DiI labeling in chicks and rats showed that RGC axons initially project diffusely to the optic tectum or superior colliculus. Axonal arbors branch in aberrant locations and are subsequently ‘pruned’ to the correct termination zone in a process that requires spontaneous neural activity in RGCs (Nakamura and O’Leary, 1989; Simon and O’Leary, 1992; Nicol et al., 2007). In frogs and fish, there are no initial diffuse projections; instead RGC axons directly target the correct termination zone (Holt and Harris, 1983; Stuermer, 1988). Then nascent branches and

synapses locally form and retract in both RGC axonal arbors and tectal cell dendritic arbors. Finally, synapses are selectively stabilized when appropriate contacts are made (O'Rourke et al., 1994; Niell et al., 2004; Meyer and Smith, 2006). Expression of tetanus neurotoxin in zebrafish RGCs indicates that RGC neural activity is not required for stable branch formation, but is required for arbor maturation and refinement, because silenced RGCs tend to have many transient filopodia and enlarged axonal arbors (Ben Fredj et al., 2010)

1.6 Cell types present in the optic tectum

Although a number of studies have focussed on axon pathfinding and map formation in the zebrafish visual system, relatively little is known about the cell types and circuitry involved in processing visual information in the optic tectum. Golgi studies and a UAS/Gal4 transgenic approach have identified about 15 morphologically distinct types of tectal cell (Meek and Schellart, 1978; Scott and Baier, 2009), with variations in soma location and dendritic and axonal arbors. An investigation into the propagation of postsynaptic depolarization in the optic tectum of rainbow trout also found that the postsynaptic response is first rapidly propagated within the SFGS and SO and then more slowly extended vertically, into the deep layers (Kinoshita et al., 2002). It is probable that processing steps upstream of the tectum segregate information into various RGC subtypes and laminae that are then fed into distinct tectal microcircuits. For example, one study found that a population of superficial GABAergic interneuron is important for the detection of large stimuli and does not respond to small moving bars (Del Bene et al., 2010).

SPV, the deepest layer, contains the largest density of cell bodies in the tectum and the two main classes of resident neurons are periventricular interneurons and periventricular projection neurons (reviewed by Nevin et al., 2010). Periventricular projection neurons receive inputs from tectal interneurons and possibly RGCs, and they contain efferent axons that project to a number of different structures. Efferent axons that project to the hindbrain revealed that each small region along the anterior-posterior and medial-lateral axes contains a different combination of projections to different hindbrain segments (Sato et al., 2007), which suggests that motor output across the tectum is not uniform.

2. Growth of the visual system

2.1 Stem cells in the visual system

After the initial development of the visual system in fish and amphibians, the retina and optic tectum continue to grow by incorporating new cells, cellular hypertrophy, and by spreading cells over a larger area (Johns and Easter, 1977; Raymond and Easter, 1983). As the eye grows, the visual world is projected onto a larger retina and thus visual acuity improves over the lifetime of the organism such that older, bigger fish exhibit improved predation over their younger, smaller rivals (Hairston et al., 1982). Not only does spatial resolution improve over time, but also the accuracy of the light intensity information relayed to the brain increases, as RGCs increase the size of their dendritic arbors over time (Hitchcock and Easter, 1986; Lee and Stevens, 2007).

As is common with post-developmental growth, in anamniotes, cell proliferation becomes restricted to two areas at the peripheries of the retina and optic tectum. In the retina, putative stem cells are located in the ciliary marginal zone (CMZ, also termed the circumferential germinal zone) and this region adds new cells in concentric rings throughout the animal's lifetime (Straznicky and Gaze, 1971; Johns, 1977). The CMZ is thought to add the majority of new retinal cells except for rod photoreceptors, which are generated by a source of lineage-restricted slowly dividing progenitors in the inner nuclear layer (Raymond and Rivlin, 1987). In the tectum, proliferating cells are situated at the caudo-medial edge and new cells are added in 'wedges' (Meyer, 1978; Raymond et al., 1983). The retinal CMZ and caudo-medial edge of the optic tectum are depicted in *Figure 2*.

In non-anamniote vertebrates, additional cells are not added to the retina after development, and consequently it was thought these vertebrate species were devoid of retinal stem cells. However, some recent data suggest that the ciliary margin in avian and mammalian retinae is homologous to the anamniote CMZ, but over the course of evolution the ciliary margin has diminished and constituent cells have gradually lost the ability to proliferate and self-renew *in vivo* (Kubota et al., 2002). In chickens, initial studies identified [^{3}H] accumulation at the periphery of the retina (Morris et al., 1976),

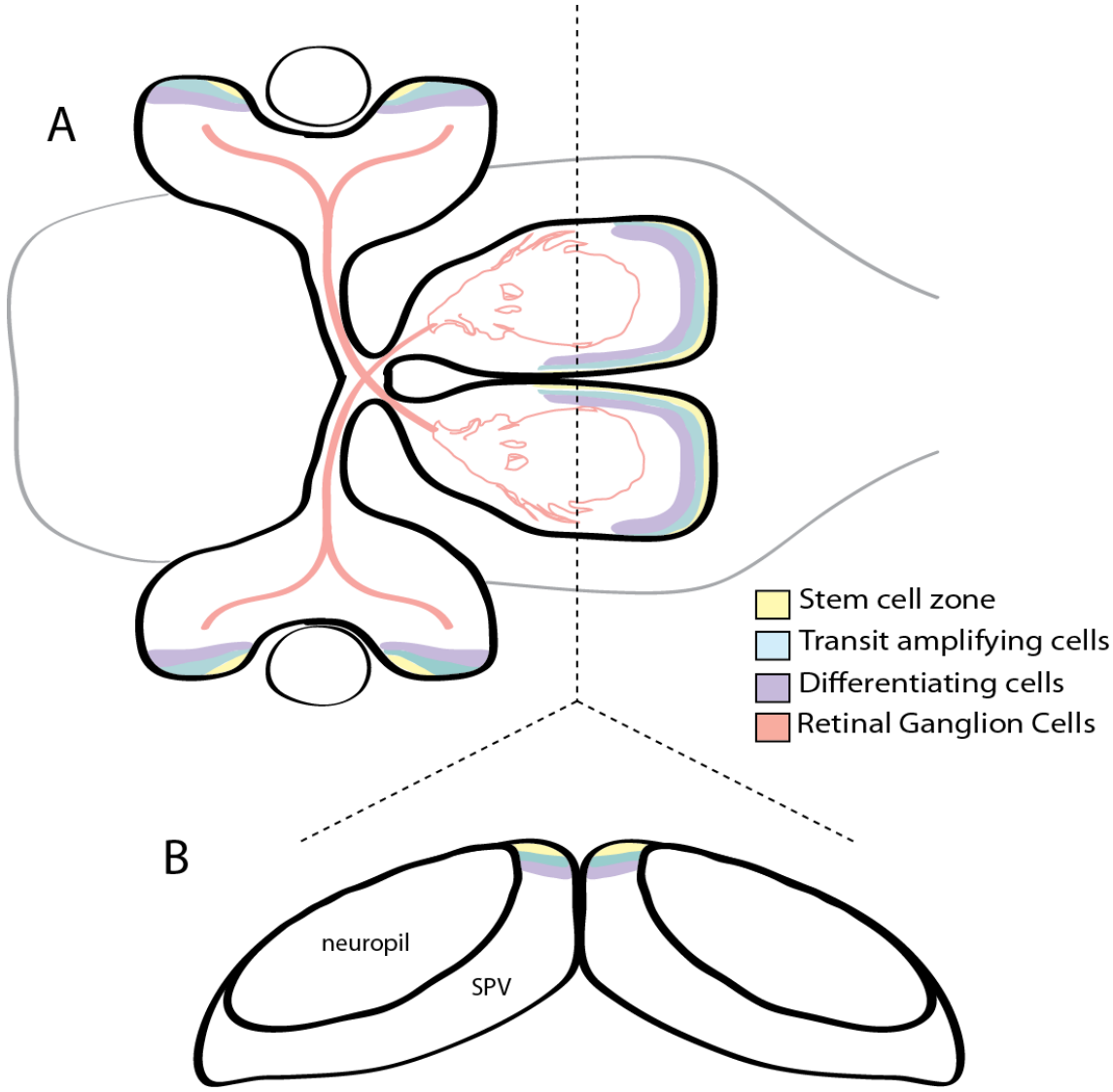

Figure 2. Zones of cell proliferation and differentiation in the CMZ and caudo-medial edge of the tectum

A cartoon dorsal view (A) and transverse view (B) of the zebrafish visual system, depicting areas of proliferation in the retina and optic tectum. Stem cells (yellow) give rise to more committed progenitors (blue), which in turn give rise to differentiating neurons (purple). New neurons integrate into the existing functional circuitry, including into the retinal ganglion cell layer, where RGCs (pink), the sole output of the retina, grow axons along the optic nerve and terminate in the optic tectum. (Image made with Leo Valdivia).

but this was not re-investigated until 2000, when BrdU incorporation was used to identify proliferating cells in the chick retinal margin up to two months after hatching (Fischer and Reh, 2000). It should be noted that although these cells express genes also found in embryonic retinal progenitors and the CMZ, their neurogenic ability is greatly reduced when compared to the retinal stem cells of anamniotes, because they do not generate ganglion cells or photoreceptors and they do not participate in regeneration post-injury.

In mammals, two papers in 2000 independently found that cells isolated from the pigmented ciliary margin have the ability to proliferate and form multipotential neural spheres *in vitro* and also have the capacity to self-renew (Ahmad et al., 2000; Tropepe et al., 2000). This suggests the presence of a quiescent population of retinal stem cells in the mammalian ciliary margin and it is thought these stem cells are evolutionary homologous to those found in the retinal margin of chicks. However, more recent studies have demonstrated that all the cells in neural spheres derived from the ciliary margin are pigmented and retain epithelial characteristics (Moe et al., 2009; Cicero et al., 2009). These results suggest that 'stem cells' in the mammalian ciliary margin may not be stem cells nor be able to produce retinal stem cells. It remains to be seen whether this population of retinal cells that are able to proliferate *in vitro* will be useful for future therapeutic strategies. Certainly a greater understanding of the CMZ in frogs and fish and the ciliary margin in chicks will help to direct future research and strategies into using and harnessing the neurogenic potential of cells in the mammalian ciliary margin.

2.2 The CMZ and tectal marginal zone

Expression patterns of transcriptional regulators and BrdU/PCNA labeling have shown that the CMZ can be subdivided into four regions. From the periphery to the more central region, distinct combinations of proneural and neurogenic genes are expressed in overlapping patterns and there is spatial separation of the progression from stem cell to differentiated neuron (Perron et al., 1998; Raymond et al., 2006). This organisation was thought to recapitulate the sequence of events that occurs during embryonic development (Perron et al., 1998), however, more recent studies suggest that similar but

not identical genetic programmes are employed in embryonic development versus the adult CMZ (Wehman et al., 2005; Cerveny et al., 2010). At the most peripheral edge of the CMZ, in contact with both the apical surface and basal lamina, lie the retinal stem cells. A transgenic approach that permanently labelled cells at the periphery and followed them for up to 1 year showed that retinal stem cells continuously supply new neurons over the course of a year and are multipotent, giving rise to different types of retinal cell across all the retinal laminae (Centanin et al., 2011). This study was extended to show that retinal stem cells mostly divide in an asymmetric way, thus maintaining the stem cell population throughout the life of the fish (Centanin et al., 2014). However, it is not clear whether rod photoreceptors are among the progeny of the labelled retinal stem cells.

Less is known about the tectal stem cell niche and unlike the retina, the tectal stem cell niche has not been fully characterized; there is not sufficient evidence to support the existence of multipotent 'tectal stem cells' that have the ability to self renew and contribute cells to all layers of the tectum throughout the lifetime of the organism. Long incubations of IdU and CldU in medaka identified a small population of slow-cycling cells at the margin of the optic tectum in adults, that rarely enter S-phase, and are adjacent to a population of more actively-dividing cells (Alunni et al., 2010). In addition, proliferating cells at the caudo-medial edge express neural stem/progenitor markers *sox2, musashi1* and *bmi1* and go on to generate neurons, radial glia and oligodendrocytes (Alunni et al., 2010; Ito et al., 2010). Interestingly, although adult neural stem cells in mammals express glial markers GFAP and S100β, $BrdU^+$ cells at the tectal cell margin in zebrafish larvae do not express either GFAP or S100β. Instead, tectal stem cells have neuroepithelial characteristics, exhibiting planar cell divisions and expressing apical polarity markers ZO1, aPKC and ϒ-tubulin (Ito et al., 2010; Recher et al., 2013).

2.3 Shift of RGC axons during growth

If the retina grows by the addition of concentric rings from the CMZ (Straznicky and Gaze, 1971), and the optic tectum grows by the addition of 'wedges' of cells from the tectal stem cell niche (Straznicky and Gaze, 1972; Raymond and Easter 1983), how is

the register of the retinotectal map maintained? Straznicky and Gaze (1972) proposed that retinotectal connections are not maintained throughout life but continuously 'shift' in order to maintain the visuotopic register. To shift, RGCs must break and reform connections as they migrate away from their initial synaptic partner. Evidence was found for and against this proposed hypothesis. In 1976 and 1977 Jacobson presented two studies, the first of which claimed that the retina grows asymmetrically in a crescent pattern, akin to the growth of the optic tectum. The second paper used [^{3}H]proline intraocular injections and [^{3}H]thymidine intraperitoneal injections to label RGCs and tectal cells. Jacobson showed that the labelled retinal and tectal cells stay in the same area following a period of growth and implied this disproved Gaze's hypothesis of shifting terminals. However, it has been argued that the results of this second paper are ambiguous and studies by other researchers, using a similar methodology, were presented in support of the hypothesis of 'shifiting terminals' (Scott and Lázár, 1976; Gaze et al., 1979; Reh and Constantine-Paton, 1984). In addition, a model for the shift of retinal axonal terminals and tectal dendritic arbors was presented by Easter and Stuermer in 1984, and provided further evidence in support of the idea of shifting terminals. From the analysis of [^{3}H]thymidine labelled retina and tecta it was suggested that RGC retinal fibres shift caudally and slightly medially over time, with the amount of displacement depending on their topographical position in the retina (Raymond, 1986).

2.4 How is growth regulated?

Continuous neurogenesis in the visual system does not proceed at a uniform rate, but is instead regulated by a number of local and systemic signals that feed into the cellular signalling network to fine-tune growth. The spatial organisation of the CMZ and optic tectum has allowed researchers to separate out the effect of extrinsic signals on the different stages of neurogenesis, taking account of proliferation, cell cycle kinetics and differentiation. Based on the similarities in cell behaviour and organisation, it is probable that similar mechanisms are involved in lifelong regulation of neurogenesis in the retina and tectum (Cerveny et al., 2012).

Retinal growth is related to the overall growth of the organism; larger fish have bigger eyes and smaller fish have smaller eyes. Systemic signals, such as growth hormone (GH), link neurogenesis to body-growth both directly and indirectly via insulin-like growth factor-I (IGF-I) (Otteson et al., 2002). Both GH and IGF-1 receptors were found in the CMZ and increasing the concentration of IGF-I increases the rate of proliferation of retinal progenitors (Boucher and Hitchcock, 1998; Otteson et al., 2002).

Multiple extracellular signals affect proliferation and differentiation in the CMZ, driving and inhibiting growth of the tissue as and when required. Pathways that have been linked to the control of proliferation in the CMZ include the Wnt-β-catenin pathway and Hedgehog (Hh) pathway. For instance, ectopic activation of the canonical Wnt pathway in *Xenopus laevis* caused increased proliferation in the CMZ and conversely, inhibition of the pathway blocked cell proliferation (Masai et al., 2005; Denayer et al., 2008). In addition, it was found that constitutive activation of the Wnt pathway in *adenomatous polyposis coli* mutant zebrafish caused expansion of the CMZ (Stephens et al., 2010). Although Hh pathway activation increased proliferation in the CMZ, it also accelerated cell cycle kinetics such that, over time, cycling cells in the retinal periphery were depleted. Inhibition of the Hh pathway decreased the rate of progression through the cell cycle, and caused slower cell cycle progression at the retinal periphery (Locker et al., 2006). In 2012, Borday et al. linked the antagonistic effects of the Wnt and Hh pathways in retinal stem cells. The authors demonstrated that the two pathways restrain each other's activity in the *Xenopus* CMZ, suggesting this interplay regulates stem/progenitor cell proliferation.

In addition to its role in proliferation, the Hh pathway has also been linked to differentiation. A wave of *shh* expression during zebrafish retinal development induces RGC differentiation (Neumann and Nuesslein-Volhard, 2000) and morpholinos against *shh* inhibit the wave of neuronal production (Masai et al., 2005).

Notch-Delta signalling is also important in both developing tissues and in the adult stem cell niche for influencing proliferation, differentiation and apoptosis (Artavanis-Tsakonas et al., 1999). In the mammalian CNS, Notch signalling has been implicated in

stem/progenitor cell maintenance (Ohtsuka et al., 2001; Hitoshi et al., 2002), and this role is conserved in the developing zebrafish spinal cord, where inhibition of Notch signalling reduces the population of neural progenitors and led to aberrant progenitor differentation (Yeo and Chitnis, 2007). Furthermore, the zebrafish telencephalic stem cell niche was used to show that different levels of Notch pathway activity controls the switch between quiescence and neurogenesis (Chapouton et al., 2010). In the retina, modifying Notch-Delta activity during different stages of development alters fate determination of the various retinal cell types in chicks (Austin et al., 1995) and frogs (Coffman et al., 1993; Dorsky et al., 1997). Several constituents of the Notch-Delta signalling pathway are expressed in the CMZ and optic tectum (Raymond et al., 2006). For example, expression of the notch ligand *jagged1a* and notch receptors *notch1a*, *notch1b* and *notch3* has been observed in the tectal proliferative zone (Jung et al., 2012; de Oliveira-Carlos et al., 2013). This indicates that the pathway is active in neurogenesis within the visual system, but further studies are required to elucidate a role for Notch-Delta signalling in the retinal and tectal stem cell niches.

The counterpart to cell proliferation, programmed cell death, is also tightly regulated to eliminate unwanted cells and protect against hyperproliferation. In the developing *Drosophila* eye, waves of mitosis are followed by programmed cell death to precisely control the number of retinal cells (reviewed by Baker, 2001). Although vertebrate eye development does not have such a precise cellular architecture, a number of signalling pathways control apoptosis. For example, increased apoptosis is detected in retinae in which cadherins (Babb et al., 2005) and Wnt/Frizzled signalling (Liu and Nathans, 2008) are abrogated. Both conditions generate a small eye phenotype, known as microphthalmia. Retinoic acid deficiency (Le et al., 2012) and mutations in a number of transcription facts are also linked to micropthalmia.

There is accumulating evidence that a wide range of neuromodulators can also influence proliferation and differentiation in adult stem cell niches in the retina (reviewed by Young et al., 2011). In the avian CMZ, glucagon immunoreactive cells have been identified at the retinal margin, and have been proposed to be part of a relay between incoming visual information and proliferation within the CMZ (Fischer et al., 2005).

Also, GABA has been implicated in control of proliferation (Ring et al., 2012) and injections of glutamate have induced Müller glia to dedifferentiate, migrate and differentiate into photoreceptors in adult mice (Takeda et al., 2008).

3. Co-ordinated growth of the retina and optic tectum

3.1 The role of innervation in growth and development

The results from surgical manipulation of sensory inputs led to the view that innervation is important for normal growth and/or development of axonal targets. For example in *Xenopus laevis*, removal of the olfactory placode during development causes hypoplasia in the olfactory bulb (Stout and Graziadei, 1980). Likewise, cochlea removal in chicks causes a rapid cessation of action potentials in the nucleus magnocellularis, followed by cell death (reviewed by Rubel et al., 1990). These types of experiments lead to the question: How does innervation influence growth and development? There is no simple answer to this question, and research suggests that neural activity and the anterograde transport of signalling molecules are both important factors.

3.2 Neural Activity

That neural activity can affect growth and development has been known for some time. Back-to-back papers in 1963 showed that monocular deprivation during the first postnatal months in cats led to deficient vision in the deprived eye and atrophy in the LGN (Wiesel and Hubel, 1963a; Wiesel and Hubel, 1963b). In these studies, the researchers sewed shut the kittens' eyelids, an experimental method that does not completely block light penetrating the eye and does not inhibit spontaneous electrical activity. This is important, as spontaneous activity and sensory-derived activity occur independently and both can influence the development of neuronal circuits (Spitzer, 2006). For example, waves of action potentials occur in mouse retinal ganglion cells before functional vision, and this spontaneous activity drives LGN neurons to fire action potentials (Mooney et al., 1996).

How does neural activity of innervating axons influence the target tissue? Neuronal activity involves the release of neurotransmitters across the synaptic cleft in response to membrane depolarization and Ca^{2+} influx. This process not only generates an action potential in the post-synaptic neuron, but can also induce secretion of signalling molecules and changes in gene expression and protein synthesis. The first gene identified as differentially expressed in response to neural activity was *c-Fos*

(Greenberg et al., 1986) and subsequent studies showed that *c-Fos* expression is upregulated across the cortex, hippocampus and limbic system after induced seizures (Morgan et al., 1986). Many more activity-regulated genes have since been identified, both through single-gene analysis (Abraham and Williams, 2003) and microarray studies (Altar et al., 2004). Amongst them are genes encoding the neurotrophins *nerve growth factor* (NGF) and *brain-dependent neurotrophic factor* (BDNF), both of which are involved in neuronal survival, neurogenesis and circuit formation (Thoenen, 1995).

3.3 Anterograde transport of signalling molecules

The development of the lamina in the insect visual system is an important example of how ingrowing axons can influence development of a target tissue through the release of signalling molecules. In *Drosophila*, retinal axons induce the final division of lamina precursor cells (Selleck and Steller, 1991). Further studies found that retinal axons transport the Hedgehog protein from the retina and that this source of Hedgehog induces terminal division and neuronal differentiation of target cells in the visual ganglia (Huang and Kunes, 1996). However, Hedgehog is not sufficient for lamina differentiation, and a second signalling molecule, the EGF ligand Spitz, is also transported along retinal axons to the lamina, where it acts downstream of Hedgehog to activate EGF signalling and induce differentiation (Huang et al., 1998).

Experiments in the rat and chick visual system have shown that anterograde transport is not restricted to the insect visual system. In the chick visual system, NT-3 and BDNF were shown to be anterogradely transported to the optic tectum, and injection of tetrodotoxin had no significant effect on their release, suggesting that this is an activity independent signalling process (von Bartheld et al., 1996). In rats, retinal-derived BDNF was also shown to be anterogradely transported from the retina to the LGN and secreted in an activity-independent manner to regulate connectivity within the LGN (Menna et al., 2003). In addition to the visual system, a recent study found that olfactory sensory neurons also anterogradely transport a neurotrophin, Neurotrophin-3, along their axons to the olfactory bulb (Liu et al., 2013). The anterograde transport of neurotrophins is significant because it suggests an activity independent mode of regulating neural circuitry and sending cell survival signals to a target tissue.

3.4 Retinal influence on the growth of the optic tectum

To study how innervation influences growth and development, researchers have often turned to the visual system of anamniotes because the optic lobes are relatively large and the eyes can easily be removed. Furthermore, in fish and most larval frogs, RGCs completely cross at the midline, which gives a clean-cut experiment: unilateral eye enucleation generates an experimental side and a control side in the same animal. Early work in the tree-frog *Hyla Regilla* demonstrated that removal of one eye led to larvae with one optic lobe significantly smaller than the other (Larsell, 1931, *Figure 3.*). In the teleost fish *Fundulus heteroclitus*, and in the salamanders *Amblystoma punctatum* and *Amblystoma tigrinum*, lack of retinal efferents to the brain also generated atrophy in the affected optic lobe (Harrison, 1929; White, 1948). These experiments along with many others led to the view that the retina positively influences growth of the optic tectum.

However, there are contrasting reports as to whether the observed atrophy is due to a reduction in the proliferative activity of the tectum stem cell zone or to other factors such as reduced cell survival. In zebrafish, it was reported that retinal innervation does not affect mitosis in the teleost tectum, but instead impaired growth of the non-innervated tecta is due to a deficiency in neuronal differentiation (Schmatolla, 1972; Schmatolla and Erdmann, 1973). These results are in contrast to experiments in goldfish *Carassius auratus auratus* and the larval frog *Rana pipiens* that detected a reduced rate of ^{3}H-thymidine incorporation in the non-innervated tectum compared to the control tectum, showing that mitosis is reduced in the absence of retinal input (Eichler, 1971; Raymond et al., 1983). At the time, it was suggested that these results conflicted because of the different species used. This suggestion was supported by a report that did not find proliferation in the optic tectum of juvenile and adult zebrafish (Rahmann, 1968), despite evidence of continuous growth in the amphibian optic tectum (Raymond and Easter, 1983).

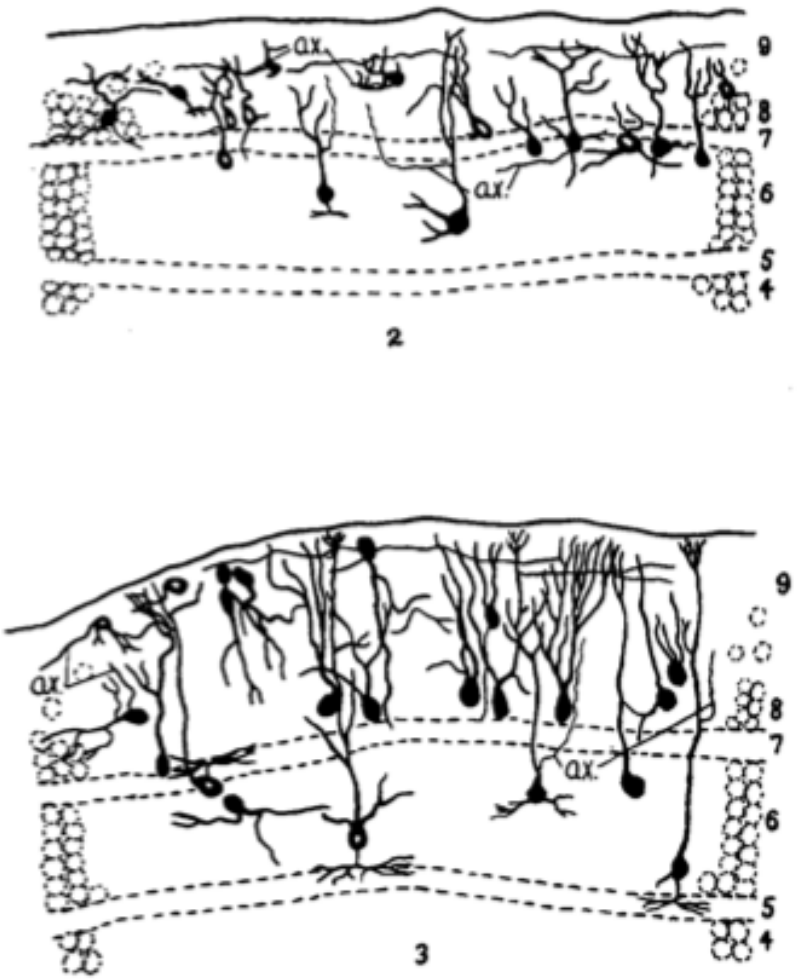

Figure 3. Composite drawing of cells and fibres in the post-metamorphic optic lobes of the tree-frog, *Hyla regilla*. The left eye was excised at the larval stage of 18mm. Cells in the outer layers of the right (affected) optic lobe are represented in **2** and cell in the outer layers of the left (normal) optic lobe are represented in **3**. Cells in the affected side have shorter dendritic processes and fewer dendritic branches than cells in the normal side of the same specimen. Source: Larsell, 1931

3.5 Methods of altering input into the visual system

Surgical enucleation is not the only method of abrogating retinal input into the optic tectum. Crushing the optic nerve temporarily deprives the contralateral tectum of retinal input. Studies in *Xenopus laevis*, showed that this method causes hypoplasia in the optic tectum that decreases over time as the visual system regenerates (McMurray, 1954). Larvae can also be grown in constant darkness, a method that removes sensory input but not spontaneous activity or activity independent signalling. Dark-rearing in the cichlid teleost *Sarotherodon mossambicus* was reported to affect lamination in the optic tectum through a reduction in ganglion cell volume (Zeutzius et al., 1984). However, no change was detected to the contralateral projection or histological appearance of the optic tecum in *Xenopus laevis* larvae reared in the dark from early life to post-metamorphosis (Grant and Keating, 1989). Instead, dark-rearing appears to affect the precision of the intertectal projection and also disrupts the topographic order of the ispilateral projection. However, it should be noted that growth of zebrafish larvae in constant light or constant dark conditions diminishes visual acuity (Bilotta, 2000).

Disrupting neuronal activity with either tetrodotoxin (TTX) injections in the retina or with a mutation in the *macho* gene lead to a dispersed retinotectal projection pattern (Gnuegge et al., 2001). Furthermore, the effect of activity blockade on development of the retinotectal projection has been studied genetically, through expression of the light chain of tetanus neurotoxin in zebrafish RGCs (Ben Fredj et al., 2010). However to date, none of these methods have been used to investigate the affect of inhibition of RGC neuronal activity on the growth of the optic tectum.

3.6 How do retinotectal projections influence optic tectum growth in zebrafish?

In this thesis, I decided to re-investigate how RGC innervation impacts growth of the optic tectum in zebrafish following the development of new tools with which to investigate tissue growth and neural circuitry. Firstly, we asked whether cell proliferation, differentiation and survival are affected by the abrogation of retinal input into the larval tectum. Our data shows that cells in the optic tectum proliferate and differentiate in response to retinal input. Specifically, we show that cell proliferation is reduced in optic tecta of *lakritz* mutants and in wild-type tecta of unilateral eye

enucleated larvae. In addition, cell differentiation, as assessed by expression of the glutamatergic marker, *slc17a6b*, appears to be decreased in the non-innervated tectum. Cell survival does not appear to be affected. Secondly, to determine which genes and pathways regulate input-dependent growth of the tectum, we assessed gene expression levels in innervated and non-innervated tecta. We provide evidence that both the Wnt/β-catenin pathway and calcium signalling promote cell proliferation and/or differentiation in an input-dependent manner. Through a candidate-gene approach, we show that the Wnt pathway components, *axin2* and *lef1,* are downregulated in non-innervated tecta. Through an RNAseq approach, we also identified two calcium signalling genes, *calb2b* and *pcp4a,* as downregulated in the non-innervated tectum. Finally, we wanted to assess whether retinal innervation influences the optic tectum by means of bursts of neural activity. We created two transgenic lines that could be used to silence neural activity specifically in retinal ganglion cells. Taken together, our data suggest that retinal input influences Wnt signalling and calcium signalling in the optic tectum, promoting tectal cell proliferation and differentiation.

Chapter 2. Materials & Methods

1.1 Zebrafish husbandry

Adult zebrafish were maintained on a 14-hour light/10-hour dark cycle at 28°C, with embryos obtained by natural spawning and reared under standard conditions (Westerfield, 1993). For larvae used at 6 dpf (days post fertilisation) onwards, embryos were transferred to a nursery at 5dpf and later culled with a lethal dose of buffered MS-222 (Sigma) anaesthetic, prior to fixation with 4% Paraformaldehyde (PFA), 4% sucrose in Phosphate Buffered Saline (PBS).

Wild-type (WT) embryos were obtained from the wild-type lines AB, Tübingen and Tup Longfin. Mutant embryos were obtained from crosses of heterozygous carriers of the *lakritz*^{th241} mutation (Kay et al., 2001). Transgenic embryos were obtained from heterozygous crosses of the transgenic lines Tg(*fli1a:EGFP*)^{y5} (Lawson and Weinstein, 2002), Tg(*elavl3:eGFP*)^{zf8} (Park et al., 2000), Tg(*hsp70l:Cre*)^{zdf13} (Feng et al., 2007; Le et al., 2007), Tg(*TOP:dGFP*)^{w25} (Dorsky et al., 2002), Tg(*-3.5ubb:loxP-EGFP-loxP-mCherry*)^{cz1701} (Mosimann et al., 2011) and those generated in this thesis.

1.2 Brain dissection

Prior to brain dissection, larvae were fixed with 4% PFA, 4% sucrose for 5 hours at room temperature, transferred to PBS and stored overnight at 4°C. Larvae were positioned laterally, in PBS, on a sylgard dish, with two dissection pins placed through the body – one through the abdomen and one through the tail. Using sharp forceps, the jaw and eye were removed, followed by the skin surrounding the brain. Dissected brains were dehydrated through 50% MeOH/PBST (0.5% Triton in PBS) to 100% MeOH, and stored at -20°C at least overnight until use.

1.3 Whole-mount *in situ* hybridization

Dissected brains stored at -20°C were rehydrated by washing with 50% MeOH/PBST, followed by 4 x 5min in PBST. They were then digested with 40µg/ml Proteinase K in PBST for 20min, and re-fixed with 4% PFA for 20min. The PFA was washed out by 4 x 5min washes in PBST, then PBST was replaced with 300µl Hyb+ and brains were

incubated at 68°C for at least 2 hours. The antisense RNA *in situ* probes were added at a 1:250 dilution in Hyb+ and incubated overnight at 68°C.

Probes were recovered the next morning and brains were washed 4 x 30min in Hyb+ at 68°C, then transferred into 2x SSC for 15min at 68°C and 0.2x SSC for 2 x 15min at 68°C. This was followed by 4 x 15min washes in PBST, then at least 1 hour at room temperature in MABlock. The brains were incubated overnight at 4°C in anti-DIG AP FAB fragments diluted 1:6000 in MABlock.

Dissected brains were washed 4 x 15min in PBST the next morning, then in freshly prepared AP buffer for 3 x 5min. The colour was developed by incubation in the dark in AP buffer with NBT (1µl per ml of AP buffer) and BCIP (3.5µl per ml of AP buffer). Once the colour was fully developed, brains were washed 2 x 10min with PBST and fixed overnight with 4% PFA at 4°C. PFA was removed and replaced by 75% glycerol for mounting and imaging.

Probes used for *in situ* hybridization

axin2	G Weidinger and R. T. Moon, 2005
cabp5b	probe amplified by qRT-PCR, primers in table below
calb2b	probe amplified by qRT-PCR, primers in table below
ccnd1	Pujic et al., 2006
cmyc	Yamaguchi et al., 2005
gad1b	Higashijima et al., 2004
gad2	Higashijima et al., 2004
gli1	Karlstrom et al., 2003
gli2	Karlstrom et al., 1999
lef1	Lee et al., 2006
npvf	probe amplified by RT-PCR, primers in table below
oxt	probe amplified by RT-PCR, primers in table below
p57	made by Kara Cerveny, Reed College, Portland, OR, USA
pcp4a	probe amplified by RT-PCR, primers in table below
ptc1	Concordet et al., 1996
ptc2	Lewis et al., 1999
si:dkey-14d8.6	probe amplified by RT-PCR, primers in table below

slc6a5 Higashijima et al., 2004

slc17a6b Higashijima et al., 2004

Gene	Forward Primer (3'-5')	Reverse Primer (5'-3')
cabp5b	GATGAGGACGATGGGCTACA	AATTAACCCTCACTAAAGGGAAGTTCAAGAATGCGTGCCC
calb2b	ACTGCGGATCCTTCAAATGC	AATTAACCCTCACTAAAGGGATCTCCAGTTCTGTGCGGAA
npvf	GCATCCTGAGCAGCTTCATG	AATTAACCCTCACTAAAGGGAGCAGGCAAGAACAGATGGA
oxt	CATCGGAGGAAAACGCTCTG	AATTAACCCTCACTAAAGGGTACAAAAGTGGGTGGCGAGT
pcp4a	TGGACAAGACCCATCCAAGA	AATTAACCCTCACTAAAGGGGCCACGCTGCCAATTAATAC
si:dkey-14d8.6	ACTCCTATGATCAGCCCCTG	AATTAACCCTCACTAAAGGGCTGATACTTCCAGCGACGGT

1.4 TUNEL assay

Dissected brains were treated as per the Whole-mount *in situ* hybridization protocol up to the post-fixation step. After this point, PFA was washed out by 4 x 5 min washes in PBST and the brains were transferred to prechilled EtOH:Acetone at a 2:1 ratio, for 10 minutes at -20°C. Samples were then washed 3 x 5min in PBST at room temperature and blocked for 1 hour in equilibration buffer prior to addition of the ApoTag® Enzyme (Chemicon) in reaction buffer (2:1 of enzyme:buffer), kept overnight at 37°C. Brains were then washed in PBST, blocked in MABlock and stained as per the Whole-mount *in situ* hybridization protocol.

1.5 Neutral red staining

Larvae were incubated in fish water containing 2.5µg/ml neutral red (Sigma Aldrich), at 28°C for 3 hours. After this, the embryos were returned to fish water at 28°C for 3 hours then anaesthetized in 0.003% tricane, mounted in 1% low-melting point agarose on a glass slide and imaged on a Nikon Eclipse E1000 microscope.

1.6 Immunohistochemistry

Samples were treated as per the Whole-mount *in situ* hybridization protocol up to the post-fixation step. After this point, PFA was washed out by 4 x 5min in PBST and the

samples were transferred to a blocking solution (10% NGS, 1% DMSO in PBST) for 1 hour at room temperature. Samples were incubated with primary antibodies diluted in blocking solution overnight at 4°C.

The next day, samples were rinsed a few times with PBST, before 4 x 30min washes with PBST. Samples were then incubated with secondary antibodies diluted in blocking solution overnight at 4°C.

Again, samples were rinsed a few times with PBST, washed 4 x 30min with PBST and then mounted and imaged on a Leica SP8 confocal microscope.

Antibodies used for immunohistochemistry

Alexa Fluor® 488 Goat anti-mouse, 1:200, Invitrogen

Alexa Fluor® 488 Goat anti-rabbit, 1:200, Invitrogen

Alexa Fluor® 568 Goat anti-rabbit, 1:200, Invitrogen

Alexa Fluor® 633 Goat anti-mouse, 1:200, Invitrogen

Chicken anti-GFP, 1:500, Abcam

Mouse anti-parvalbumin, 1:250, Chemicon/Millipore

Mouse anti-acetylated tubulin, 1:1000, Sigma

Rabbit anti-calretinin, 1:250, Swant

Rabbit anti-dsRed, 1:300, Clontech

1.7 EdU treatment and EdU staining

Embryos at 3dpf were anaesthesised in 0.003% tricane and mounted in 1% agarose with the heart facing upwards. 1nl of 0.1mM EdU was injected into the heart, and embryos were then transferred to fish water for 3 hours prior to being culled with 4% PFA, 4% sucrose.

Larvae older than 4dpf were swum in 0.1mM EdU dissolved in fish water for 24hrs in a dark 28°C incubator. Larvae were then washed out of EdU and transferred to fish water for 3 hours prior to being culled with 4% PFA, 4% sucrose.

Dissected brains were stained for EdU using the Click-iT ® EdU Alex Fluor ® 555 Imaging Kit (Invitrogen) according to the manufacturers instructions.

1.8 Imaging and confocal microscopy

Brains stained by *in situ* hybridization were mounted on a glass slide with the dorsal side uppermost in 100% glycerol and imaged on a Nikon Eclipse E1000 microscope using a Micropublisher 5.0 RTV camera (Q imaging).

Brains stained by immunohistochemistry and/or EdU treatment were mounted on a glass slide with the dorsal side uppermost in 1% low melting point agarose. The mounted brains were covered with H_2O and imaged by confocal laser-scanning microscopy using a Leica SP8 confocal microscope and x25 water immersion lens or x20 water immersion lens. *z*-stacks were acquired at 1-2µm intervals and rendered into 3D projections using Velocity (PerkinElmer).

1.9 Cell counting

<u>EdU^+ cells</u>

EdU^+ cells in larval brains, imaged by confocal microscopy, were counted using a cell counter plugin on the open-source platform, Fiji (Schindelin et al., 2012). In each wholemounted brain, all the EdU^+ cells in a 1950µm^2 area (75µm by 26µm) were counted, from the most dorsal region of the tectum to a ventral position containing no EdU^+ cells. The two regions counted in the left and right tectum of each larval brain were at the same position along the anterior-posterior axis, and the same distance from the midline. Two boxes in *Chapter 3. Figure 1.A* represent the position and size of the areas used to count EdU^+ cells in each tectum. In images of 16µm transverse sections, all the EdU^+ cells in a region close to the tectal midline were counted, as shown in *Chapter 3. Figure 1.8.*

<u>TUNEL cells</u>

Cells marked by the TUNEL assay were counted using a Nikon Eclipse E1000 microscope. In each tectum, all TUNEL stained cells in the SPV layer were counted, from the dorsal midline to the lateral edge of the tectum. The black box in *Chapter 3. Figure 5.B* represents the position and size of the area used to count apoptotic cells in each tectum.

<u>Calretinin and Parvalbumin containing neurons</u>

Calretinin and Parvalbumin immunopositive neurons in larval brains imaged by confocal microscopy were counted using a cell counter plugin on the open-source

platform, Fiji (Schindelin et al., 2012). In each tectum, all the positive neurons were counted in the SPV lamina, up to a distance of 60μm from the midline.

1.10 Eye enucleation

At 24hpf to 32hpf

Embryos were dechorionated at 24hpf – 32hpf in fish water and anaesthetised in 0.003% tricane. Embryos were then mounted on their side, with the left eye facing upwards, in 1% low melting point agarose in a 35mm culture dish. With the agarose set, 1x Ringers solution was added to the dish. A wedge was cut in the agarose with a surgical blade such that the tip of the wedge was by the head of the embryo. The left eye was manually removed from the embryo using a tungsten wire, sharpened at the end and bent into a hook. The embryos were released from the agarose and transferred to fish water with antibiotics (1% penicillin and streptomycin).

At 5pdf

Eye enucleation was performed as for 24hpf to 32hpf embryos (above), except that larvae were mounted in 2% low melting point agarose instead of 1% low melting point agarose and the left eye was manually removed using a pair of finely sharpened surgical forceps.

1.11 RNA extraction

All RNA was extracted from Tup Longfin wild type fish. Larvae at 9dpf were fixed in 4% PFA, 4% sucrose for 5 hours at room temperature, then transferred to PBS and stored at 4°C overnight. Fixed larvae were mounted on their side on a sylgard dish with 2 pins placed vertically through the body of the fish. The pins were placed one through the tail and one through the abdomen. The skin, jaw and eyes were removed from the head of the fish, then the pins were removed from the sylgard and placed horizontally on the sylgard dish so that the dorsal part of the fish was uppermost. Using a microsurgical knife, the forebrain was cut off and the midbrain was cut down the midline. Each half of the midbrain was transferred directly into digestion solution using a capillary pipette, with as little PBS as possible.

RNA was isolated using the RecoverAll^{TM} total nucleic acid isolation kit for FFPE (Ambion), with the deparaffinization step omitted. Midbrains were dissected on

multiple days and frozen after protease digestion before being pooled together through the same extraction column, such that each extracted RNA sample contained 74 midbrain halves. RNA was eluted into 60µl nuclease-free water. RNA integrity was identified by OD_{260}/OD_{280} nm absorption ratio > 2.0 and RQI > 7.6, where 0 corresponds to fully degraded RNA and 10 corresponds to intact DNA (Experion RNA Highsens Analysis, BIORAD).

1.12 RNAseq and analysis

RNAseq library samples were prepared at UCL Genomics and sequencing was performed on an Illumina HiSeq Machine at the BRC GSTT Genomics Core facility at Kings College London. Three biological replicates of four distinct samples were analysed using RNAseq:

- Left midbrains from 74 Tup Longfin larvae, culled at 9dpf
- Right midbrains from 74 Tup Longfin larvae, culled at 9dpf
- Left midbrains from 74 Tup Longfin larvae, with the left eye removed at 24hpf and the larvae culled at 9dpf
- Right midbrains from 74 Tup Longfin larvae, with the left eye removed at 24hpf and the larvae culled at 9dpf

The resulting 12 sets of RNA were run on one lane, generating 100nt paired end reads. De-multiplexed raw data files were imported onto the Galaxy server at http://usegalaxy.org/ (Goecks et al., 2010, Blankenberg et al., 2010 and Giardine et al., 2005). The quality of raw sequence data was checked using FastQC and all the reads at each base position had a bottom quartile score greater than 28. The processed reads were mapped to the genome with TopHat2 (Kim et al., 2013), using a mean inner distance between mate pairs of 0, standard deviation for distance between mate pairs of 81 and the zebrafish V9 assembly, version 65. Known junctions from the zebrafish V9 assembly were used, but the alignment software also looked for unsupplied junctions. Each BAM dataset (in a binary version of a sequence alignment/map format) produced by TopHat was assembled into a parsimonious set of transcripts using Cufflinks and a merged transcript dataset from all the Cufflinks transcripts was created using Cuffmerge

(Trapnell et al., 2010). Differential expression analysis was performed on the BAM files from all three biological replicates and the merged transcript dataset using Cuffdiff. Differential expression between samples was only counted as significant if $q < 0.05$.

1.13 cDNA synthesis and quantitative real-time PCR

cDNA was synthesized and amplified using the TransPlex® Complete Whole Transcriptome Amplification Kit (Sigma-Aldrich). 144ng of RNA was used from each sample and all cDNA after amplification had OD_{260}/OD_{280} nm absorption ratio >1.86.

For RT-qPCR, primers were designed with a T_M of 60°C give products of 100-250bp long, using Primer3 (MIT). Primer efficiency was calculated by qRT-PCR standard curve analysis using 1:5 serial dilutions of cDNA over at least four samples. Only primers with a high amplification efficiency (90-105%) were used.

$$\text{Amplification efficiency} = 10^{-1/\text{gradient}}$$

cDNA for qRT-PCR analysis was diluted 1:4 in H_2O. Samples and standards were run in triplicates on 96 well PCR plates. qRT-PCR amplification was performed using SYBR Green JumpStart Taq ReadyMix (Sigma) on a CFX96 R-T qPCR machine (BIO-RAD). 40 amplification cycles were used, with each cycle consisting of 94°C for 15 seconds, 60°C for 30 seconds and 72°C for 30 seconds. Relative gene expression was calculated using the $2^{-\Delta\Delta Ct}$ method, with elongation factor 1α (*ef1*α) as a reference gene. Melt-curve analysis was used to identify and remove reactions with nonspecific products.

Gene	Forward Primer (3'-5')	Reverse Primer (5'-3')	Product size, bp	Amplif. efficiency (%)
axin2	AGCCTTACCCTCGGACACTT	CGAGGATTTTGCCCTCATAC	157	103.53
cabp5b	AGCTGTCATGAGTCTAGGGC	TTCCATCTCAGTGGGCATGT	196	100.39
calb2b	GCCTGTCCAGCTCAAAGAAG	GATTGGGGTGGGTGAAGGTA	159	93.97
dlx2b	GCCCCATCGTTCTTAACAAACT	AACAGGTGTATTCGGCCATTTT	154	92.61
ef1α	GTACTTCTCAGGCTGACTGTG	ACGATCAGCTGTTTCACTCC	136	100.18
ephb1	AGATCTGTCGAACTGCCACA	CAGGGAGTTTCAGTCGACCT	213	92.94
lef1	AGCACGAGCAGAGAAAGGAG	CATCCTGGGTAAAGCTGCAT	244	99.10
lhx8a	CCCAGTTTGCTCAGGACAAC	GTGCAGCTGAAGAGTGGTTC	153	102.48
lrrtm4	CCTCCGTGCTTTGTATCTGC	TTCCCTGCAAGACTGATGGT	243	95.91
dvmap3k10	CAGCAGGTTTAGGGTCAGGA	ACAGGGAAAGGGAGAGTGTG	237	93.15
npvf	GGGACAGTTTTCAGAGAATGCT	AGGTTGATGGTAGACTTGGGAG	225	94.46
osbp	CAGCAAGTTCAGGGGCAAAT	AATTTGAGATGGCAGCGGTC	201	92.30
oxt	CGGCCTGCTACATCTCAAAC	TCACACGGAGAAGGGAGAAA	205	94.52
pcp4a	CTCTTCTGCCCAATCCAGC	ATGTCGAAGTCCTCAGCCG	150	97.90
rhpn1	GGAGGCTGCTAGGGTATCAG	TGGCTGTCTGGTGTGAATCT	238	92.73
rimbp2	TACCGCACCATTCTCACCAT	TTTCCCCTGTCGCTGAAGAT	205	90.02
si:dkey-14d8.6	AGTATGAAGACCGGGTGTGG	AGACGCGGTTACCTCTACAG	210	96.04
tcf4	CCAGTTATGAACCACCGCTG	AGAGTGTGAAGGCGTGATCA	164	92.15

1.14 Generation of transgenic lines

Tg(*ath5:cre*^{nls}*,clmc:EGFP*) and Tg(*isl2b:loxP-dsRed-N1-loxP,TeNT-Lc-EGFP*) transgenic lines were both constructed using Gateway® Three-Fragment Vector Construction Kit (Invitrogen).

The p5E-Isl2b-deltaBX construct was a kind gift from Chi-Bin Chien (University of Utah). LoxP-dsRed-N1-loxP was PCR amplified from the pCMV-Lox-dsRed2-pA-Lox-EGFP plasmid (Langenau et al., 2005) using the following primers: GGGGACAAGTTTGTACAAAAAAGCAGGCTCCAAGCTTATAACTTCGTATAG (F) and GGGGACCACTTTGTACAAGAAAGCTGGGTGGATCCACCGGTATAACTTC (R). TeNT-Lc-EGFP was PCR amplified from the 5UAS TeNT-Lc-EGFP construct (Ben Fredj et al., 2010) using primers GGGGACAGCTTTCTTGTACAAAGTGGAGTTCGCCCTTGCCGAGCGCC (F) and GGGGACAACTTTGTATAATAAAGTTGTGTAGTGGGCCATCGCCCTGA (R). The loxP-dsRed2-pA-loxP and TeNT-Lc:EGFP PCR products were inserted into pDONR-221 and pDONRP2R-P3 respectively using BP clonase II enzyme mix (Invitrogen). The three entry vectors were then inserted into the pDestTol2pA2 destination vector using LR clonase II enzyme mix (Invitrogen).

Cre^{nls} was inserted into a middle entry vector by Mario E. Sanchez Rubio (University of Chile). The *ath5* promoter was PCR amplified from an *ath5* promoter plasmid (gift from Clemens Riegler, Harvard University), using primers TTTTTAAGCTTCTGTGACTGTCTGAATCTG (F) and TTTTTGGATCCGGATGGTTCTTAATCGCTT (R) and the PCR product was inserted into pENTR5'-TOPO vector. The *ath5* promoter, the Cre^{nls} construct and a 3' polyA sequence were inserted into the pDestTol2CG2 destination vector using LR clonase II enzyme mix (Invitrogen).

1nl of 25ng/ul DNA and 25ng/ul *Tol2* transposase mRNA were injected into embryos at the one cell stage. Tg(*isl2b:loxP-dsred-loxP,TeNT-Lc-EGFP*) embryos were identified by dsRed expression in the retina and brain at 3dpf. Tg(*ath5:cre^{nls},clmc:EGFP*) embryos were identified by EGFP expression in the heart at 1-2dpf. Positive embryos were raised to adulthood and crossed to AB^{*} wild-type fish, with positive F1 embryos raised to adulthood.

1.15 List of solutions

AP buffer: 5ml of 1M Tris-HCl (pH 9.5), 2.5ml of 1M $MgCl_2$, 1.25ml of 4M NaCl, 0.25ml of 20% TX-100, 41ml H_2O

Hyb+: 25ml Formamide, 12.5ml 20x SSC, 500µl of 50mg/ml Torula RNA, 25µl of 100mg/ml Heparin, 250µl of 20% Tween-20, 460µl og 1M Citric acid, 11.27ml H_2O

MABlock: 150mM NaCl, 100mM Malic Acid, 2% Roche Blocking Reagent in H_2O, pH 7.5

Ringers soln. 116mM NaCl, 3mM KCl, 4mM $CaCl_2$ (anhydrous), 1mM $MgCl_2.6H_2O$, 5.0mM HEPES, 1% Penicillin + Streptomycin

Chapter 3. Results I.

Innervation from Retinal Ganglion Cells promotes tectal cell proliferation and survival

1. Introduction

It has been suggested that retinal input regulates growth of the optic tectum, with a number of reports demonstrating atrophy of the tectum upon abrogation of retinal input (Larsell, 1931; White, 1948; Kollros (1953); Schmatolla, 1972; Schmatolla and Erdmann, 1973; Currie and Cowan, 1974; Kollros; 1982; Raymond et al., 1983). However published reports conflict on how retinal innervation affects growth of the optic tectum. For example Schmatolla and Erdmann (1973) concluded that despite a smaller non-innervated tectum, the rate of mitosis and the number of cells between innervated and non-innervated tecta was nearly identical. On the other hand, Raymond et al. (1983) reported decreased proliferation in non-innervated tecta, with decreased [^{3}H] incorporated into the non-innervated tectum compared to the innervated tectum. These disagreements may have arisen from differences in the species used in each study, as Schmatolla and Erdmann (1973) used zebrafish and Raymond et al. (1983) used goldfish. With the development of new tools to study proliferation, apoptosis and differentiation, we decided to re-investigate the affect of retinal input on growth of the optic tectum

2. Results

2.1 Proliferation is reduced in the tectum of *lakritz* mutants

We first asked if abrogation of retinal efferents affects proliferation in the optic tectum. Atoh7, expressed solely in the retina, is required for the generation of retinal ganglion cells (RGCs), and the *atoh7* mutant, *lakritz*, completely lacks RGCs (Kay et al., 2001), thus providing us with a mutant in which to assess the affect of retinal innervation on the optic tectum. *lakritz; atoh7:RFP* mutants can be distinguished from wild-type siblings as early as 32hpf, when RGC axons exit the retina (Burrill and Easter 1994). We examined the number of proliferating cells in *lakritz* mutants at 5, 7 and 9dpf and found that the number of proliferating cells decreases as larvae age, with a greater

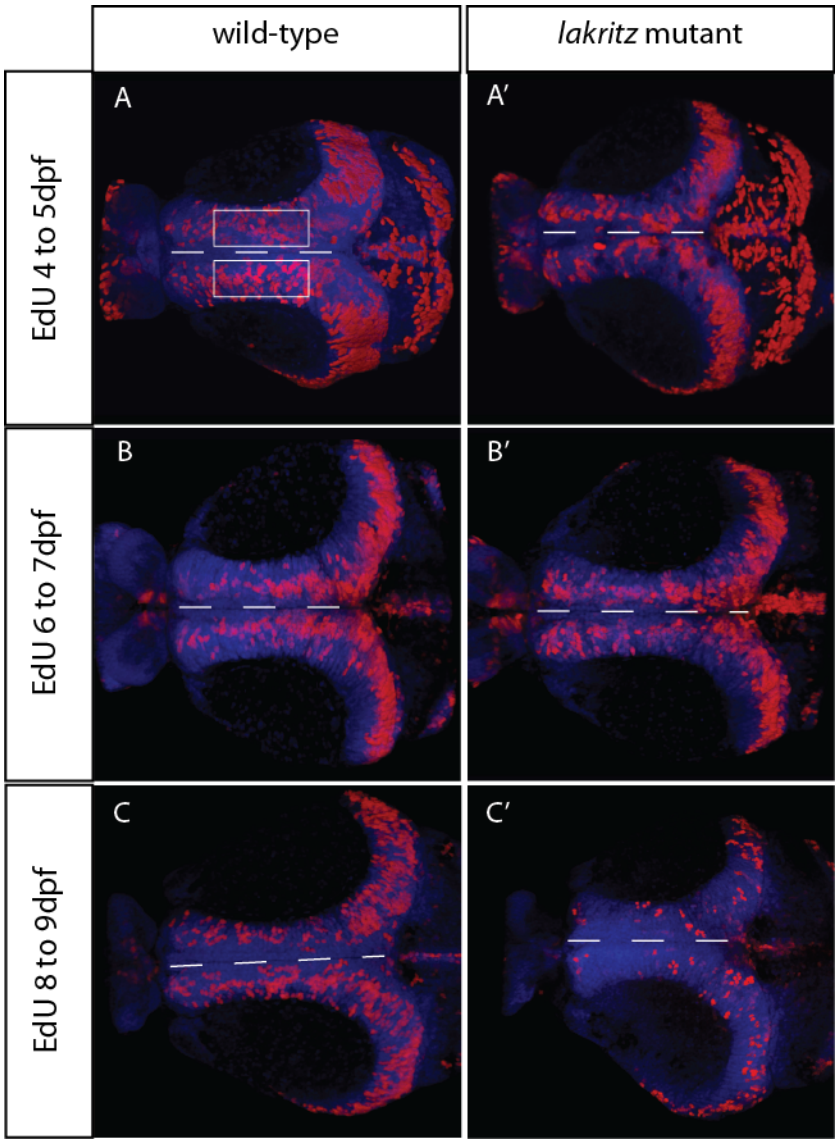

Figure 1. Proliferation is reduced in the tectum of *lakritz* mutants

3D reconstructions of dorsal views of dissected brains from wild-type larvae **(A-C)** and *lakritz* mutant larvae **(A'-C'),** swum for 24 hours in EdU and culled at 5dpf **(A-A'),** 7dpf **(B-B')** and 9dpf **(C-C').** Brain morphology is visualised with the nuclear marker TOPRO-3 (blue) and proliferating cells with EdU (red).

(A-B') The optic tecta of both wild-type and mutant larvae show similar levels of EdU incorporation at 5dpf and 7dpf

(C'-C') At 9dpf, mutant larvae show decreased levels of EdU incorporation compared to their wild-type siblings

The two boxes in **A** represent the position and size of the area used to count the number of EdU positive cells in each larvae.

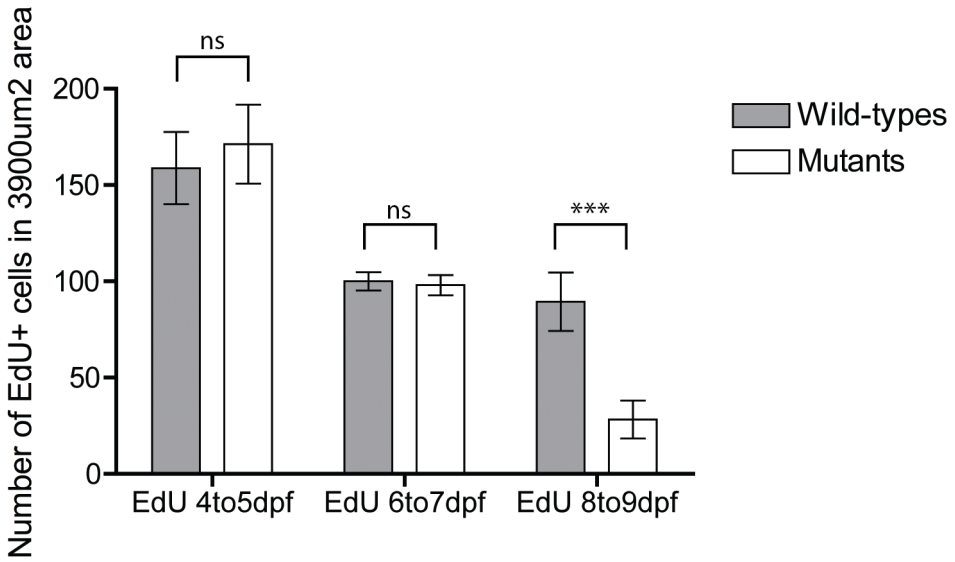

Graph 1. Proliferation is significantly reduced in the *lakrtiz* mutant tectum at 9dpf

Graph representing the number of cells incorporating EdU at 5dpf, 7dpf and 9dpf in wild-type sibling larvae and *lakritz* mutant larvae. EdU+ cells were counted in a 390um2 area in each larval brain, as represented by the white boxes in ***figure 1.1***. Data represents the mean ± s.e.m. n = 6 (wt, 5dpf), 5 (mutants, 5dpf), 12 (wt and mutants, 7dpf), 13 (wt, 9dpf), 11 (mutants, 9dpf). The number of EdU cells in wild-type and mutant tecta was compared using a Student's t-test (paired, ns = not significant, *p<0.05, **p<0.01 ***p<0.001).

reduction in the absence of retinal input. To label cells proliferating in the tectum, we swam *lakritz; atoh7:RFP* larvae in the nucleoside analog EdU, which is incorporated into replicating cells during DNA replication. We labelled as many proliferative cells as possible and reduced variance between larvae by swimming both wild-types and *lakritz* mutants for 24 hours in 0.1mM EdU, then returned the larvae to normal fish water and culled them 3 hours later. Dissected brains were stained for EdU, using a "click-it reaction" (see methods), and the nuclear marker TOPRO-3, which shows the positions of EdU^+ cells within the optic tectum. At 5dpf and 7dpf, EdU incorporation is similar between the tecta of wild-types and *lakritz* mutants (*Figure 1.A-B'*). At 9dpf, *lakritz* mutant tecta show visibly reduced EdU incorporation compared to their wild-type siblings (*Figure 1.C-C'*).

When we quantified the number of EdU^+ cells in wild-type and *lakritz* tecta we found that there was no significant change at 5dpf or 7dpf, but at 9dpf, *lakritz* tecta have a 68.4% reduction in the number of EdU^+ cells in two 1950μm^2 zones either side of the midline compared to their wild-type siblings ($p = 0.0004$, *Graph 1.*). This data suggests that abrogation of retinal input reduces proliferation in the optic tectum. However there is also the possibility that this decrease is an effect of the mutation, or due to a difference in the rate of development between larvae, and so we next assessed the effect of retinal abrogation in wild-type fry.

2.2 Proliferation is not reduced in the non-innervated tectum after eye removal between 24hpf and 32hpf

To exclude the possibility that decreased proliferation in *lakritz* mutants is a secondary consequence of either the mutation or a difference in the rate of development between larvae, we assessed the effect of retinal abrogation in wild-type larvae. We surgically removed the retina between 24hpf and 32hpf, before any axons reach the tectum. Throughout this work, only the left eye was surgically removed, which resulted in a non-innervated tectum on the right side of experimental larvae, and an innervated tectum on the left side.

Using the *Tg(atoh7:GFP)* transgenic line and DiI retinal injections, we observed that manual eye removal does not generally cause ipsilateral projections to the tectum from the remaining eye (*Figure 2.A-B'*). This allowed us to use the innervated tectum as an

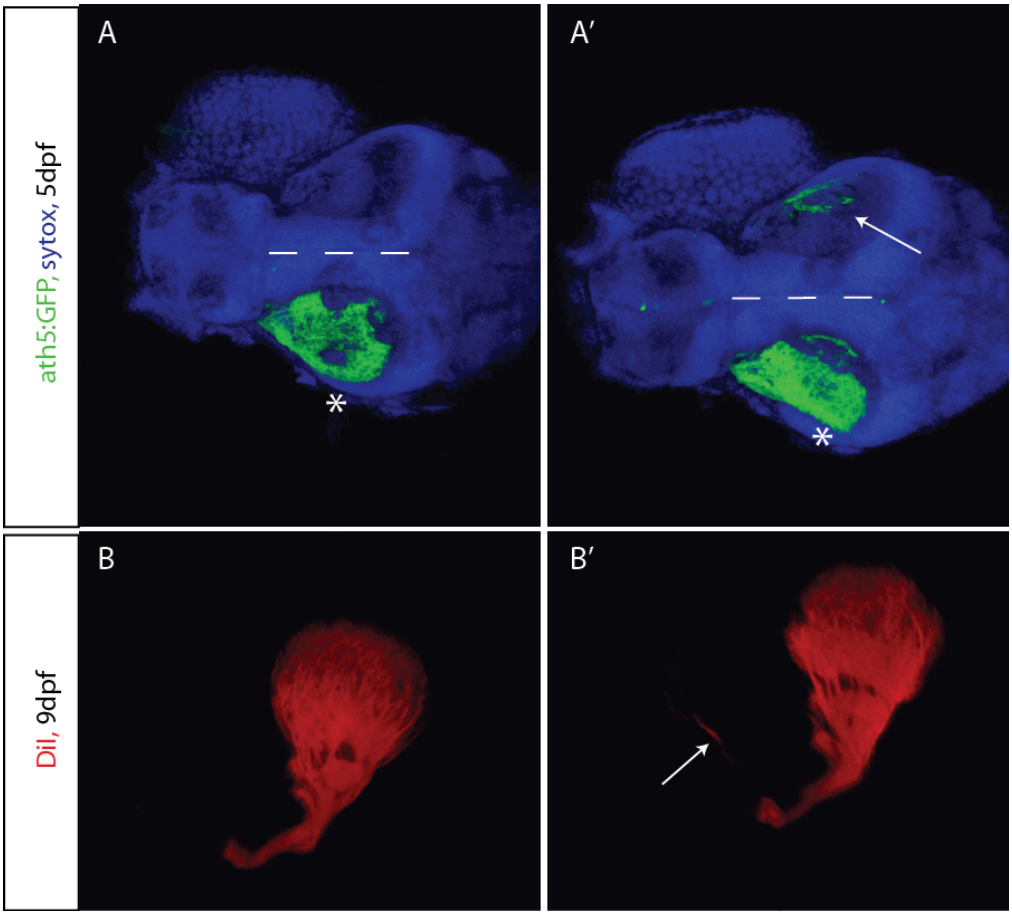

Figure 2. The de-innervated optic tectum generally does not receive ipsilateral RGC projections from the remaining eye

(A-A') 3D reconstructions of dorsal views of the larval brain at 5dpf in *Tg(atoh7:GFP)* embryos with the left eye surgically removed between 24 and 32hpf. Brain morphology is visualised with the nuclear marker TOPRO-3 (blue). **(B-B')** 3D reconstructions of the innervation from the remaining eye at 9dpf, injected with DiI, with the left eye surgically removed between 24 and 32hpf.

(A-A') The majority of larvae have innervation only to the contralateral tectum (with an asterisk. 1 out of 10 embryos have small ipsilateral projections from the remaining eye.

(B-B') The majority of larvae have innervation only to the contralateral tectum. 2 out of 10 embryos have small ipsilateral projections from the remaining eye.

Figure 3. Proliferation in the non-innervated tectum is not greatly altered following eye removal between 24hpf and 32hpf

3D reconstructions of dorsal views of dissected brains from wild-type larvae **(A-E)** and larvae with the left eye surgically removed between 24 and 32hpf **(A'-E'). (A-A')** Embryos were injected with EdU at 3dpf and culled 3 hours later. **(B-E')** Larvae were swum for 24 hours in EdU and culled 3 hours later at 5dpf **(B-B'),** 7dpf **(C-C'),** 9dpf **(D-D')** and 14dpf **(E-E').** Brain morphology is visualised with the nuclear marker TOPRO-3 (blue) and proliferating cells with EdU (red).

(A-E) Wild-type larvae display similar levels of EdU incorporation in both tecta.

(A'-B') The innervated (with a white asterix) and non-innervated tecta of one-eyed larvae display similar levels of EdU incorporation at 3dpf and 5dpf

(C'-E') Innervated tecta of one-eyed larvae appear to incorporate higher levels of EdU than their non-innervated counterparts at 7dpf, 9dpf and 14dpf.

The two boxes in **A** represent the position and size of the area used to count the number of EdU positive cells in each tectum.

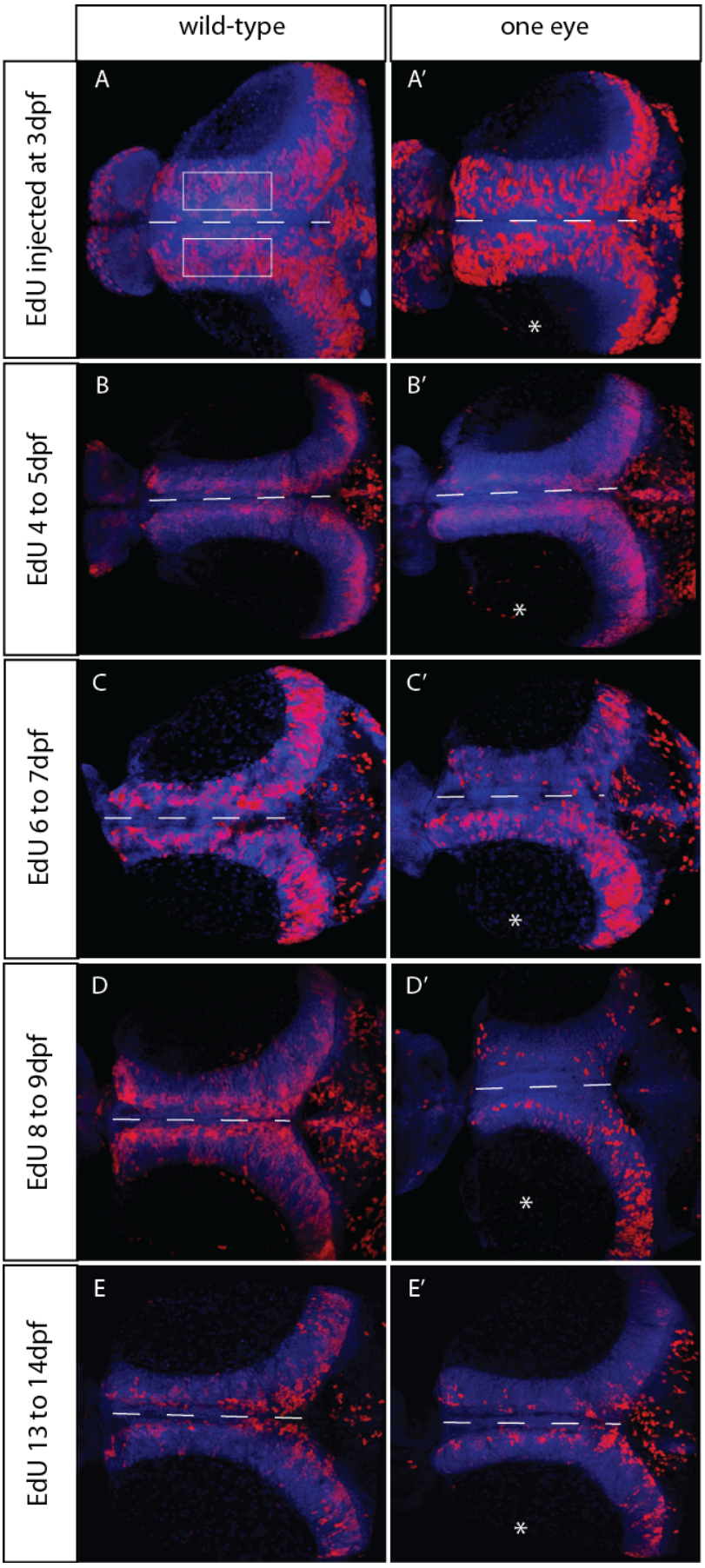
wild-type
one eye
EdU injected at 3dpf
EdU 4 to 5dpf
EdU 6 to 7dpf
EdU 8 to 9dpf
EdU 13 to 14dpf
A
A′
B
B′
C
C′
D
D′
E
E′

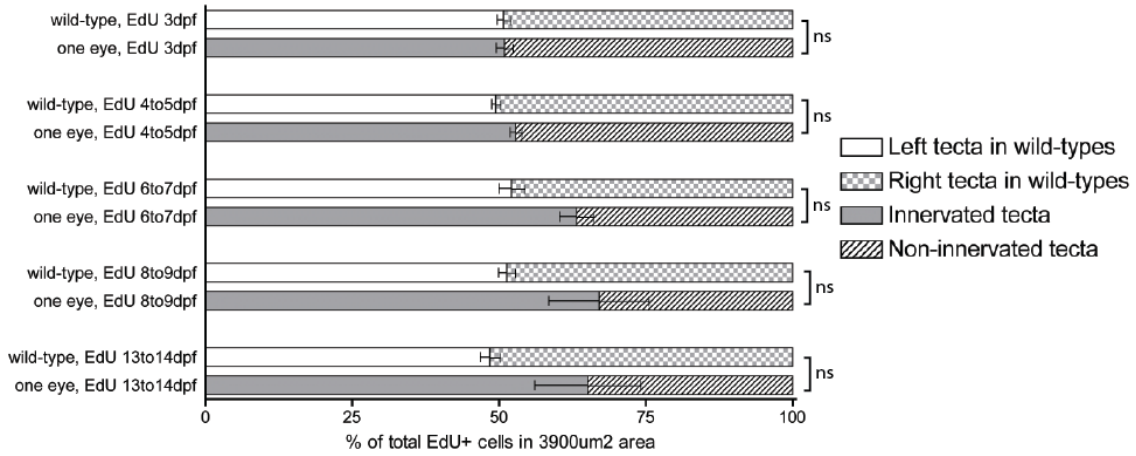

Graph 2. Proliferation is not reduced in the non-innervated tectum when the eye is removed between 24 and 32hpf

Graph representing the proportion of cells incorporating EdU at 3dpf, 5dpf, 7dpf, 9dpf and 14dpf in the left and right tecta of wild-type larvae and the innervated and non-innervated tecta of larvae with the eye removed between 24 and 32hpf. EdU^{+} cells were counted in a 1950μm^2 area in each tectum, as represented by the white boxes in ***figure 1.2***. Data represents the mean ± s.e.m. n = 9 (wt, 3dpf), 11 (1eye, 3dpf), 8 (wt, 5dpf), 12 (1eye, 5dpf), 7 (wt, 7dpf), 4 (1eye, 7dpf), 5 (wt, 9dpf), 4 (1eye, 9dpf), 11 (wt, 14dpf), 5 (1eye, 14dpf). The proportion of EdU cells in wild-type left tecta and non-innervated tecta was compared using a Student's t-test (paired, ns = not significant, *p<0.05, **p<0.01, ***p<0.001).

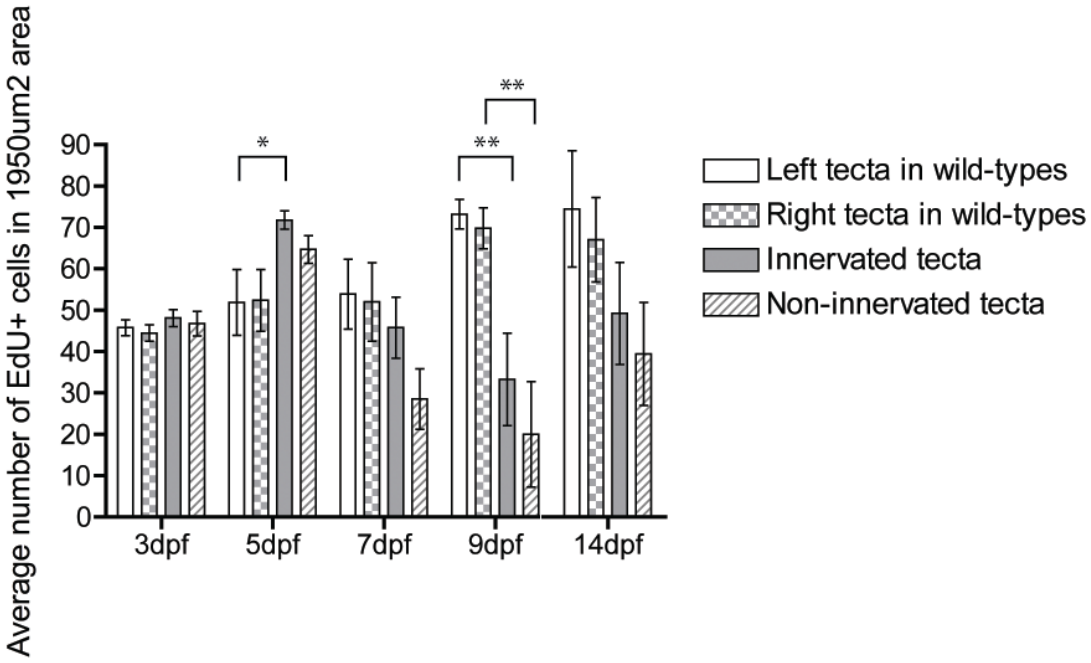

Graph 3. Proliferation is reduced in both innervated and non-innervated tecta when an eye is removed between 24hpf and 32hpf

Graph representing the average number of cells incorporating EdU at 3dpf, 5dpf, 7dpf, 9dpf and 14dpf, in the left and right tecta of wild-type larvae and the innervated and non-innervated tecta of larvae with the eye removed between 24 and 32hpf. EdU^+ cells were counted in a 1950μm^2 area in each tectum, as represented by the white boxes in ***figure 1.2***. Data represents the mean ± s.e.m. n = 9 (wt, 3dpf), 11 (1eye, 3dpf), 8 (wt, 5dpf), 12 (1eye, 5dpf), 7 (wt, 7dpf), 4 (1eye, 7dpf), 5 (wt, 9dpf), 4 (1eye, 9dpf), 11 (wt, 14dpf), 5 (1eye, 14dpf). The number of EdU cells counted in each tectum were compared using a Student's t-test (paired, ns = not significant, *$p<0.05$, **$p<0.01$, ***$p<0.001$). Only significant results are represented on the graph.

internal control to the non-innervated tectum in unilaterally enucleated larvae. We also used wild-type controls to ascertain that there is no latent asymmetry in wild-type non-enucleated larvae and that any effects we see are not due to the experimental methods performed after enucleation.

After 4dpf, larvae can take up EdU when it is dissolved in fish water, but to label proliferating cells at 3dpf, we injected 0.1mM EdU directly into the heart and culled the larvae 3 hours later. All older larvae were swum for 24 hours in EdU, then 3 hours in normal fish water before being culled. As with the experiments using *lakritz* mutants, tecta of young larvae at 3dpf and 5dpf do not display a change in the number of cells incorporating EdU (*Figure 3.A-B'*). At 7dpf, 9dpf and 14dpf, there appears to be a slight reduction in the number of EdU^+ cells in non-innervated tecta compared to innervated tecta (*Figure 3.C'-E'*). This difference in proliferation is not present in wild-types and could be due to the abrogation of retinal innervation into the optic tectum.

To validate this finding, we counted the number of EdU^+ cells in wild-type and surgically enucleated brains. To account for the possible difference in size between the tecta and for variance between larvae, we first counted cells in a 1950μm^2 area in each tectum (representative boxes are in *Figure 3.A*) and then calculated the proportion of EdU^+ cells in each tectum out of the total for the left and right tectal areas together. Quantification shows that there is no significant decrease in the proportion of cells in non-innervated tecta that incorporated EdU at 3dpf, 5dpf, 7dpf, 9dpf and 14dpf (*Graph 2*.). This data contrasts with that from *lakritz* mutants and suggests that tectal cell proliferation is not affected by RGC innervation.

When we compared the average number of cells counted in a 1950μm^2 area in each tectum, we noticed an initial increase in EdU^+ cells in the innervated tectum compared to the left wild-type tectum ($p=0.0105$) at 5dpf, followed by a decrease in the average number of EdU^+ cells in both the innervated tectum ($p=0.0071$) and non-innervated tectum ($p=0.0054$) when compared to their corresponding wild-type tectum at 9dpf. However no significant change was found at 3dpf, 7dpf or 14dpf (*Graph 3*.). This suggests that larval growth rates can be affected by unilateral eye enucleation, but the effect is variable. To investigate whether removal of retinal input alters proliferation in the tectum after RGC axons innervate and form functional synapses with tectal cells, we decided to analyse wild-type larvae, unilaterally enucleated at 5dpf.

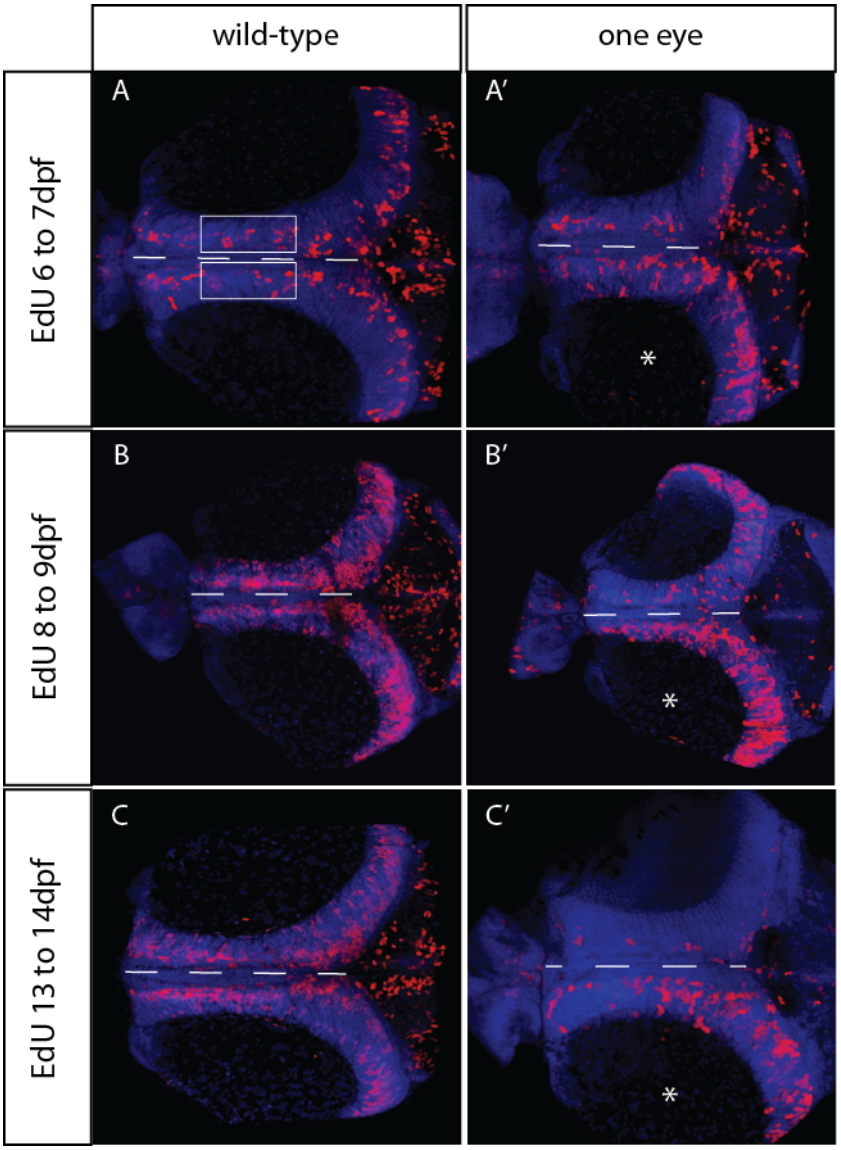

Figure 4. Proliferation decreases in the non-innervated tectum after eye removal at 5dpf

3D reconstructions of dorsal views of dissected brains from wild-type larvae **(A-D)** and larvae with the left eye surgically removed at 5dpf **(A'-D'),** swum for 24 hours in EdU and culled at 7dpf **(A-A'),** 9dpf **(B-B')** and 14dpf **(C-C').** Brain morphology is visualised with the nuclear marker TOPRO-3 (blue) and proliferating cells with EdU (red).

(A-C) Wild-type larvae display similar levels of EdU incorporation in both tecta.

(A'-C') Innervated tecta of one-eyed larvae (with a white asterix) incorporate considerably higher levels of EdU than their non-innervated counterparts at each time point.

The two boxes in **A** represent the position and size of the area used to count the number of EdU positive cells in each tectum.

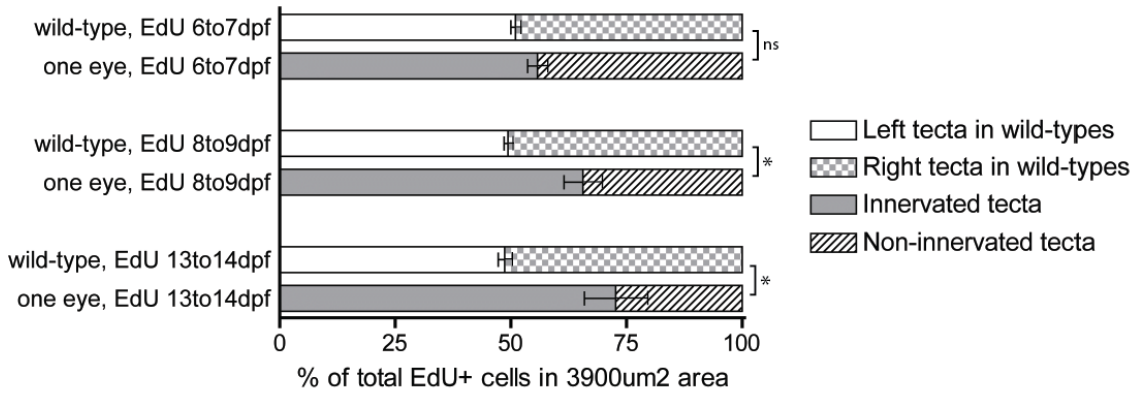

Graph 4. Proliferation is significantly reduced in the non-innervated tectum when the eye is removed at 5dpf

Graph representing the proportion of cells incorporating EdU at 7dpf, 9dpf and 14dpf in the left and right tecta of wild-type larvae and the innervated and non-innervated tecta of larvae with the eye removed at 5dpf. EdU^+ cells were counted in a 1950µm^2 area in each tectum, as represented by the white boxes in ***figure 1.4***. Data represents the mean ± s.e.m. n = 9 (wt, 7dpf), 6 (1eye, 7dpf), 15 (wt, 9dpf), 6 (1eye, 9dpf), 7 (wt and 1eye, 14dpf). The proportion of EdU cells in wild-type left tecta and non-innervated tecta was compared using a Student's t-test (paired, ns = not significant, *p<0.05, **p<0.01, ***p<0.001).

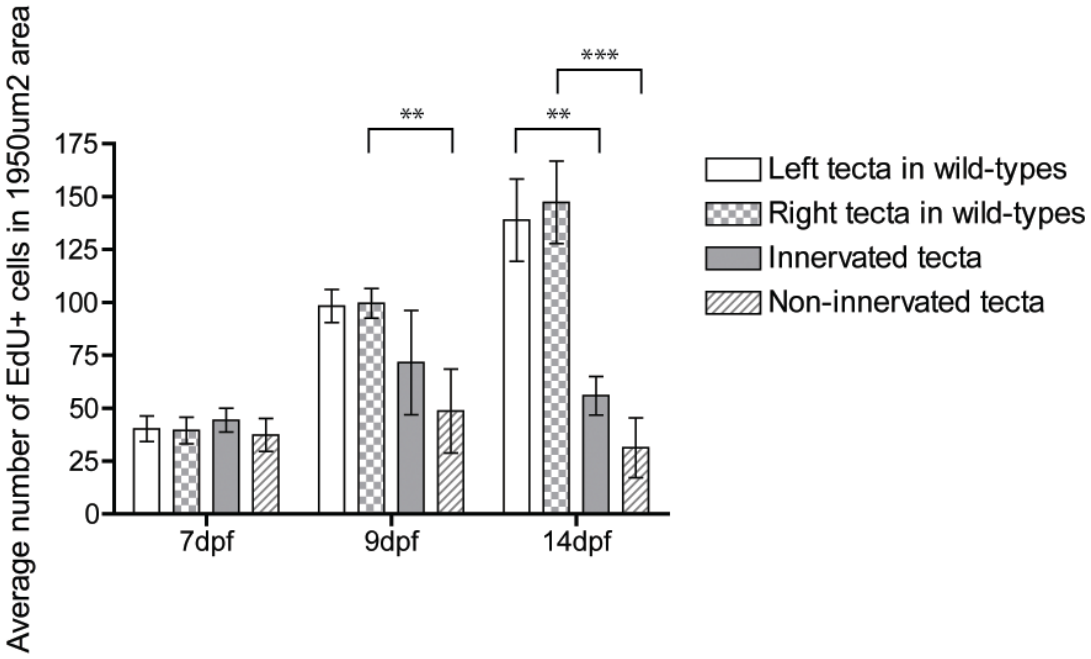

Graph 5. Proliferation is significantly reduced in both innervated and non-innervated tecta when an eye is removed at 5dpf

Graph representing the average number of cells incorporating EdU at 7dpf, 9dpf and 14dpf in the left and right tecta of wild-type larvae and the innervated and non-innervated tecta of larvae with the eye removed at 5dpf. EdU^{+} cells were counted in a 1950µm2 area in each tectum, as represented by the white boxes in ***figure 1.4***. Data represents the mean ± s.e.m. n = 9 (wt, 7dpf), 6 (1eye, 7dpf), 15 (wt, 9dpf), 6 (1eye, 9dpf), 7 (wt and 1eye, 14dpf). The number of EdU cells counted in each tectum were compared using a Student's t-test (paired, ns = not significant, *p<0.05, **p<0.01, ***p<0.001). Only significant results are represented on the graph.

2.3 Proliferation is reduced in the non-innervated tectum after eye removal at 5dpf

Although RGCs reach the tectum at 48hpf, their axonal arbors do not fully cover the tectum until 72hpf (Burrill and Easter, 1994), the same time at which the optokinetic response begins to develop (Easter and Nicola, 1996). From 3dpf to 7dpf, tectal cells start to mature, with the rapid development of nascent dendritic arbors and stable synapses. After which, the RGC axonal arbors and tectal dendritic arbors become relatively stable (Niell et al., 2004; Meyer and Smith, 2006).

To look at the effect of unilateral enucleation on proliferation in the tectum after retinal innervation, we decided to remove the eye at 5dpf, at the onset of prey/capture behaviour (Westerfield, 1993) and after the initial growth of retino-tectal axonal and dendritic arbors in the tectum. We swam fish for 24 hours in 0.1mM EdU, then 3 hours in normal fish water before being culled. At 7dpf, 9dpf and 14dpf, there appears to be a reduction in the number of EdU^+ cells in the non-innervated tectum compared to the innervated tectum (*Figure 4.A'-C'*) and this difference in proliferation between tecta is not present in wild-types (*Figure 4.A-C*).

When we quantified proliferation, by measuring the proportion of EdU^+ cells in the non-innervated tectum out of the total for the non-innervated and innervated tecta combined, we found that the non-innervated tectum had 44.3% of the EdU^+ cells at 7dpf (not significant), 34.4% of the EdU^+ cells at 9dpf ($p = 0.0139$) and 27.3% of the EdU^+ cells at 14dpf ($p = 0.0183$), (*Graph 4.*). This data suggests that retinal input regulates cell proliferation in the optic tectum and that this regulation requires a period of tectal innervation by RGC axons. When we compared the average number of cells counted in a $1950\mu m^2$ area in each tectum, we found a decrease in the average number of EdU^+ cells in the non-innervated tectum at 9dpf ($p=0.0043$) and both the innervated tectum ($p=0.0011$) and non-innervated tectum ($p=0.0004$) at 14dpf when compared to the average number of EdU^+ cells in their corresponding wild-type tecta (*Graph 5.*). This again suggests that growth of both innervated and non-innervated tecta, or by extrapolation, the larvae themselves are affected by unilateral eye enucleation. We next wanted to ask how lack of retinal innervation regulates this change in proliferation in the optic tectum.

Figure 5. Tectal expression of cell cycle markers *ccnD1, cmyc* and *p57* is unaffected by lack of retinal innervation

Dorsal views of dissected brains at 9dpf from wild-type larvae **(A-C),** larvae with the left eye surgically removed between 24 and 32hpf **(A'-C')** and larvae with the left eye surgically removed at 5dpf **(A''-C'').** Dissected brains have been stained for the expression of cell cycle regulators *ccnD1* **(A-A''),** *cmyc* **(B-B'')** and *p57* **(C-C'').**

(A-C) Wild-type larvae display similar levels of *ccnd1, cmyc* and *p57* expression between the two tecta.

(A'-C') Non-innervated tecta from larvae with the eye removed between 24 and 32hpf display similar levels of *ccnD1, cmyc* and *p57* expression to their innervated counterparts (with a black asterix).

(A"-C") Non-innervated tecta from larvae with the eye removed at 5dpf display similar levels of *ccnD1, cmyc* and *p57* expression to their innervated counterparts.

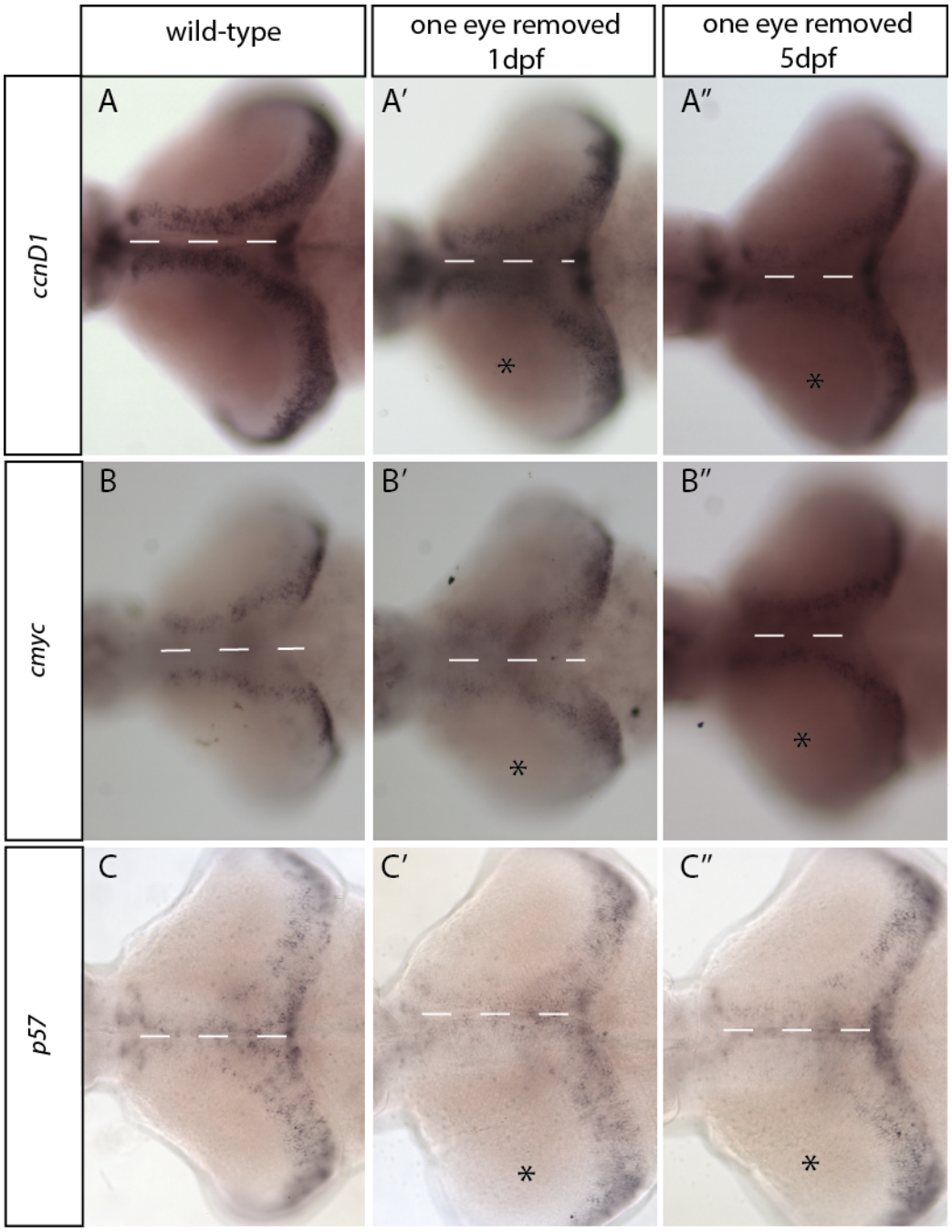
wild-type
one eye removed 1dpf
one eye removed 5dpf
ccnD1
cmyc
p57
A
A′
A″
B
B′
B″
C
C′
C″

2.4 Tectal expression of cell cycle regulators *ccnD1, cmyc* and *p57* is not overtly affected by lack of retinal innervation

There are four different phases of the cell cycle (G1, S, G2, M), with cells committed to a round of cell division once passing the restriction checkpoint towards the end of G1 (reviewed by Malumbres and Barbacid, 2009). During G1, several different signalling systems, including growth factor signalling, target Cyclin proteins to drive or inhibit progression past the restriction point. A master regulator of the cell cycle is C-myc, a proto-oncogene whose activity is regulated by growth factors and which acts to stimulate cell proliferation (Eilers et al., 2008; Dang, 2012). CyclinD1 (CcnD1) expression and activity is also heavily dependent on mitogens (reviewed by Sherr and Roberts, 1999).

Analysis of *ccnd1* and *cmyc* in unilaterally enucleated brains revealed no visible difference in their expression between non-innervated and innervated tecta (*Figure 5.A-B"*). In addition, we could not detect a difference in the expression of *cyclinA2* (data not shown), the basic helix-loop-helix transcription factor *neuroD* (data not shown) or genes encoding the cyclin kinase inhibitors *p57,* required for cell cycle exit in the retina *(Figure 5.C-C";* Dyer and Cepko, 2000) and *p27* (data not shown). Our observation of no change in the expression of *ccnD1*, *cmyc, ccnA2, neuroD, p27* and *p57* suggests that the cell cycle is regulated by other means, possibly at the protein level, or perhaps that the cell cycle is not altered in non-innervated tecta, but instead more cells enter programmed cell death. This prompted us to investigate whether the regulation of apoptosis is affected by retinal input.

2.5 Eye removal between 24hpf and 32hpf does not affect apoptosis in the non-innervated tectum

We have shown that retinal innervation regulates proliferation in the optic tectum of *lakritz* mutants and larvae unilaterally enucleated at 5dpf. Another way of regulating tissue growth is through the control of programmed cell death. We used the TdT-mediated dUTP-biotin nick-end labelling (TUNEL) assay to look at nuclei in the tectum containing fragmented DNA.

When we performed unilateral enucleation between 24hpf and 32hpf, there was no visible difference between the number of stained nuclei in innervated and non-

Figure 6. Eye removal between 24 and 32hpf does not affect apoptosis in the non-innervated tectum

Dorsal views of live larvae **(A,A')** and dissected brains **(B-E')** from wild-type larvae **(A-E)** and larvae with the left eye surgically removed between 24 and 32hpf **(A'-E')** Larvae have been culled at 3dpf **(A-B'),** 5dpf **(C,C'),** 7dpf **(D,D')** and 9dpf **(E,E')** and the brains stained using the neutral red assay **(A,A')** for microglia or TUNEL assay **(B-E')** for apoptotic cells.

(A-E) Wild-type larvae display similar numbers of microglia and apoptotic cells between the two tecta.

(A'-E') Non-innervated tecta of one-eyed larvae also display similar numbers of microglia and apoptotic cells to their innervated counterparts (with a black asterix).

The black box in **A** represents the position of the area used to count the number of apoptotic cells in each tectum

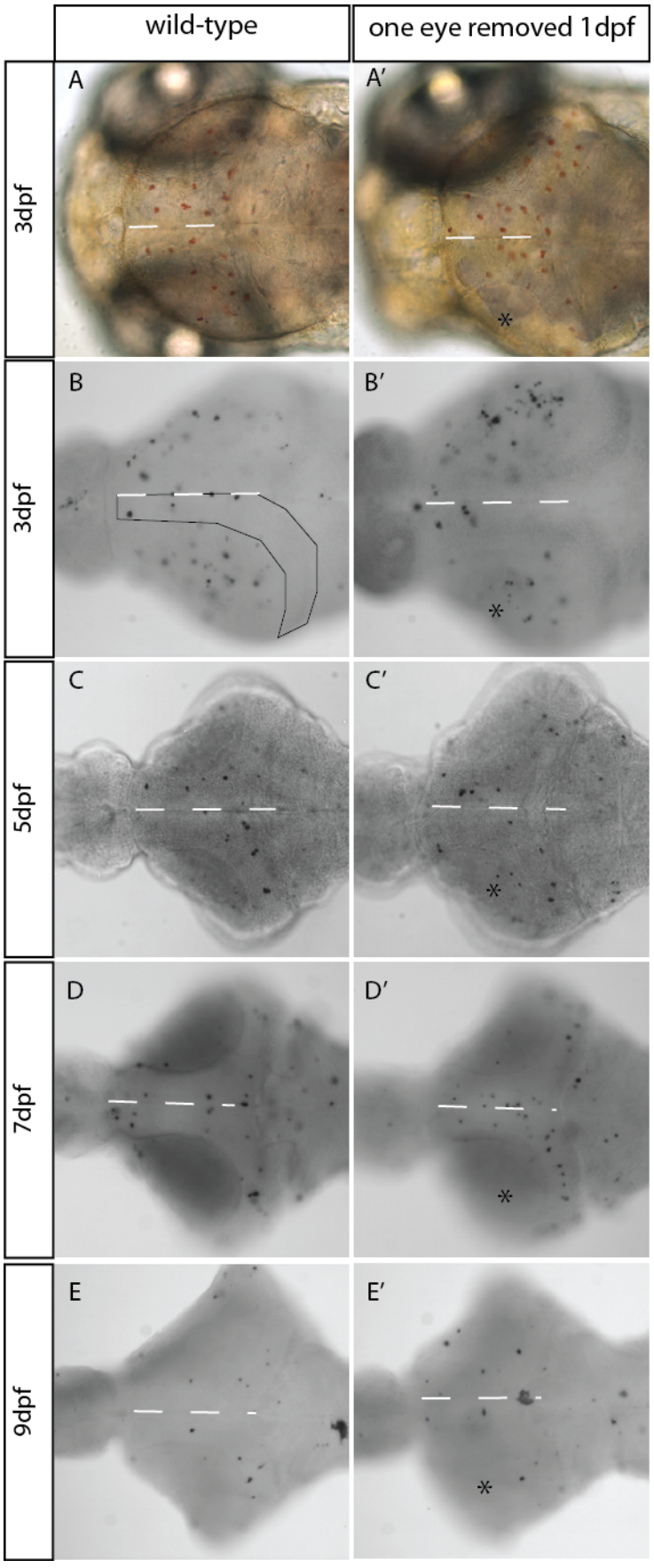
wild-type
one eye removed 1dpf
3dpf
A
A′
3dpf
B
B′
5dpf
C
C′
7dpf
D
D′
9dpf
E
E′

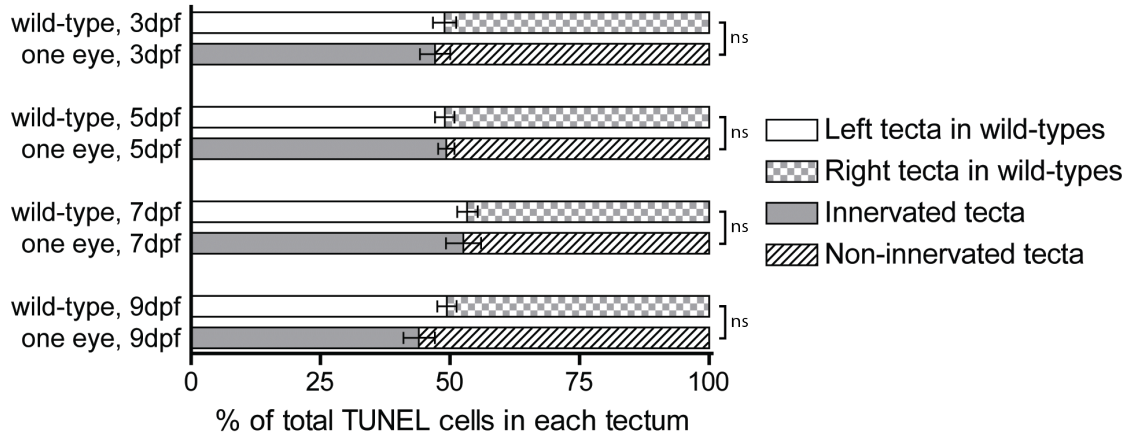

Graph 6. Eye removal between 24 and 32hpf does not significantly alter the number of apoptotic cells in the tectum

Graph representing the proportion of TUNEL cells in the left and right tecta of wild-type larvae and the innervated and non-innervated tecta of one-eyed larvae with an eye removed between 24 and 32hpf. TUNEL cells were counted in the SPV lamina, as represented by the black box in ***figure 1.6.*** Data represents the mean ± s.e.m. n = 10 (WT, 3dpf), 7 (one eye, 3dpf), 27 (WT, 5dpf), 16 (one eye, 5dpf), 14 (WT, 7dpf), 11 (one eye, 7dpf), 17 (WT, 9dpf), 15 (one eye, 9dpf). The percentage of TUNEL cells in wild-type left tecta and non-innervated tecta were compared using a Student's t-test (paired, ns = not significant, *$p<0.05$, **$p<0.01$, ***$p<0.001$).

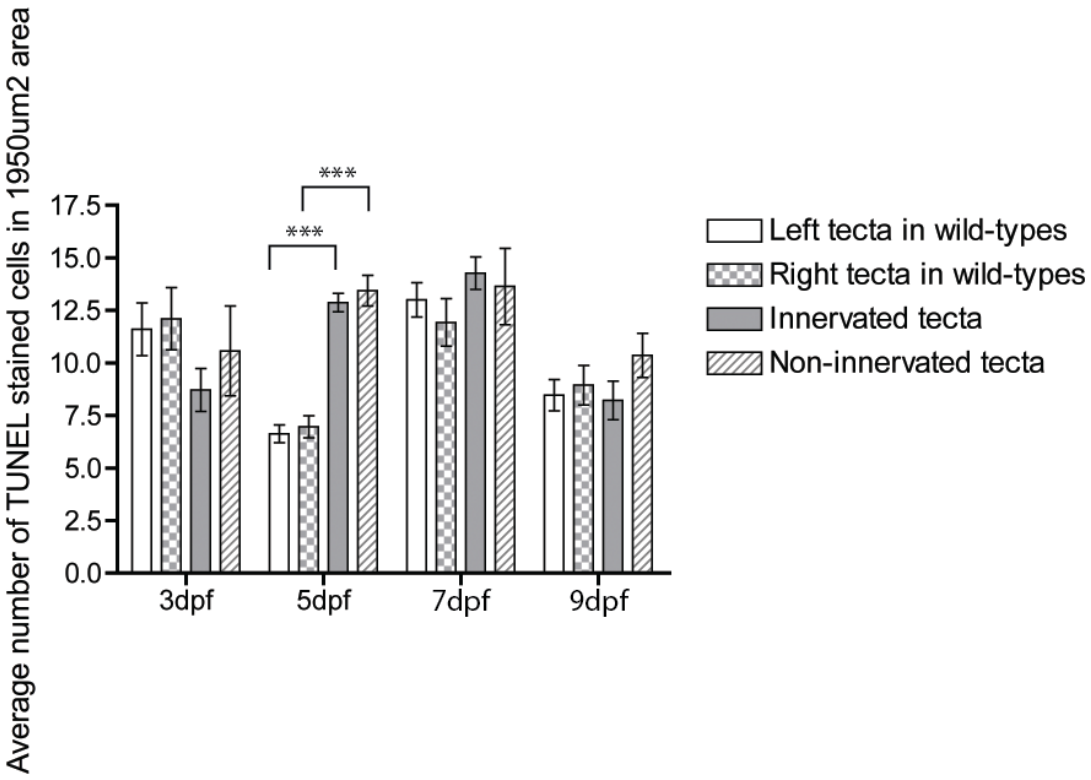

Graph 7. Cell survival in both innervated and non-innervated tecta is affected by eye removal between 24hpf and 32hpf

Graph representing the number of TUNEL cells in the left and right tecta of wild-type larvae and the innervated and non-innervated tecta of one-eyed larvae with an eye removed between 24 and 32hpf. TUNEL cells were counted in the SPV lamina, as represented by the black box in ***figure 1.6.*** Data represents the mean ± s.e.m. n = 10 (WT, 3dpf), 7 (one eye, 3dpf), 27 (WT, 5dpf), 16 (one eye, 5dpf), 14 (WT, 7dpf), 11 (one eye, 7dpf), 17 (WT, 9dpf), 15 (one eye, 9dpf). The number of TUNEL stained cells counted in each tectum were compared using a Student's t-test (paired, *$p<0.05$, **$p<0.01$, ***$p<0.001$). Only significant results are represented on the graph.

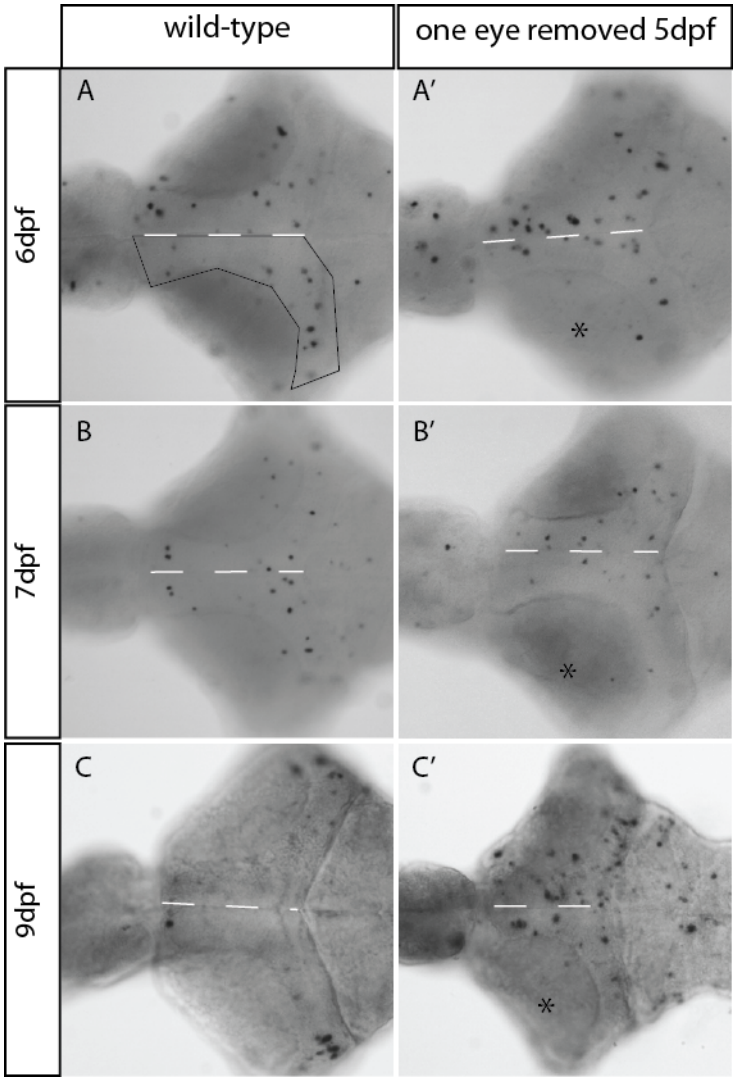

Figure 7. Eye removal at 5dpf generates increased apoptosis in the non-innervated tectum
Dorsal views of dissected brains at 9dpf from wild-type larvae **(A-C)** and larvae with the left eye surgically removed at 5dpf **(A'-C')**. Larvae have been culled at 6dpf **(A, A'),** 7dpf **(B,B'),** and 9dpf **(C, C')** and the dissected brains stained using the TUNEL assay.
(A-C) Wild-type larvae display similar numbers of apoptotic cells between the two tecta.
(A'-C') Non-innervated tecta of one-eyed larvae show more apoptotic cells in the cell body region than their innervated counterparts (with a black asterix).

The black box in **A** represents the position of the area used to count the number of apoptotic cells in each tectum.

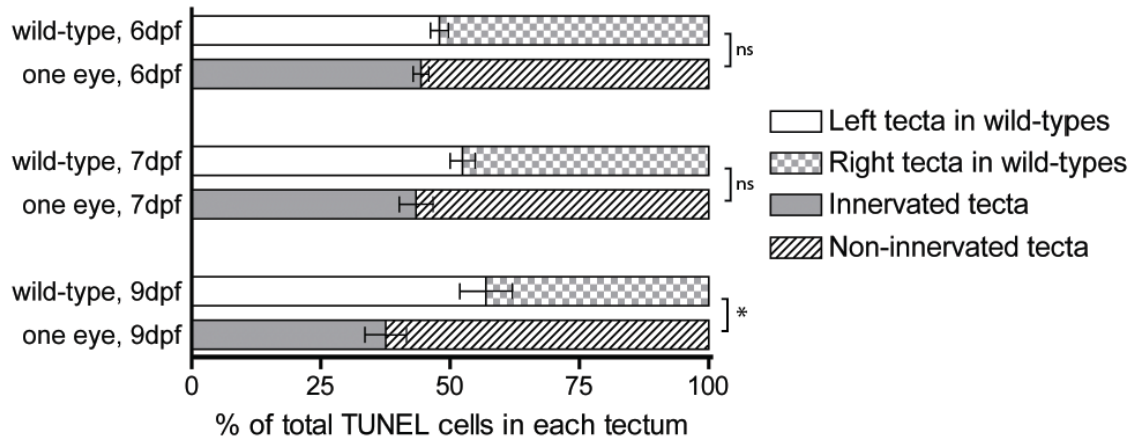

Graph 8. Eye removal at 5dpf significantly alters the number of apoptotic cells in the tectum

Graph representing the proportion of TUNEL cells in the left and right tecta of wild-type larvae and the innervated and non-innervated tecta of one-eyed larvae. TUNEL cells were counted in the SPV lamina, as represented by the black box in ***figure 1.7.*** Data represents the mean ± s.e.m. n = 17 (WT, 6dpf), 11 (one eye, 6dpf), 17 (WT, 7dpf), 10 (one eye, 7dpf), 10 (WT, 9dpf), 13 (one eye, 9dpf). The percentage of TUNEL cells in wild-type left tecta and non-innervated tecta were compared using a Student's t-test (paired, ns = not significant, *$p<0.05$, **$p<0.01$, ***$p<0.001$).

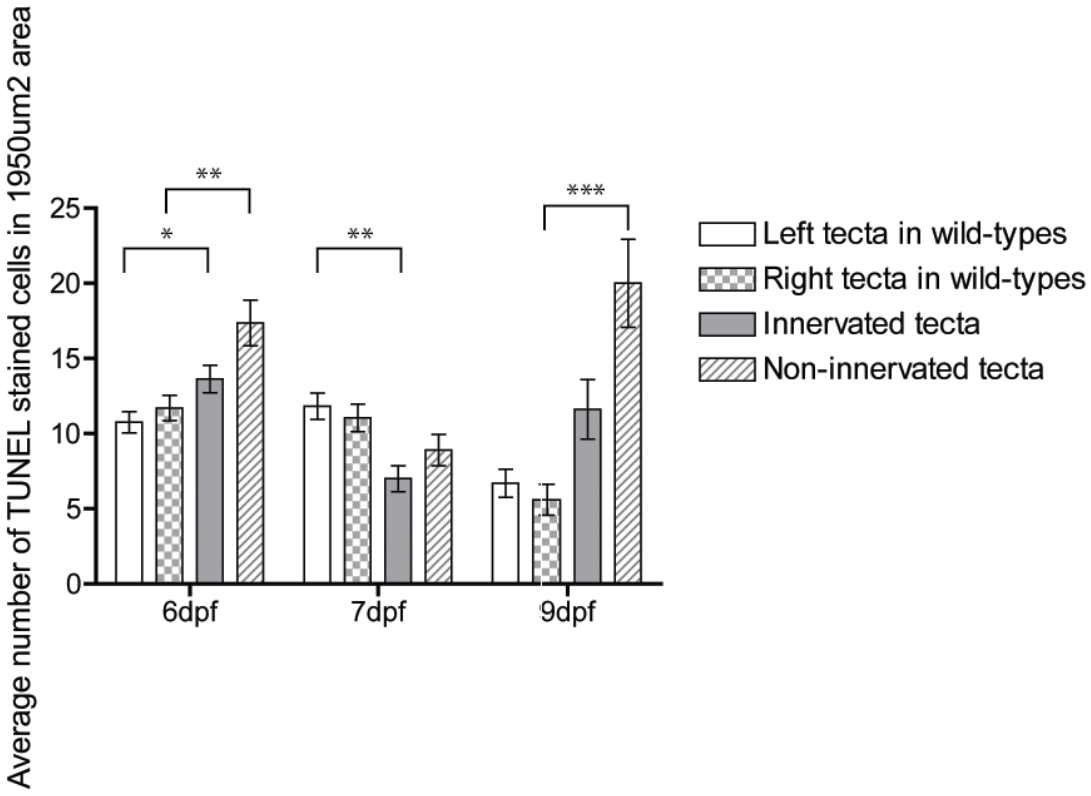

Graph 9. Cell survival in both innervated and non-innervated tecta is affected by eye removal at 5dpf

Graph representing the number of TUNEL cells in the left and right tecta of wild-type larvae and the innervated and non-innervated tecta of one-eyed larvae with an eye removed at 5dpf. TUNEL cells were counted in the SPV lamina, as represented by the black box in ***figure 1.7.*** Data represents the mean ± s.e.m. n = 17 (WT, 6dpf), 11 (one eye, 6dpf), 17 (WT, 7dpf), 10 (one eye, 7dpf), 10 (WT, 9dpf), 13 (one eye, 9dpf). The number of TUNEL stained cells counted in each tectum were compared using a Student's t-test (paired, *$p<0.05$, **$p<0.01$, ***$p<0.001$). Only significant results are represented on the graph.

innervated tecta (*Figure 6.B-E'*). We noticed that at 3dpf, there appeared to be some stained nuclei in the neuropil region of the tectum. This prompted us to look at the population of microglial cells in the optic tectum, which are present by 72hpf, but are usually excluded from the neuropil region (Herbomel et al., 2001). Larvae were stained with 2.5µg/ml neutral red for 3 hours, to label microglia cells and this revealed no change in the distribution of microglia in the optic tectum following eye removal (*Figure 6.A-A'*).

In order to quantify and compare the number of apoptotic cells in the tecta, we counted TUNEL stained cells in the tectal cell body region only, from the dorsal midline to the lateral edge (area represented by a black box in *Figure 6.B*) and then determined the proportion of such cells in the innervated tectum and non-innervated tectum (*Graph 6.*). We found that there is no significant change in the proportion of apoptotic cells between innervated and non-innervated tecta. However, when we compared the number of apoptotic cells in one eyed larval tecta and wild-type larval tecta, we noticed that both innervated ($p=0.0001$) and non-innervated ($p=0.0001$) tecta have increased TUNEL stained cells when compared to their respective wild-type tecta at 5dpf (*Graph 7*). No significant changes were found at 3dpf, 9dpf or 14dpf, which suggests that removal of retinal input affects growth of the tectum and/or larval fish specifically around the point at which larvae start to exhibit prey/capture behaviour. To explore changes in apoptosis levels further, we decided to look in wild-types with unilateral enucleation after retinal innervation of the tectum.

2.6 Eye removal at 5dpf generates increased apoptosis in the non-innervated tectum

After eye removal at 5dpf, at the onset of prey/capture behaviour, we do not notice an initial change in the distribution of apoptotic cells in the optic tectum (*Figure 7.A-B'*), but at 9dpf, we observe more apoptotic cells in the non-innervated tectum when compared to the innervated tectum (*Figure 7.C-C'*).

When we quantified the number of TUNEL stained cells in the tecta of wild-type and unilaterally enucleated larvae, we observed a gradual shift in the proportion of TUNEL cells between innervated and non-innervated tecta (*Graph 8.*). At 6dpf, the non-innervated tectum has 55.6% of the TUNEL stained cells (not significant), this increases

to 56.6% at 7dpf (not significant), and 62.5% at 9dpf (p = 0.0361). As with our results on proliferation in unilaterally enucleated larvae, this increase in apoptosis contrasts with the data from larvae enucleated between 24 and 32hpf. When we compared the number of apoptotic cells in one eyed larval tecta and wild-type larval tecta, we noticed that innervated tecta have increased TUNEL stained cells at 6dpf (p=0.0187) and decreased TUNEL stained cells at 7dpf (p=0.0013) when compared to left wild-type tecta. In addition, non-innervated tecta have increased TUNEL stained cells at both 6dpf (p=0.0016) and 9dpf (p=0.0004) when compared to right wild-type tecta (*Graph 9*). As the change in apoptosis is not consistent for innervated tecta relative to left wild-type tecta, it is difficult to interpret this result, but this could be because there is variability between the growth of wild-type and one eyed larvae.

Taken together, our data suggests that removal of retinal input leads to decreased tectal cell proliferation and decreased tectal cell survival. Furthermore, the discrepancy between removal of an eye before retinal input reaches the tectum and afterwards suggests that an initial period of innervation by RGCs is required for the retina to affect growth of the optic tectum. We next wanted to ask whether the proliferating cells we see in the non-innervated tectum survive and contribute to the growth of the optic tectum.

2.7 Cells that have proliferated in non-innervated tecta migrate away from the tectal margin (and differentiate)

As the optic tectum grows, neural stem/progenitor cells proliferate in the medial and caudal margins and cells are added to the tissue in a caudo-medial wedge (Straznicky and Gaze, 1972; Ito et al., 2010). We decided to look at the fate of proliferating cells, by swimming fish from a transgenic line that labels differentiated neurons, *Tg(elavl3:eGFP)*^{zf8}*,* for 24 hours in 0.1mM EdU at 8dpf to 9dpf, then looking at the position of EdU^+ cells in the tectum 7 days later.

At 16dpf, unlike at earlier time points (*Figure 3., Figure 4.*), the torus longitudinalis is now just below the tectal commissure and proliferating cells at the ventricular surface of the torus are now visible. The presence of proliferating cells in the torus longitudinalis masks the possible identification of any EdU^+ cells remaining at the midline in wholemount images. Nevertheless, it is clear that in both innervated and non-innervated

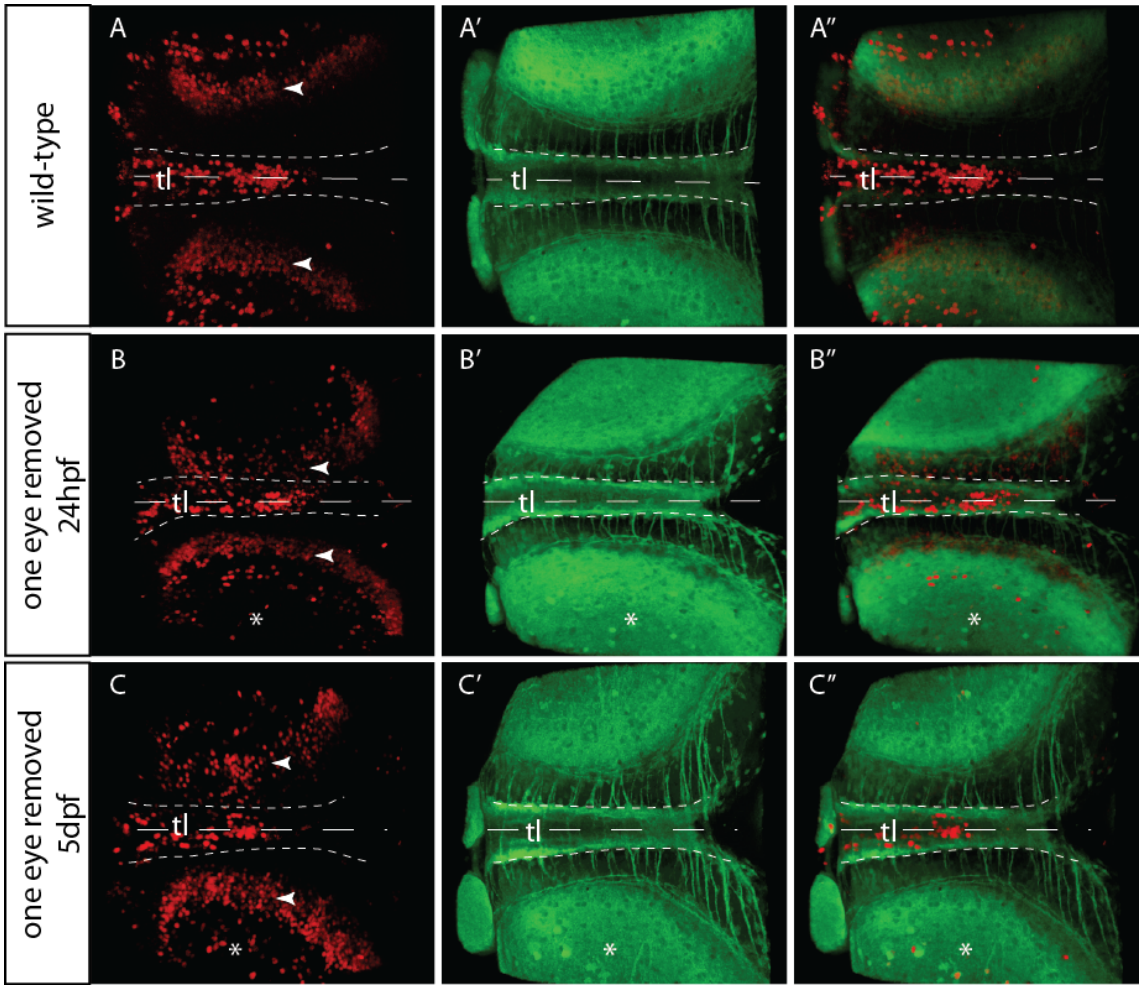

Figure 8. Cells that have proliferated in non-innervated tecta migrate away from the midline

(A-C'') 3D reconstructions of dorsal views of 16dpf dissected brains from *Tg(elavl3:GFP)* wild-type larvae **(A-A''),** larvae with the left eye surgically removed at 24hpf **(B-B'')** and larvae with the left eye surgically removed at 5dpf **(C-C'').** All larvae were swum in EdU for 24 hours from 8dpf to 9dpf, culled at 16dpf and stained for elavl3 (green) and EdU (red).

(A-A") Wild-type larvae display similar levels of EdU retention (white arrowheads) in both tecta.

(B-C") The innervated tecta (with a white asterix) of one-eyed larvae show slightly increased numbers of EdU+ cells than their corresponding non-innervated tecta. In both innervated and non-innervated tecta, the EdU positive cells (white arrowheads). migrate away from the midline Small white dashed lines either side of the midline, demarcate the torus longitudinalis (tl).

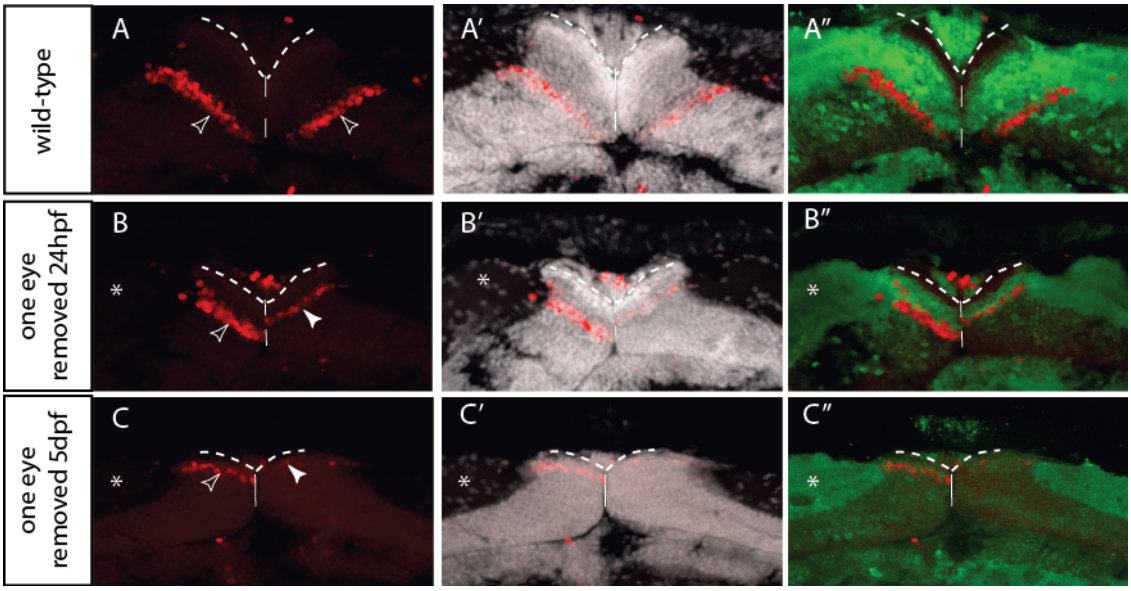

Figure 9. Proliferating cells in non-innervated tecta do not migrate as far from the margin as those in innervated tecta

(A-C'') 3D reconstructions of transverse sections through 16dpf dissected brains from *Tg(elavl3:GFP)* wild-type larvae **(A-A''),** larvae with the left eye surgically removed at 24hpf **(B-B'')** and larvae with the left eye surgically removed at 5dpf **(C-C'').** All larvae were swum in EdU for 24 hours from 8dpf to 9dpf, culled at 16dpf and stained for DAPI (grey), EdU (red) and elavl3 (green).

(A-A") Cells that incorporated EdU (clear arrowheads) migrate away from the tissue margin (dashed lines) to the same extent in the two wild-type tecta.

(B-C") Cells that incorporated EdU in the innervated tecta (clear arrowheads/with a white asterix) migrate away from the tissue margin (dashed lines) to a greater extent than EdU+ cells (white arrowheds) in the non-innervated tecta.

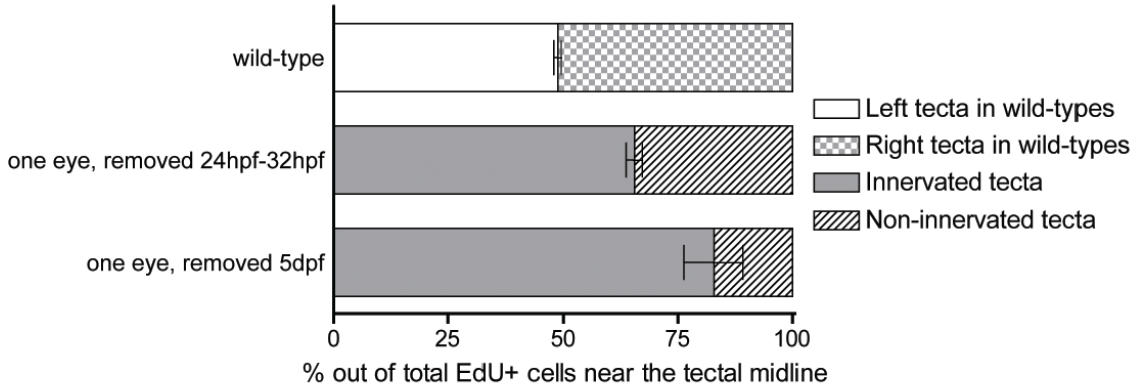

Graph 10. EdU+ cells retained in the non-innervated tectum are reduced in number after a 7 day EdU chase

Graph representing the proportion of cells retaining EdU at 16dpf in the left and right tecta of wild-type larvae and the innervated and non-innervated tecta of one-eyed larvae after removing an eye between 24hpf and 32hpf, or at 5dpf, then swimming larvae in EdU for 24 hours between 8dpf and 9dpf. EdU+ cells were counted from transverse section images, in the region close to the tectal midline, as shown in ***figure 1.9.*** Data represents the mean ± s.e.m. n = 9 (wt), 3 (1eye removed 24hpf-32hpf) and 2 (1eye removed 5dpf).

tecta, there is still a large population of EdU^+ cells remaining, and they have migrated away from the midline over the course of 7 days (*Figure 8.A-C"*). To further investigate the migration of EdU^+ cells away from the midline, we next decided to look at transverse sections (This work was carried out in collaboration with Kara Cerveny, a former post-doc in the Wilson lab, who performed the cryo-sectioning). We used *Tg(elavl3:eGFP)*^{zf8} larvae for this experiment to see whether EdU^+ cells migrate into regions containing $elavl3^+$ neurons, which would indicate that proliferating cells then differentiate and contribute to the growth of the tectum. As with wholemounts, we swum wild-type and unilaterally enucleated larvae in 0.1mM EdU for 24 hours from 8dpf to 9dpf and culled them at 16dpf. We then created 16µm transverse sections through the brain using a cryostat and stained the sections for GFP, DAPI and EdU. Co-staining the sections with DAPI showed that there are $Elavl3^-$ cells at the edge of the tectum, where cells proliferate and start to differentiate.

In transverse sections, EdU^+ cells have shifted away from this margin, with similar levels of EdU^+ migration between both wild-type tecta (*Figure 9.A-A"*). In larvae enucleated between 24hpf and 32hpf, we saw that not only have EdU^+ cells migrated away from the margin to a lesser extent in non-innervated tecta than innervated tecta, but there also appear to be less of them (*Figure 9.B-B"*). In larvae enucleated at 5dpf, there was also reduced migration of EdU^+ cells away from the margin and fewer EdU^+ cells in the non-innervated tectum (*Figure 9.C-C"*).

Due to the difficulties encountered growing unilaterally enucleated larvae up to 16dpf, we had only a few sections in which to count the number of EdU^+ cells retained in the optic tectum. With this in mind, although the *n* numbers are small, we still observed an equal ratio between the two wild-type tecta and a reduced proportion of the EdU^+ cells in the non-innervated tecta compared to the innervated tecta (*Graph 10.*).

Our results show that proliferating cells go on to contribute to the growth of the optic tectum in wild-type larvae. When retinal input is abrogated, cells still proliferate, then migrate away from the ventricular zones at the margins of the tectum and we can observe EdU^+ cells in areas of $Elavl3^+$ expression suggesting that these cells differentiate.

Figure 10. Expression of GABA synthesis and glycine transporter genes does not change in the non-innervated tectum

Dorsal views of dissected brains at 9dpf from wild-type larvae **(A-E)** and larvae with the left eye surgically removed between 24hpf and 32hpf **(A'-E').** Dissected brains have been stained for the expression of GABA synthesis genes *gad1b* **(A-B'),** and *gad2* **(C-D')** and the glycine transporter gene *slc6a5* **(E-E').**

(A-E) Wild-type larvae display similar levels of *gad1b, gad2* and *slc6a5* expression between the two tecta.

(A'-E') Non-innervated tecta of one-eyed larvae also display similar levels of *gad1b, gad2* and *slc6a5* expression to their innervated counterparts (with a white asterix).

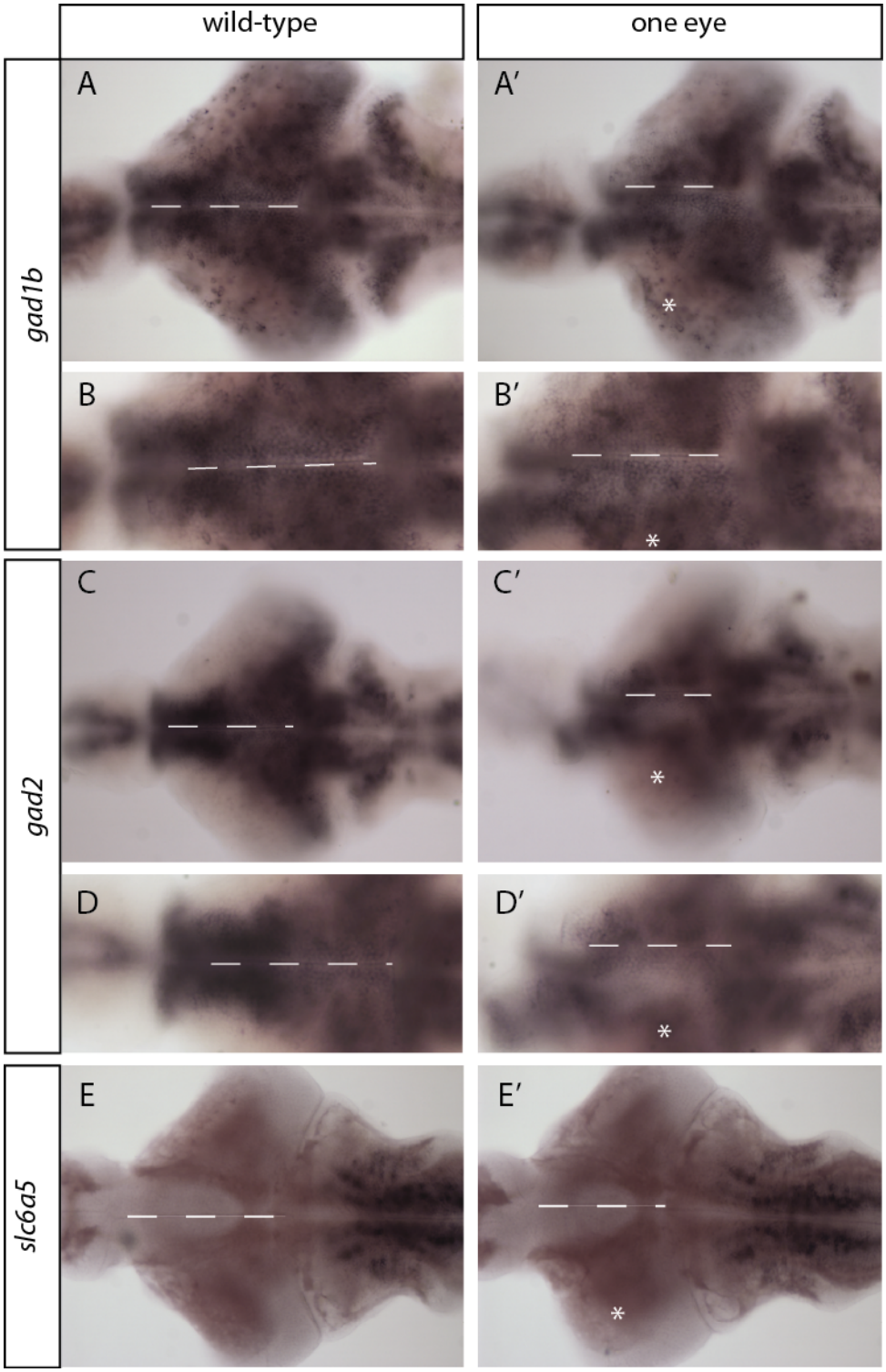
wild-type
one eye
gad1b
gad2
slc6a5
A
A′
B
B′
C
C′
D
D′
E
E′

2.8 Expression of GABA synthesis and glycine transporter genes does not obviously change in the non-innervated tectum

In the zebrafish optic tectum there are about 15 different types of neuron, which have been described anatomically using cell-tracing studies (Meek and Schellart, 1978). However, there are no current immunological or genetic methods to distinguish between these different types of tectal neuron. Instead, a simple starting point is to look at the distribution of excitatory and inhibitory neurons by *in situ* hybridization. We used markers against *glutamic acid decarboxylase 1b* and 2 (*gad1b* and *gad2,* respectively) for inhibitory GABAergic neurons, and *solute carrier family 6 member 5* (*slc6a5*) for excitatory glycinergic neurons. Probes against *gad1b* and *gad2* detect GABAergic neurons in overlapping regions within the tectum, covering both the synaptic laminae and the SPV.

We could not detect differences in the expression of markers of GABAergic neurons between wild-type and innervated/non-innervated tecta (*Figure 10.A-D'*). Also, in agreement with previous studies (Higashijima et al., 2004), we did not detect any glycinergic neurons in the optic tectum using probes against *slc6a5* (*Figure 10.E-E'*). These results suggest that there is no major change to the distribution of GABAergic or glycinergic neurons in the non-innervated tectum and so we next decided to look at the distribution of excitatory glutamatergic neurons.

2.9 Expression of the vesicular glutamate transporter *slc17a6b* is reduced in non-innervated tecta

The vesicular glutamate transporter*, solute carrier family 17, member 6b* (*slc17a6b*; sometimes referred to as *vglut2.1*), is a marker for excitatory glutamatergic neurons. In the optic tectum, *slc17a6b* is expressed in the SPV. In control conditions we did not detect a difference in its expression pattern between left and right wild-type tecta (*Figure 11.A-C*). However, when we analysed the expression of *slc17a6b* in larvae unilaterally enucleated between 24hpf and 32hpf, we found a large decrease in expression in the non-innervated tectum relative to the innervated tectum (*Figure 11.A'*). Because of expression in midbrain regions underneath the tectum, this difference is not obvious in dorsal wholemount images and therefore we decided to analyse both transverse sections of dissected brains stained as wholemounts (*Figure 11.B'*) and

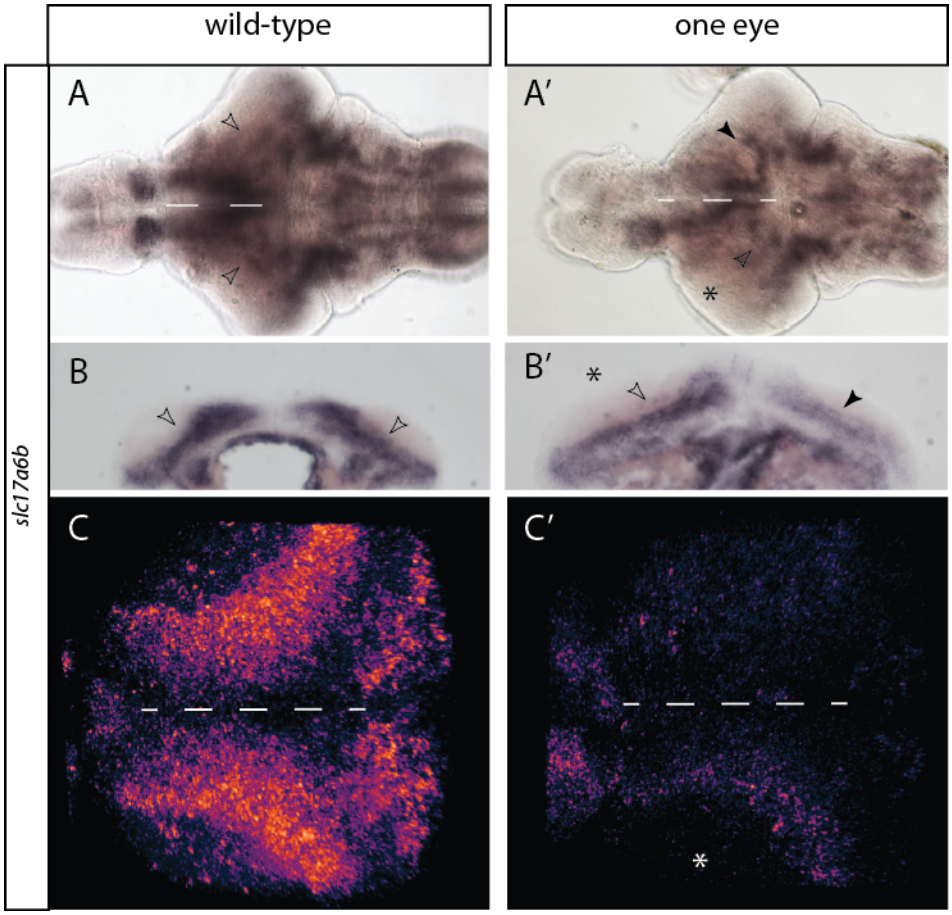

Figure 11. Expression of the vesicular glutamate transporter *slc17a6b* is reduced in non-innervated tecta

Dorsal, **(A, A'; C, C')** and transverse **(B-B')** views of dissected brains at 9dpf from wild-type larvae **(A-C)** and larvae with the left eye surgically removed between 24 and 32hpf **(A'-C').** Dissected brains have been stained for the expression of *slc17a6b*, using digoxigenin probes and either NBT/BCIP **(A-B')** or fluorescent Cy3 **(C-C')** development.

(A-C) Wild-type larvae display similar levels of *slc17a6b* expression in the SPV lamina (marked with clear arrowheads) between the two tecta.

(A'-C') Non-innervated tecta of one-eyed larvae display reduced expression of *slc17a6b* in the SPV lamina (marked with black arrowheads) compared to their innervated counterparts (with a white/black asterix, marked with clear arrowheads).

fluorescent *in situ* hybridization on wholemounts for the same marker (*Figure 11.C'*). Both of these approaches also show decreased expression of *slc17a6b* in the non-innervated tectum relative to the innervated tectum. Wholemount fluorescent labelling is weaker on both sides of the brain of unilaterally enucleated brains when compared to wild-type. This is because we stained for the same amount of time, rather than to the same level of expression and curiously, probe development often takes a shorter time in wild-types than in enucleated brains. Altogether, these results show that expression of the glutamatergic marker *slc17a6b* is reduced in non-innervated tecta, which suggests that neuronal activity within tectal neurons may be attenuated. To further investigate the affect of eye removal on the different neuronal populations within the optic tectum, we decided to analyse the distribution of calcium binding proteins in the non-innervated tectum.

2.10 Calcium-binding proteins calretinin and parvalbumin are not affected by lack of retinal innervation

Calretinin, calbindin and parvalbumin are constituents of a subset of calcium binding proteins that act as Ca^{2+} buffers, regulating internal Ca^{2+} levels (reviewed by Schwaller, 2010). These three proteins have been found to mark overlapping populations of neurons. Given that we found reduced levels of *slc17a6b* in non-innervated tecta, we decided to investigate the distribution of calretinin and parvalbumin in the optic tectum when retinal input is abrogated. We identified calretinin and parvalbumin immunopositive neurons in both the synaptic laminae and the SPV layer of the optic tectum at 9dpf.

Both proteins displayed a similar neuronal distribution between wild-type tecta (*Figure 12.A-B*) and between the innervated and non-innervated tecta of larvae enucleated between 24hpf and 32hpf (*Figure 12.A'-B'*) and at 5dpf (*Figure 12.A''-B''*). We then quantified the number of parvalbumin and calretinin positive neurons in the SPV lamina, within 60μm of the midline, and calculated the proportion of the total number in each tectum. We did not find a significant change in the distribution between wild-type tecta and between innervated and non-innervated tecta (*Graph 11.*). These results suggest that lack of innervation does not influence the distribution of calcium-binding protein-immunoreactive neurons in the optic tectum.

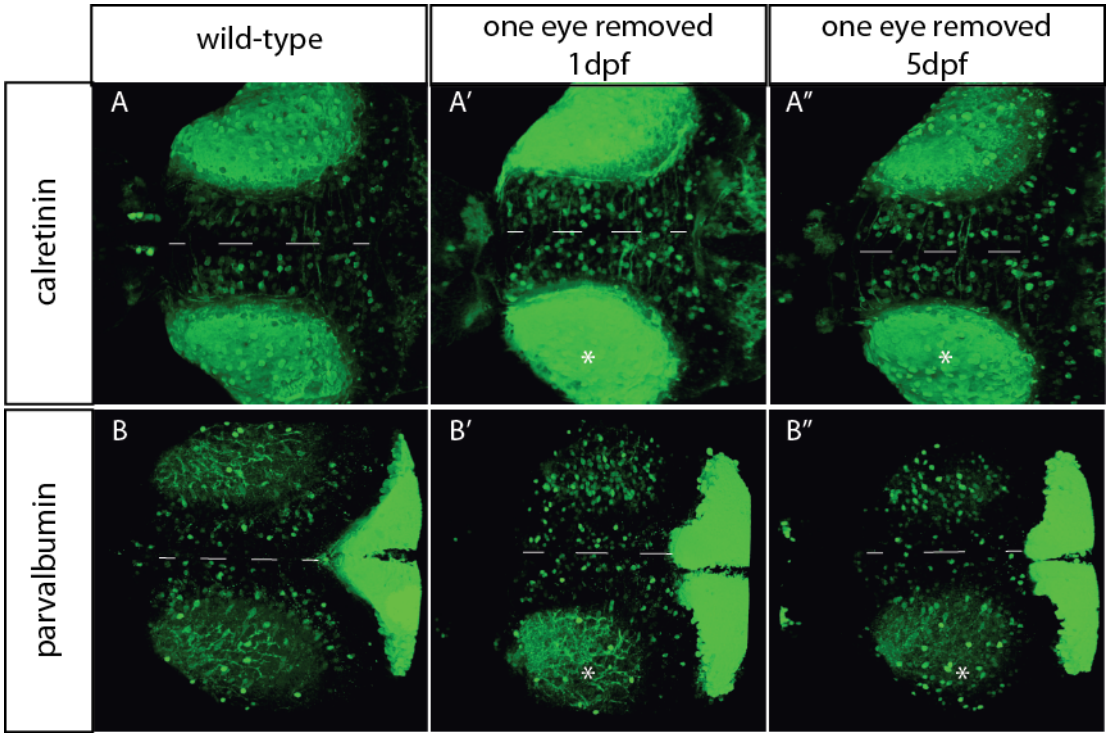

Figure 12. Calcium binding proteins Calretinin and Parvalbumin are not affected by lack of retinal innervation

3D reconstructions of dorsal views of 9dpf dissected brains in wild-type larvae **(A, B),** larvae with the left eye surgically removed between 24 and 32hpf **(A', B')** and larvae with the left eye surgically removed at 5dpf **(A"-B").** Brains were stained for the calcium binding proteins calretinin **(A-A")** and parvalbumin **(B-B").**

(A, B) Wild-type tecta display similar numbers of Calretinin and Parvalbumin positive nuclei **(A'-A"; B'-B")** Non-innervated tecta display similar numbers of Calretinin and Parvalbummin positive nuclei when compared to their innervated counterparts (with white asterisks)

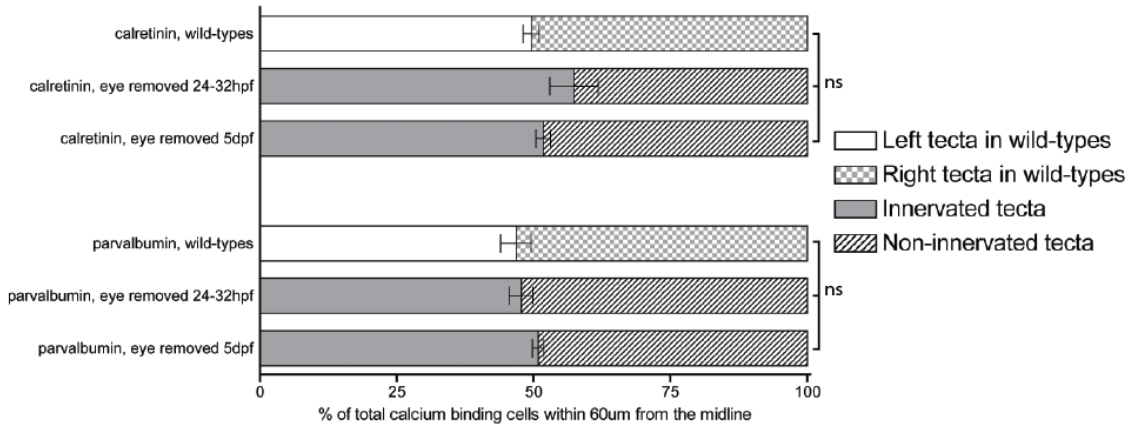

Graph 11. The distribution of Calretinin containing neurons and Parvalbumin containing neurons in tecta is not altered in the absence of retinal input

Graph representing the proportion of Calretinin containing neurons and the proportion of Parvalbumin containing neurons at 9dpf in the left and right tecta of wild-type larvae, the innervated and non-innervated tecta of larvae with the eye removed between 24 and 32hpf and the innervated and non-innervated tecta of larvae with the eye removed at 5dpf. All positive neurons were counted in the stratum periventriculare layer of each tectum, up to a distance of 60um from the midline. Data represents the mean ± s.e.m. For calretinin, n = 10 (wt), 3 (1eye 24-32hpf), 6 (1eye 5dpf). For parvalbumin, n = 7 (all larvae types). The percentage of calcium binding protein immunopositive cells in wild-type left tecta and non-innervated tecta were compared using a Student's t-test (paired, ns = not significant, *$p<0.05$, **$p<0.01$, ***$p<0.001$).

2.11 Summary

Altogether, our results demonstrate that retinal innervation regulates proliferation and differentiation in the optic tectum. We find that in *lakritz* mutants, there is reduced tectal proliferation when compared to their wild-type siblings. This result is replicated when we removed an eye from wild-type larvae at 5dpf but not when we removed an eye between 24hpf and 32hpf. Furthermore, programmed cell death, an important aspect of tissue growth regulation, is significantly increased in the non-innervated tectum after eye removal at 5dpf, but not when an eye was removed between 24hpf and 32hpf. This suggests that the disruption of retio-tectal synapses after their formation affects proliferation and survival of tectal cells. If tectal cells never receive RGC input, then growth of the tectum is not affected. By performing a 'pulse-chase' experiment with EdU, we have shown that cells proliferate and then migrate away from the margin into Elavl3^{+} regions, which suggests that the reduced numbers of proliferating cells in the non-innervated tectum still contribute to the growth of the tissue. Lastly, our results show that although the distribution of GABAergic, glycinergic and parvalbumin and calretinin containing neurons is unaffected by abrogation of retinal input into the optic tectum, there is a significant decrease in the distribution of glutamatergic neurons, with reduced expression of the *slc17a6b* marker in non-innervated tecta. The reduction in *slc17a6b* expression suggests that activity in the tectum is affected by abrogation of retinal input.

These results are discussed in more depth in Chapter 6.

Chapter 4. Results II

Analysis of differential gene expression in the optic tectum following removal of Retinal Ganglion Cell input

1. Introduction

We have shown that retinal input may be linked to the control of proliferation and cell death in the optic tectum. Alongside an observed reduction in proliferation in the non-innervated tectum when an eye was removed at 5dpf, we found that cell survival is affected, but there is no change in the expression of genes encoding important cell cycle regulators *ccnD1, cmyc* and *p57*.

To unravel genes and cell signalling pathways differentially expressed in the non-innervated tectum we used a candidate approach, analysing the expression of readouts for the Hedgehog and Wnt pathways. We also took an unbiased quantitative approach to compare RNA extracted from innervated and non-innervated midbrains by RNAseq.

2. Results

2.1 Tectal expression of Hedgehog pathway members is not obviously affected by removal of retinal innervation

Hedgehog is a conserved signalling molecule that has been implicated in a number of developmental events, including neuronal progenitor proliferation and differentiation. In *Drosophila*, the Hedgehog protein is transported along the length of retinal axons and induces terminal division, neuronal differentiation and synaptic cartridge organisation in the visual ganglia (Huang and Kunes, 1996; Huang and Kunes, 1998). In rodents, Sonic hedgehog (Shh) is transported along retinal axons and stimulates *patched* expression in astrocytes of the optic nerve (Wallace and Raff, 1999; Dakubo et al., 2003). Similarly, it has been shown that Shh drives retinal neurogenesis in teleosts (Neumann and Nuesslein-Volhard, 2000). Nevertheless, the effect of RGC-derived Shh on growth of vertebrate visual processing centres has not been examined.

Figure 1. Tectal expression of Hedgehog pathway members is unaffected by the lack of retinal innervation

Dorsal views of dissected brains at 9dpf from wild-type larvae **(A-D),** larvae with the left eye surgically removed between 24 and 32hpf **(A'-D')** and larvae with the left eye surgically removed at 5dpf **(A''-D'').** Dissected brains have been stained for the expression of hedgehog pathway members *gli1* **(A-A''),** *gli2* **(B-B''),** *ptc1* **(C-C'')** and *ptc2* **(D-D").**

(A-D) Wild-type larvae display similar levels of *gli1, gli2, ptc1* and *ptc2* expression between the two tecta.

(A'-D') Non-innervated tecta from larvae with the eye removed between 24 and 32hpf display similar levels of *gli1, gli2, ptc1* and *ptc2* expression to their innervated counterparts (with a black asterix).

(A"-D") Non-innervated tecta from larvae with the eye removed at 5dpf display similar levels *of gli1, gli2, ptc1* and *ptc2* expression to their innervated counterparts.

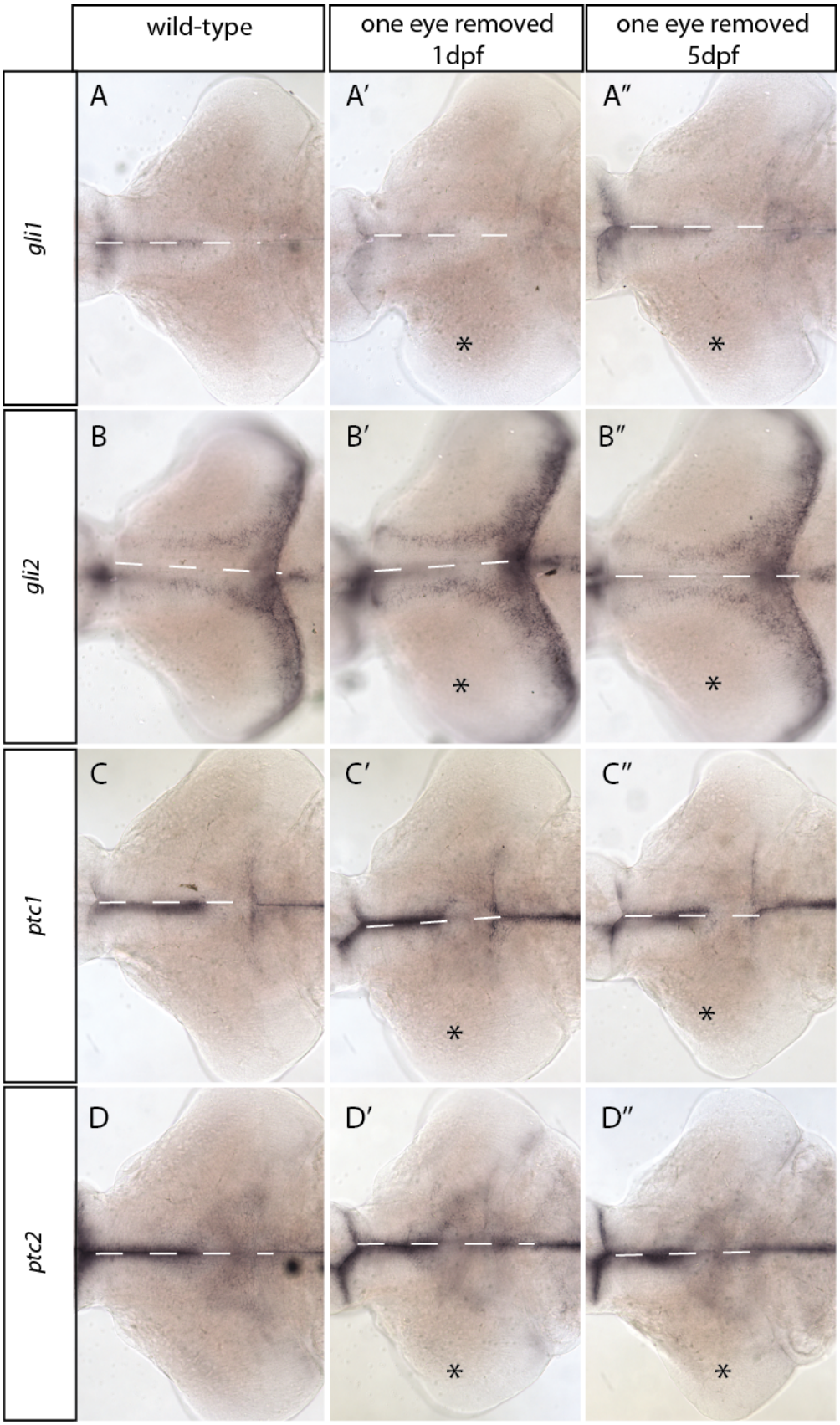
wild-type
one eye removed 1dpf
one eye removed 5dpf
gli1
gli2
ptc1
ptc2
A
A′
A″
B
B′
B″
C
C′
C″
D
D′
D″

To examine whether RGC-derived Shh might influence tectal growth, we analysed the expression of Hedgehog pathway target genes *gli1, gli2*, *patched 1* (*ptc1*) and *patched 2* (*ptc2*) in wild-type tecta and unilaterally eye enucleated tecta. These genes are targets of the Hedgehog signalling pathway and are often used as readouts of Hedgehog pathway activity. In wild-types, we found *gli1, ptc1* and *ptc2* expression in or near the tectal midline and *gli2* symmetrically expressed in both tectal neuroepithelia (*Figure 1.A-D*). In larvae unilaterally enucleated between 24hpf and 32hpf and at 5dpf, we did not detect any overt change in expression of any of these genes (*Figure 1.A'-D"*). Taken together, this data indicates that removal of RGC-derived Shh does not have a significant effect on the activity of the Hedgehog pathway in the optic tectum.

2.2 Expression of the Wnt pathway member *axin2* is downregulated in non-innervated tecta

A number of different signalling proteins have been implicated in the regulation of neurogenesis, including Wnts (Lie et al., 2005). In frogs and chicks, Wnts are expressed in the tectum and have a role in retinotectal mapping (Schmitt et al., 2006; Lim et al., 2010). In zebrafish, the Wnt transgenic reporter, *Tg(TOP:dGFP)* shows localized expression in the dorsal midbrain (Dorsky et al., 2002) and we detected expression of the gene encoding the Frizzled 10 (Fzd10) Wnt receptor in tectal neuroepithelia (*Figure 2.A-A"*), which suggested to us that the Wnt pathway might have a role in the regulation of proliferation in the optic tectum.

We analysed expression of *axin2*, a direct target of the Wnt pathway that is involved in negative feedback (Jho et al., 2002), and *lef1*, a downstream effector and target of Wnt signalling (Kengaku et al., 1998; Hovanes et al., 2001). In 9dpf wild-type larvae, *axin2* and *lef1* have similar levels of expression in both tecta (*Figure 2.B-C*). In contrast, in larvae enucleated between 24hpf and 32hpf, we observed reduced expression of *axin2* and *lef1* in the non-innervated tectum relative to the innervated tectum (*Figure 2.B'-C'*). Interestingly, in larvae enucleated at 5dpf we only observed a visible difference in the expression of *axin2* (*Figure 2.B"-C"*). Only the finding of reduced *axin2* expression in the non-innervated tectum of larvae enucleated between 24hpf and 32hpf was confirmed by qRT-PCR (see below). *axin2* transcriptional activation is targeted by Wnt pathway activity (Ota et al., 2012), therefore our results suggest that Wnt signalling is

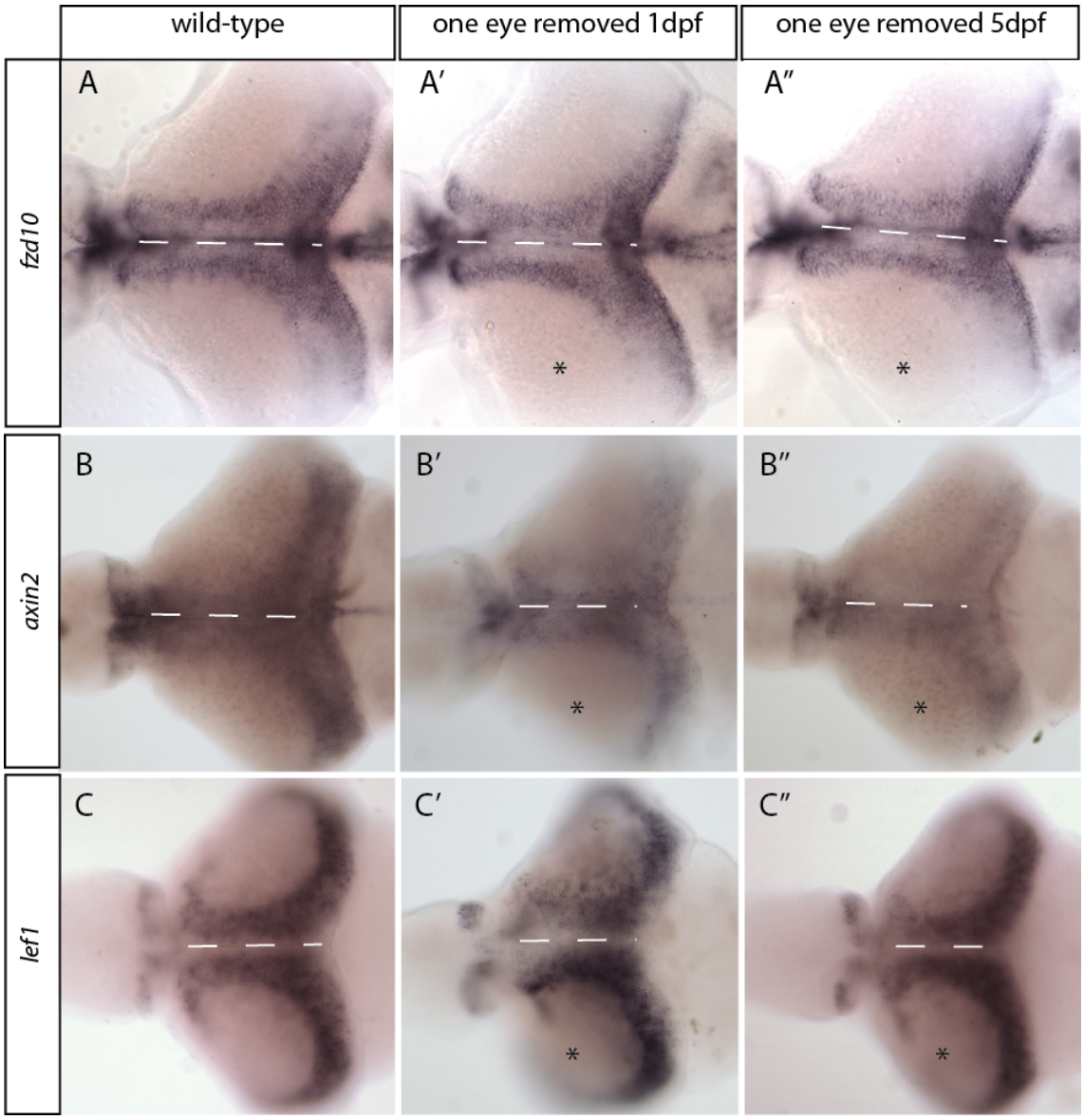

Figure 2. Expression of Wnt pathway member *axin2* is downregulated in non-innervated tecta

Dorsal views of dissected brains at 9dpf from wild-type larvae **(A-B),** larvae with the left eye surgically removed between 24 and 32hpf **(A'-B')** and larvae with the left eye surgically removed at 5dpf **(A''-B'').** Dissected brains have been stained for the expression of Wnt pathway members *axin2* **(A-A'')** and *lef1* **(B-B'').**

(A-B) Wild-type larvae display similar levels of *axin2* and *lef1* expression between the two tecta.

(A'-B') Non-innervated tecta from larvae with the eye removed between 24 and 32hpf display reduced expression of both *axin2* and *lef1* compared to their innervated counterparts (with a black asterix).

(A"-B") Non-innervated tecta from larvae with the eye removed at 5dpf display reduced expression of *axin2*, but not *lef1* compared to their innervated counterparts.

downregulated in the optic tectum upon abrogation of retinal input. To investigate this further, we next wanted to examine Wnt pathway gene expression in *lakritz* mutants.

2.3 Expression of Wnt pathway members *axin2* and *lef1* are downregulated in *lakritz* mutant tecta

We have previously shown that proliferation is reduced in the *lakritz* mutant optic tectum at 9dpf, a result that mirrors what was observed in wild-type larvae with an eye surgically removed at 5dpf. To ascertain whether Wnt pathway activity is also affected in the *lakritz* mutant tectum, we decided to assess the expression of *axin2* and *lef1* in these embryos. Similar to the larvae enucleated between 24hpf and 32hpf, we found reduced expression of both *axin2* and *lef1* in mutants compared to wild-type siblings (*Figure 3.A-B*'). Colour development in both wild-type sibling and *lakritz* mutant larvae was stopped at the same point, and a control probe, *cmyc*, showed no difference in the level of expression between larvae (data not shown). These results support our finding that retinal input affects activity of the Wnt pathway in the optic tectum.

2.4 The Wnt transgenic reporter line, *Tg(TOP:dGFP)* does not detect an obvious difference in Wnt pathway activation in the absence of retinal input

To further extend our finding that activation of the Wnt signalling pathway in the tectum is compromised in the absence of innervation from the eye, we used a well established transgenic readout of this pathway, the *Tg(TOP:dGFP)* transgene reporter. This transgenic reporter was the first zebrafish Wnt reporter line developed and consists of four TCF/Lef binding sites upstream of a minimal *cFos* promoter sequence driving expression of destabilized GFP (Dorsky et al., 2002).

When we analysed dissected *Tg(TOP:dGFP)* brains, stained with an anti-GFP antibody, we did not detect any asymmetry in the number or distribution of GFP^+ cells in wild-types (*Figure 4.A*). Surprisingly, we also did not note a change in the number or distribution of GFP^+ cells in the optic tectum when the retina was removed between 24 and 32hpf (*Figure 4.A'*), or when the retina was removed at 5dpf (*Figure 4.A''*). This result raises the possibility that activation of the Wnt pathway in the optic tectum is not affected upon abrogation of retinal input. However, it could also be that the transgene is reporting a different Wnt response in tectal cells and/or that responsiveness and

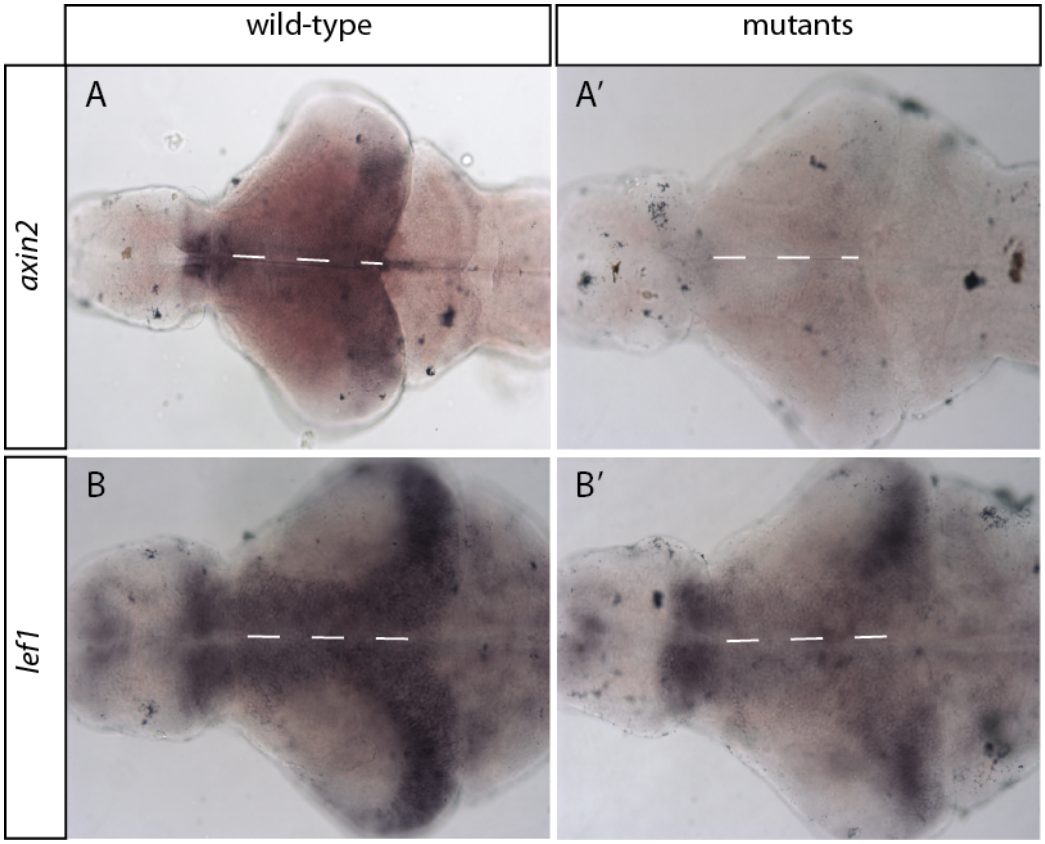

Figure 3. Expression of Wnt pathway members *axin2* and *lef1* are downregulated in *lakritz* mutant tecta

Dorsal views of dissected brains at 9dpf from wild-type sibling larvae **(A-B)** and mutant larvae **(A'-B').** Dissected brains have been stained for the expression of Wnt pathway members *axin2* **(A-A'')** and *lef1* **(B-B'').**

(A-A') Mutant larvae show reduced expression of *axin2* compared to their wild-type sibllings

(A'-B') Mutant larvae also show reduced expression of *lef1* compared to their wild-type siblings.

Small dashed lines mark the boundary between the SPV lamina and the tectal neuropil region

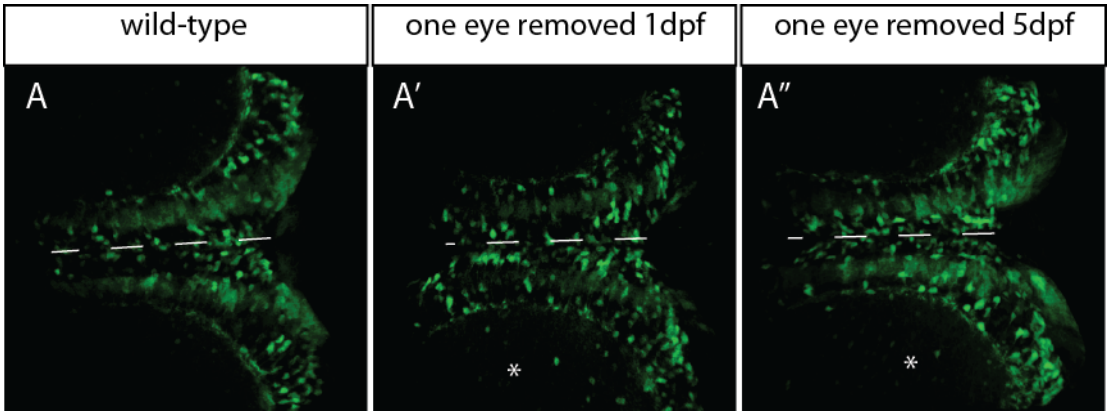

Figure 4. The Wnt transgenic reporter line, *Tg(TOP:dGFP)* does not detect a difference in Wnt pathway activation in the absence of retinal input

3D reconstructions of dorsal views of dissected brains at 9dpf from *Tg(TOP:dGFP)* wild-type larvae **(A),** larvae with the left eye surgically removed between 24 and 32hpf **(A')** and larvae with the left eye surgically removed at 5dpf **(A'').** Dissected brains have been stained with an anti-GFP antibody to detect Wnt-signalling cells.

(A-A") Wild-type and unilaterally enucleated larvae display similar numbers of Wnt activated cells in both tecta (innervated tecta in one-eyed brains are labelled with an asterisk).

sensitivity of the *Tg(TOP:dGFP)* line makes it inadequate to faithfully report variation in Wnt activity level in the optic tectum. Therefore, further confirmation is required from other Wnt activity reporters.

2.5 Extraction of RNA from dissected brains at 9dpf

To further understand how retinal input influences cell division and differentiation in the tectum, we took an unbiased approach and investigated differences in the transcriptome of innervated and non-innervated tecta. Total RNA was extracted from two sets of dissected brains at 9dpf; one set from wild-type larvae and the second set from larvae which had their left eye removed between 24hpf and 32hpf. Larvae were fixed in 4% PFA, 4% sucrose and the brains were dissected, the forebrain removed, manually cut down the midline with a microsurgical scalpel and finally cut just caudal to the midbrain-hindbrain boundary (*Figure 5.*).

From each brain used, the left and right sides of the midbrain were isolated, generating 4 different samples:

- Left midbrains from WT larvae
- Right midbrains from WT larvae
- Left (innervated) midbrains from surgically enucleated larvae
- Right (non-innervated) midbrains from surgically enucleated larvae

In order to compensate for the error introduced by manually cutting the dissected brains with a scalpel, each sample was collected from 74 larval brains. Total RNA was extracted from the samples using the RecoverAll^{TM} Total Nucleic Acid Isolation Kit for FFPE (Ambion), omitting the de-paraffinization step. Although fixation caused the formation of cross-linkages between proteins and nucleic acids in the samples, the quality of RNA produced was sufficient for RNAseq analysis, as identified using OD_{260}/OD_{280} absorption spectra and RNA Electropherograms (*Appendix 3.*).

To validate our methodology and confirm that the extracted RNA could be used to identify differentially expressed genes, we used quantitative RT-PCR (qRT-PCR) against *axin2* and *lef1*, two genes we had previously found to be downregulated in non-innervated tecta. The isolated RNA was amplified using the Whole Transcriptome Amplification 2 (WTA2) kit (Sigma-Aldrich), to generate cDNA. Gene expression was

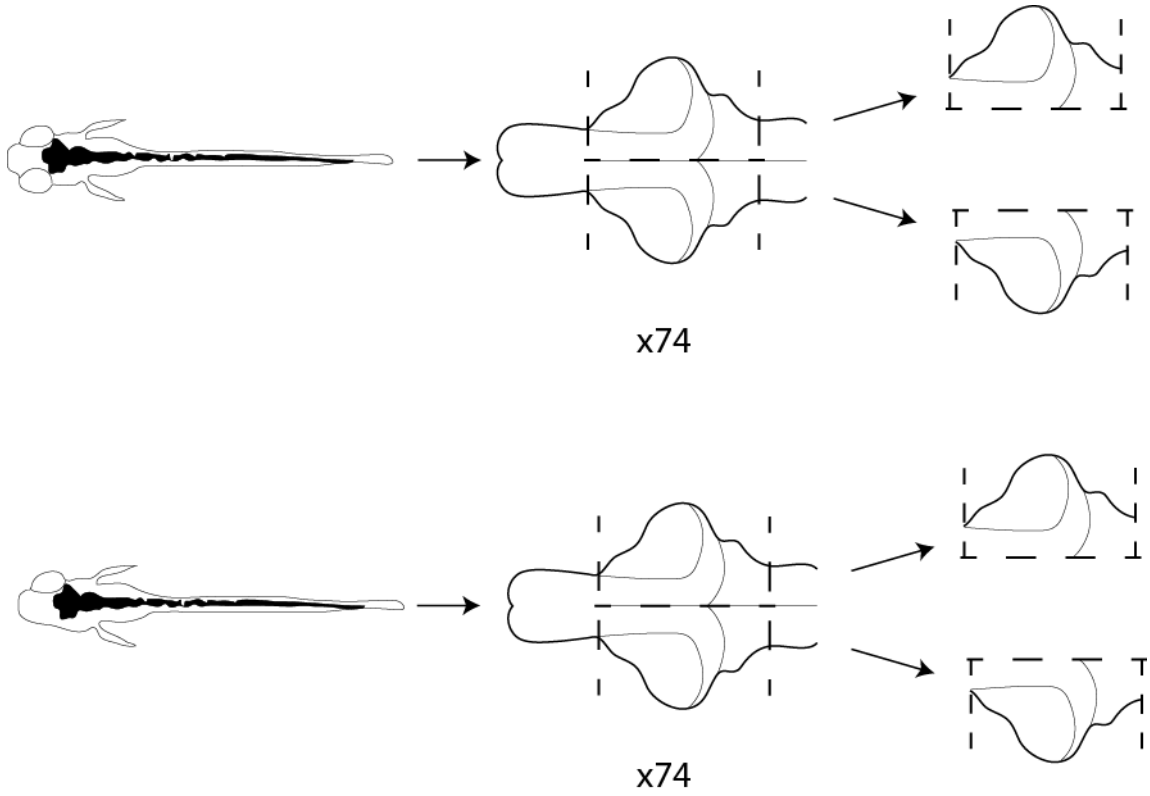

Figure 5. Extraction of RNA from dissected brains at 9dpf

Brain samples were collected from 74 zebrafish larvae at 9dpf from each of 2 groups: one group with two eyes, and the other group with one eye surgically removed between 24 to 32hpf. In each dissected brain, the forebrain was cut and removed, the left and right sides of the brain were separated down the midline and then the hindbrain was cut and removed. The incision planes are indicated by dashed lines.

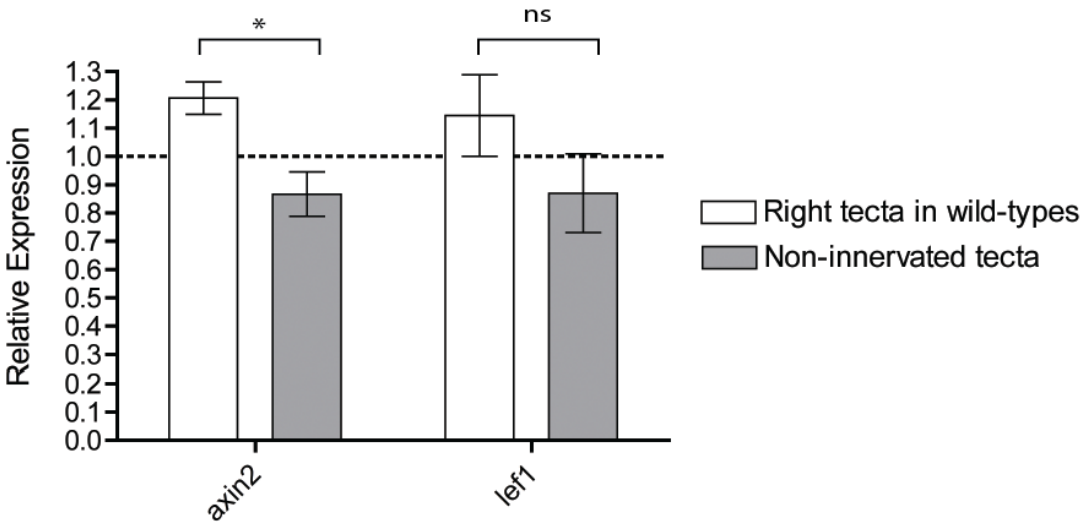

Graph 1. The decrease in *axin2* gene expression in non-innervated midbrains can be verified by qRT-PCR

qRT-PCR of *axin2* and *lef1*. Gene expression levels were measured by qPCR and normalized to the reference gene *ef1a*. Relative expression was calculated and plotted using the ΔΔC(t) method. Expression of both genes is normalized to their relative expression in the left midbrain of one-eyed or wild-type larvae. Data represents the mean ± s.e.m. from 4 biological samples, each extracted from 74 dissected midbrains.

Relative expression was compared using a Student's t-test (paired, ns = not significant, *$p<0.05$, **$p<0.01$, ***$p<0.001$).

normalized to the reference gene *ef1α* and expression in non-innervated tecta and right wild-type tecta was determined relative to expression in innervated tecta and left wild-type tecta respectively across four biological replicates.

We only found a decrease in the relative expression of *axin2* ($p = 0.0129$) in non-innervated tecta when compared to right wild-type tecta (*Graph 1.*). Differential expression of *lef1* was not significant ($p = 0.3025$), which is not surprising given that we did not detect a difference in the expression of *lef1* between innervated and non-innervated tecta of larvae unilaterally enucleated at 5dpf. This result confirms that expression of *lef1* is not affected by retinal innervation and shows that the RNA we extracted could be used to identify differentially expressed genes. We also noted that both genes show increased relative expression in right wild-type tecta, suggesting that we might have introduced some error into extracting RNA and our RNAseq results should be validated *in vivo* as well as by qRT-PCR.

2.6 Identification of differentially expressed genes by RNAseq

RNAseq libraries were prepared by Anthony Brooks (UCL Genomics), and for each of the four samples analysed, there were three biological replicates (all three were also used for qRT-PCR). 12 samples were run in a single lane on an Illumina sequencing machine and reads were aligned to the Zv9 genome using Bowtie (Kim et al., 2013), and a merged transcript dataset was assembled using the Cufflinks and Cuffmerge scripts (Trapnell et al., 2010). Differentially expressed genes were identified from all three biological replicates and the merged transcript dataset using Cuffdiff. Differentially expressed genes were only counted as significant if $q<0.05$ and $\log2(\text{Foldchange})>0.5$ or <-0.5.

The RNAseq datasets showed 183 genes with different expression between the RNA samples from left and right midbrains in wild-type larvae, 69 genes as differentially expressed between the left and right midbrain in unilaterally enucleated larvae and 76 genes as differentially expressed in both sets. Of the 69 genes differentially expressed between the left and right midbrain in unilaterally enucleated larvae, 9 were downregulated and 60 were upregulated in the non-innervated midbrain samples when compared to the innervated midbrain samples. We decided to focus on a set of genes with either a log (fold change) <-0.5 (9 genes, *Table 2.*) or a log (fold change) >1.2 (18

Gene	Log (Fold Change)	p-value	q-value
rhpn1	2.11748	0.00105	0.03345
CABZ01024428.1	1.68537	0.00015	0.00913
CASKIN2	1.54455	0.00100	0.03238
rimbp2	1.50021	0.00060	0.02352
osbp	1.48853	0.00055	0.02224
usp34	1.47566	0.00185	0.04779
bbx	1.46473	0.00170	0.04516
tcf4	1.46019	0.00070	0.02596
vdr	1.42085	0.00095	0.03143
foxn3	1.37579	0.00195	0.04935
wnk1	1.31877	0.00025	0.01309
ephb1	1.27423	0.00005	0.00406
kiaa1024	1.25539	0.00055	0.02224
lrrtm4	1.23835	0.00045	0.01959
map3k10	1.21327	0.00025	0.01309
phf15	1.21146	0.00195	0.04935
CABZ01079241.1	1.20690	0.00100	0.03238

Table 1. Upregulated genes in the non-innervated midbrain, identified by RNAseq

Genes significantly upregulated in the non-innervated midbrain, relative to the innervated midbrain in one-eyed larvae at 9dpf, as identified by RNAseq. Log (Fold change) >1.2, $q<0.05$ and the genes do not have significant changes in gene expression when comparing the wild-type right midbrain to the wild-type left midbrain (apart from *wnk1*, where the log(fold change) between the two wild-type midbrains is 1.30695).

Gene	Log (Fold Change)	p-value	q-value
cabp5b	-1.82055	0.00010	0.00686
lhx8a	-1.48706	0.00045	0.01959
si:dkey-14d8.6	-1.48209	0.00165	0.04436
apod	-1.46859	0.00015	0.00913
oxt	-1.27193	0.00005	0.04061
dlx2b	-1.20145	0.00145	0.04090
amy2a	-1.19074	0.00075	0.02708
npvf	-1.18310	0.00005	0.00406
try	-0.81648	0.00020	0.01148
si:ch73-103b2.3	-0.74094	0.00125	0.03733
calb2b	-0.73382	0.00015	0.00913
npy	-0.69467	0.00090	0.03026
pcp4a	-0.58470	0.00195	0.04935

Table 2. Downregulated genes in the non-innervated midbrain, identified by RNAseq

Genes significantly downregulated in the non-innervated midbrain, relative to the innervated midbrain in one-eyed larvae at 9dpf, as identified by RNAseq. Log(Fold change)<-0.5, q<0.05 and the genes do not have significant changes in gene expression when comparing the wild-type right midbrain to the wild-type left midbrain (apart from *lhx8a* where the log(fold change) between the two wild-type midbrains is -1.0887, *oxt* (log(fold change) of -1.22254), *dlx2b* (log(fold change) of -1.36066) and *npvf* (log(fold change) of -1.49073).

genes, *Table 1*). We also included *LIM homeobox 8a* (*lhx8a), oxytocin (oxt), distal-less homeobox 2b (dlx2b)* and *neuropeptide VF precursor (npvf)* as controls to validate the RNAseq analysis results. These genes had a log (fold change) <-1.0 in both the right tectum of wild-type larvae and the non-innervated tectum of unilaterally enucleated larae *(Table 2)*. This is intriguing because asymmetric expression has not previously been reported for any of these genes, yet our RNAseq analysis suggests that they are differentially expressed between the left and right sides of the midbrain in wild-type situations.

When we considered the differentially expressed genes in the non-innervated midbrain samples compared to the innervated midbrain samples, as identified by RNAseq, we did not notice *axin2* or *lef1*, which emphasizes the limitation of this approach in the identification of differentially expressed genes. We also did not notice multiple targets or members of a signalling pathway, which would have led us towards a mechanism for how RGC input influences growth of the optic tectum. Despite this, we did note multiple genes that are involved in calcium signalling: *calcium binding protein 5b (cabp5b)*, *calbindin 2b (calb2b)*, *purkinje cell protein 4a (pcp4a)* and *CASK interacting protein 2 (caskin2)*, which is interesting given that Ca^{2+} signalling can affect many cellular processes (reviewed by Clapham, 2007) and has been implicated in cell proliferation (Rodrigues et al., 2007).

2.7 qRT-PCR of genes upregulated in the non-innervated midbrain, as identified by RNAseq

To assess the validity of results from RNAseq analysis, we assessed differences in the levels of expression of selected number of genes by qRT-PCR. As with previous experiments, four biological replicates were used per experimental condition. Of the genes implicated as upregulated in the non-innervated midbrain by RNAseq, we did not detect significant upregulation in the relative expression of *rhophilin, Rho GTPase binding protein 1* (*rhpn1), RIMS binding proteins 2 (rimbp2), oxysterol-binding protein (osbp), transcription factor 4 (tcf4), EPH receptor B1 (ephb1), leucine rich repeat transmembrane neuronal 4 (lrrtm4)* or *mitogen-activated protein kinase kinase kinase* 10 (*map3k10)* in either non-innervated midbrain samples or right wild-type midbrain samples (*Graph 2*.). Also, although *osbp* was identified as upregulated, by qRT-PCR we

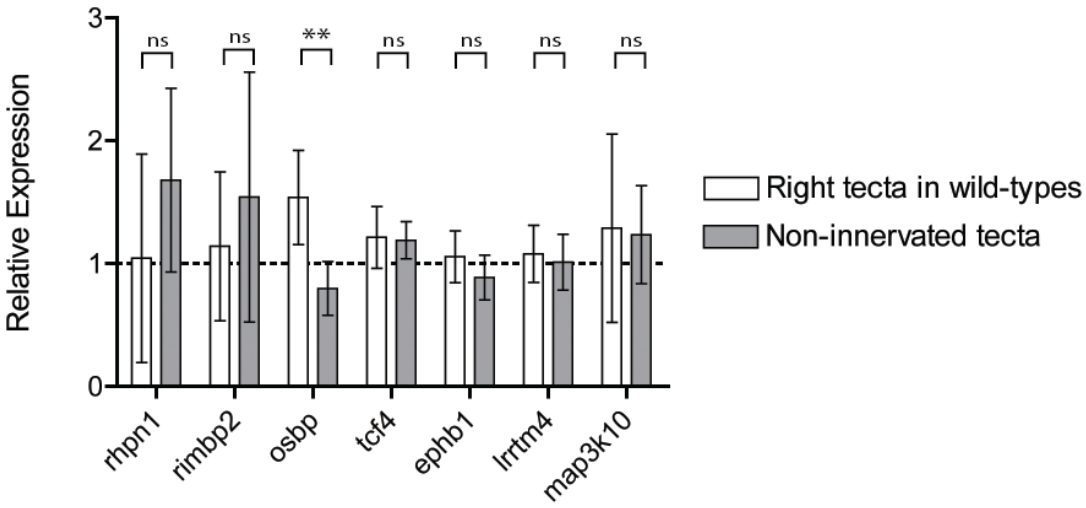

Graph 2. qRT-PCR of genes upregulated in the non-innervated midbrain, as identified by RNAseq

qRT-PCR of *rhpn1, rimbp2, osbp, tcf4, ephb1, lrrtm4* and *map3k10.* Gene expression levels were measured by qPCR and normalized to the reference gene *ef1a*. Relative expression was calculated and plotted using the ΔΔC(t) method. Expression of all genes is normalized to their relative expression in the left midbrain of one-eyed or wild-type larvae. Data represents the mean ± s.e.m. from 4 biological samples, each extracted from 74 dissected midbrains.

Relative expression was compared using a Student's t-test (paired, ns = not significant, *p<0.05, **p<0.01, ***p<0.001).

found relative expression in the non-innervated (right) midbrain to be significantly downregulated when compared to the relative expression in the right wild-type midbrain ($p = 0.0038$). We noticed a large amount of variability between the four biological replicates, which could account for why we detected these genes by RNAseq and/or why we were unable to replicate our findings with qRT-PCR. These results lead us to treat the RNAseq data with caution, as many genes do not show comparable changes when assessed by a different method.

2.8 qRT-PCR of genes downregulated in the non-innervated midbrain, as identified by RNAseq

As with the genes identified as upregulated by RNAseq, we were unable to validate the RNAseq results by qRT-PCR for various genes implicated as downregulated in the non-innervated midbrain (*Graph 3*.). We found decreased, but not significant, relative expression in non-innervated midbrain samples compared to right wild-type midbrain samples for *cabp5b*, *calb2b* and *pcp4a.* The only gene with significantly decreased relative expression in non-innervated midbrain samples when compared to right wild-type midbrain samples by both RNAseq and qRT-PCR was *si:dikey-14d8.6*, ($p = 0.0155$). However, we also detected a change in the expression of *si:dkey-14d8.6* (and *cabp5b*) in right wild-type midbrain samples relative to left wild-type midbrain samples by qRT-PCR. This difference in expression between wild-type midbrain samples was not detected in our RNAseq analysis and again suggests that some of our RNAseq results may not be authentic. *in vivo* confirmation of differential gene expression between the innervated and non-innervated midbrain will be required for each gene, before we can suggest that there is altered expression in the absence of retinal input.

qRT-PCR of *lhx8a, oxt, dlx2b* and *npvf* replicated what was found by RNAseq: all four genes had decreased relative expression in both right-sided non-innervated and right-sided wild-type midbrain samples (*Graph 3*.). *oxt* also had significantly reduced relative expression in non-innervated midbrain samples compared to right wild-type midbrain samples ($p = 0.0224$). This result suggests that these genes show a left right asymmetry in wild-type as well as experimental conditions.

In summary, we could not convincingly validate our RNAseq results for genes identified as upregulated in the non-innervated tectum, but we could for genes identified

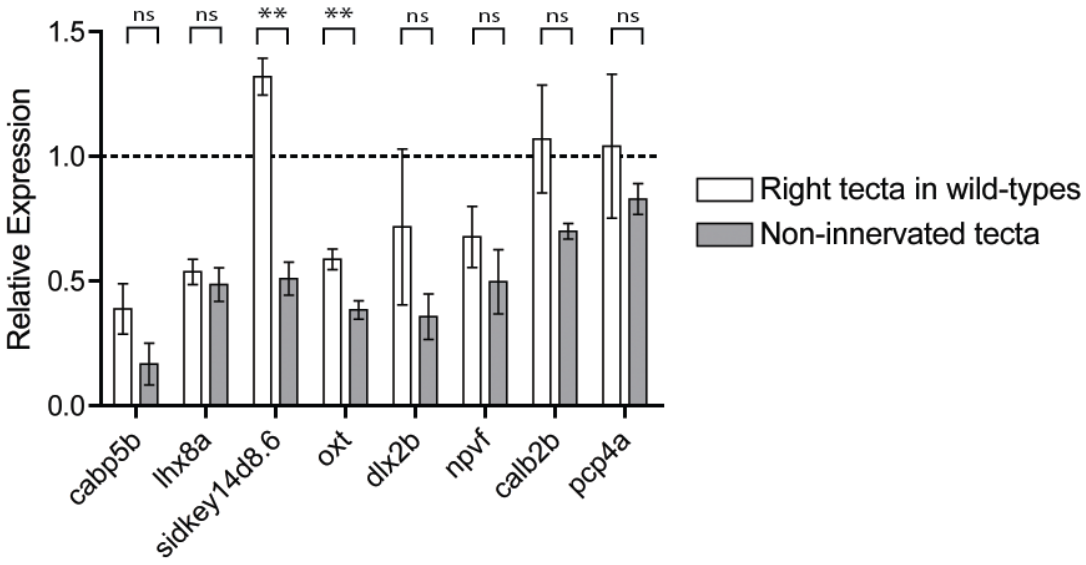

Graph 3. qRT-PCR of genes downregulated in the non-innervated midbrain, as identified by RNAseq

qRT-PCR of *cabp5b, lhx8a, si:dkey14d8.6, oxt, dlx2b, npvf* and *calb2b*. Gene expression levels were measured by qPCR and normalized to the reference gene *ef1a*. Relative expression was calculated and plotted using the ΔΔC(t) method. Expression of all genes is normalized to their relative expression in the left midbrain of one-eyed or wild-type larvae. Data represents the mean ± s.e.m. from 4 biological samples, each extracted from 74 dissected midbrains.

Relative expression was compared using a Student's t-test (paired, ns = not significant, *p<0.05, **p<0.01, ***p<0.001)

as downregulated in the non-innervated tectum and we next decided to analyse these genes *in vivo*.

2.9 Genes involved in calcium signalling are not downregulated in the non-innervated tectum

We have identified *si:dkey-14d8.6* as downregulated in non-innervated tectal samples, both by RNAseq and qRT-PCR. To understand the biological significance of this result and to confirm that *cabp5b*, *calb2b* and *pcp4a* are not downregulated we decided to probe for the expression pattern of these genes by *in situ* hybridization. As previously described (Di Donato et al., 2013) we found that *cabp5b* is expressed at a low level in the optic tectum of 9dpf wild-type embryos (*Figure 6.A-A"*). Confirming our qRT-PCR results, we also observed that the expression of *cabp5b* is not downregulated in non-innervated tecta. (*Figure 6.A'-A"*).

si:dkey-14d8.6 is expressed in the SPV layer, but has overtly symmetric expression in both wild-type and unilaterally enucleated larvae (*Figure 6.B-B"*). However, the overall high level of *in situ* hybridization signal makes it difficult to detect any subtle changes to the expression of *si:dkey-14d8.6* by wholemount analysis.

calb2b is expressed throughout the tectum and expression levels are equal in both wild-type tecta (*Figure 6.C*) and in the non-innervated tectum when the eye is removed between 24hpf and 32hpf (*Figure 6.C'*) and at 5dpf (*Figure 6.C"*).

pcp4a is symmetrically expressed in tectal synaptic laminae in wild-type embryos (*Figure 6.D*), and when the eye is removed between 24hpf and 32hpf (*Figure 6.D'*) and at 5dpf (*Figure 6.D"*).

When we analysed genes identified as downregulated in both right-sided non-innervated and right-sided wild-type samples, we observed expression close to the midline and variable expression between both left and right sides in wild-type and unilaterally enucleated larvae. This may explain why we detected these genes in our RNAseq analysis, as the RNA extraction method involved manual cutting down the midline that could have incorporated a human error for genes close to the midline if the surgical separation was not exact and more often off-centre. Or, if gene expression either side of the midline is variable, a bias to be more highly expressed on one side over the other could have been detected by our RNAseq analysis.

Figure 6. Genes involved in calcium signalling are not downregulated in the non-innervated tectum

Dorsal views of dissected brains at 9dpf from wild-type larvae **(A-D),** larvae with the left eye surgically removed between 24 and 32hpf **(A'-D')** and larvae with the left eye surgically removed at 5dpf **(A''-D'').** Dissected brains have been stained for the expression of *cabp5b* **(A-A''),** *si:dkey-14d8.6* **(B-B"),** *calb2b* **(C-C'')** and *pcp4a* **(D-D").**

(A-A") *cabp5b* is not strongly expressed in the optic tectum.

(B-B") *si:dkey-14d8.6* is expressed in the SPV lamina at simliar expression levels in both wild-type tecta and innervated and non-innervated tecta.

(C-C") Expression of *calb2b* and *pcp4a* is similar in left and right wild-type tecta, and non-innervated tecta do not have reduced expression of either gene when compared to their expression levels in innervated tecta.

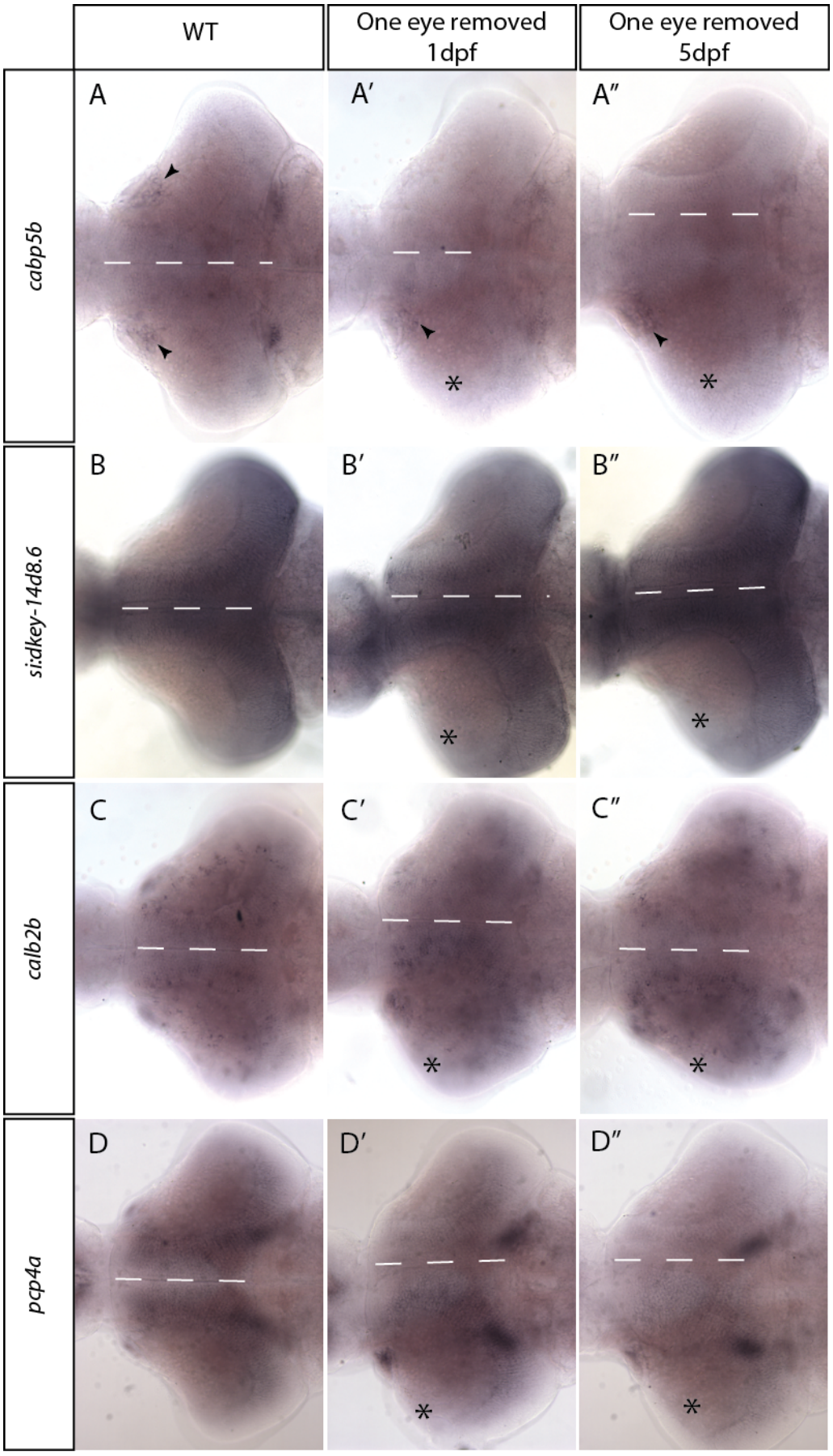
WT
One eye removed 1dpf
One eye removed 5dpf
cabp5b
si:dkey-14d8.6
calb2b
pcp4a
A
A′
A″
B
B′
B″
C
C′
C″
D
D′
D″

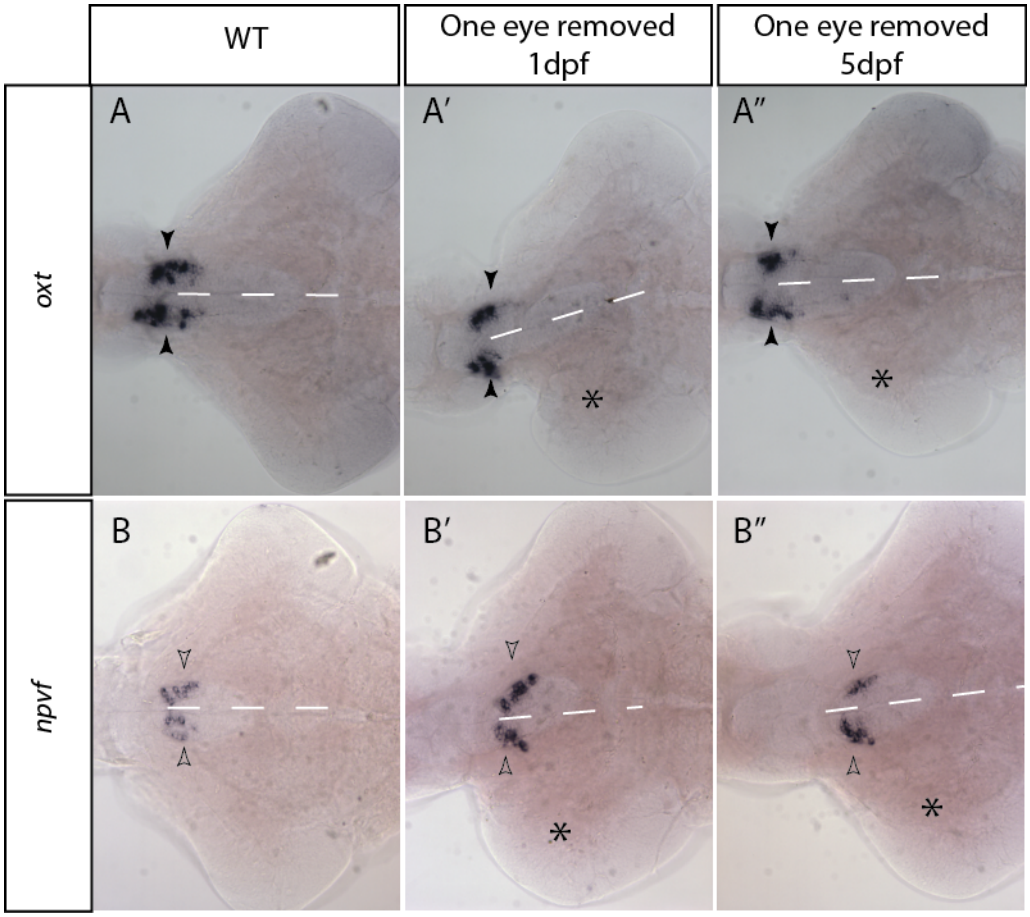

Figure 7. Genes identified as downregulated both in the right wild-type midbrain and the non-innervated midbrain show asymmetric expression patterns

Dorsal views of dissected brains at 9dpf from wild-type larvae **(A-B),** larvae with the left eye surgically removed between 24 and 32hpf **(A'-B')** and larvae with the left eye surgically removed at 5dpf **(A''-B'').** Dissected brains have been stained for the expression of *oxt* **(A-A")** and *npvf* **(B-B'').**

(A-A") *oxt* is expressed in the preoptic region (marked with full arrowheads), where the forebrain and midbrain were manually separated. Staining appears to be in variable numbers of cells either side of the midline in both wild-type and non-innervated (marked with an asterisk) brains.

(B"-B") *npvf* also appears to be in variable numbers of cells (marked with empty arrowheads) either side of the midline in both wild-type and non-innervated brains (marked with an asterisk). Expression of *npvf* is ventral to the optic tectum

oxt is expressed in the preoptic region, where we separated the midbrain from the forebrain and we found variable numbers of *oxt*-expressing cells between the two sides of the brain (*Figure 7.A-A"*). Recently, variability in the location of many different zebrafish preoptic cell types, including Oxtytocin immunoreactive cells has also been described (Herget et al., 2014), which supports our results. We could not detect a bias in *oxt* expression for one side over the other.

npvf is expressed ventrally to the tectum, with variable expression either side of the midline (*Figure 7.B-B"*). This gene has previously been described as an RFamide family member, with possible chemosensory function (Tessmar-Raible et al., 2007), although no variable expression was observed. We also could not detect a bias in *npvf* expression for one side over the other.

These results show that we were unable to use RNA we extracted from fixed tissue to identify genes that are downregulated when the eye is removed earlier in development.

2.10 Summary

Altogether, our results suggest that Wnt pathway activity in the optic tectum may be regulated by innervation from retinal ganglion cells. We find that *axin2* expression in non-innervated tecta is downregulated. However, symmetric expression of *lef1* and symmetric expression of GFP in the Wnt transgenic reporter line, *Tg(TOP:GFP)*, challenges these findings. We also developed a method to extract RNA in separated larval midbrains and through RNAseq, were able to identify downregulated expression of calcium signalling genes in midbrains with abrogated retinal input. However, these results could not be confirmed by either qRT-PCR or *in situ* hybridization.

These results are discussed in depth in Chapter 6.

Chapter 5. Results III.

A transgenic approach to assess the importance of Retinal Ganglion Cell neuronal activity on growth of the optic tectum

1. Introduction

In chapter two, we used a candidate approach and an unbiased quantitative approach to assess differential gene expression in the non-innervated tectum relative to the innervated tectum. By using a candidate approach, we found reduced expression of *axin2*, a gene involved in Wnt signalling. An important outstanding question,,is whether release of trophic, pro-growth factors from RGC axonal arbors or whether RGC neuronal activity is dominant in coordinating growth of the retina and tectm? We set out to test the importance of RGC neuronal activity in the co-ordination of growth between the retina and optic tectum.

2. Results

2.1 An intersectional strategy to activate tetanus neurotoxin expression specifically in retinal ganglion cells

To identify the mechanism by which retinal input regulates growth of the optic tectum, we generated a transgenic fish in which neurotransmission is silenced specifically in the RGC population. To silence neurons in the retinal ganglion cells, we decided to use a sequence for the light chain of the tetanus neurotoxin (TeNT-Lc), fused to EGFP (Ben Fredj et al., 2010). TeNT is a neurotoxin that prevents neurotransmission by cleaving the synaptic vesicle SNARE, synaptobrevin (also called VAMP2), preventing the association of synaptic vesicles with t-SNAREs on the pre-synaptic membrane and thus preventing the release of neurotransmitters across synaptic clefts. Fusion to EGFP has been shown to not affect TeNT-Lc proteolytic activity (Ben Fredj et al., 2010).

Transient expression of TeNT-Lc:EGFP in RGCs would not be appropriate in this context, because transient transgenics often generate a mosaic expression pattern. To see a balanced affect across multiple larvae, we needed to remove RGC synaptic activity from the entire RGC population. However, generation of a stable transgenic

with TeNT-Lc:EGFP under the control of a tissue specific promoter would be difficult, because we would expect complete lack of visual function to affect growth and behaviour. Therefore, to create a stable transgenic line, we used a conditional gain-of-function approach, whereby, under normal conditions transgenic fish would not be affected by the expression of this toxic gene. We decided to use a Cre/lox recombinase system to create a conditional gain-of-function of the tetanus neurotoxin. Cre (cyclization recombination) is a DNA recombinase that causes site-specific recombination between two *loxP* (locus of crossover of phage P1) sequences (Sauer, 1993). By placing a TeNT-Lc:EGFP sequence downstream of a *loxP*-flanked STOP sequence, TeNT-Lc:EGFP is not normally expressed and there would be no toxic affects to the fish. Only in the presence of a Cre-recombinase, is the STOP sequence excised and TeNT-Lc:EGFP expressed.

We decided to drive expression of TeNT-Lc:EGFP downstream of a loxP-dsRed2-STOP-loxP cassette, which contains dsRed2 (a red fluorescent protein) followed by multiple transcription stop sites and flanked by loxP sites. A version of this loxP cassette has previously been shown to cause expression of dsRed in the absence of Cre recombinase, with no read through to the next part of the transgene until the cassette is excised (Langenau et al., 2005). To drive loxP-dsRed2-STOP-loxP;TeNT-Lc:EGFP we decided to use the upstream promoter sequence from the *isl2b* gene, which drives expression throughout the life of the fish in RGCs as well as other neuronal populations along the anterior-posterior axis (Pittman et al., 2008). In cells where only the *isl2b* promoter is active, there should be no excision of the loxP-dsRed2-STOP-loxP cassette and cells should only express dsRed2.

Spatial specificity for the RGC population is obtained by Cre-induced expression under the control of the *atoh7* promoter, which activates gene expression in newborn RGCs, but is switched off after differentiation.

Therefore only in RGCs would Cre recombinase be expressed, where it would mediate the excision of the loxP cassette. Once the loxP cassette is excised, *isl2b* can drive expression of TeNT-Lc:EGFP throughout the life of the cell.

2.2 Generation of isl2b:loxP-dsRed-STOP-loxP:TeNT-Lc:EGFP and atoh7:cre^{nls} constructs

To generate the isl2b:loxP-dsRed-STOP-loxP:TeNT-Lc:EGFP and atoh7:cre^{nls} constructs, we used a Gateway® Three-Fragment Vector Construction kit. This kit is based on the bacteriophage lambda recombination system and it mediates site-specific recombination between different recombination sites, to construct a plasmid from three entry clones (5' clone, middle clone and 3' clone).

10kb of the upstream sequence of the *isl2b* was supplied in the 5' Gateway vector (kind gift from Chi-Bin Chien). loxP-dsRed-STOP-loxP was PCR amplified from a pCMV-Lox-dsRed2-pA-Lox-EGFP plasmid (Langenau et al., 2005) and inserted into the middle Gateway vector using a BP enzyme reaction. TeNT-Lc:EGFP was PCR amplified from a 5UAS TeNT-Lc-EGFP construct (Ben Fredj et al., 2010) and inserted into a 3' Gateway vector using a BP enzyme reaction. Both clones from the BP reaction were verified by sequencing (data not shown).

2kb of the upstream sequence from *atoh7* was PCR amplified from an *atoh7* promoter plasmid and inserted into a 5' entry vector. The *atoh7* entry vector was checked by restriction digest (data not shown). cre^{nls} was supplied in a middle entry vector (kind gift from Mario E. Sanchez Rubio, University of Chile). A polyA 3' entry Gateway plasmid was also available to use.

The three constituent entry vectors for isl2b:loxP-dsRed-STOP-loxP:TeNT-Lc:EGFP and atoh7:cre^{nls}:polyA mentioned above were recombined into a destination vector. Either side of the recombination sites were two Tol2 sequences, to enable efficient insertion of both constructs into the genome when injected in combination with Tol2 transposase (Kawakami, 2007). The atoh7:cre^{nls} destination vector also contained a *clmc2:EGFP* sequence, to activate EGFP expression in the heart and enable identification of larvae with the transgene inserted into their genome.

2.3 Generation of *Tg(isl2b:loxP-dsRed-STOP-loxP:TeNT-Lc:EGFP)* and *Tg(atoh7:cre^{nls})* transgenic lines

Two stable transgenic lines were generated: *Tg(atoh7:cre^{nls})* (*Figure 1.A*) and *Tg(isl2b:loxP-dsRed-STOP-loxP:TeNT-Lc:EGFP)* (*Figure 1.B*). We injected embryos at the one cell stage with 1nl of 25ng/µl transgene-containing plasmid and 25ng/µl Tol2

Figure 1. ***atoh7:cre*** **and** ***isl2b:loxP-dsRed-STOP-loxP:TeNT-Lc:EGFP*** **transgenes both recombine into the genome**

Schematic of the *atoh7:cre* **(A)** and isl2b:*loxP-STOP-loxP:TeNT-Lc:EGFP* **(B)** transgenes and images of agarose gels showing PCR amplification from the plasmid **(C, D)** and genomic DNA of the different transgenic lines made from the plasmids **(C'; D'-D").**

(A; C-C') *atoh7:cre* recombines into the genome of AB x Tup(LF) wild-type fish. The position of amplification within the transgene of each primer pair are indicated in **A**. The size of the products are as follows: PCR using primer pair 1 (595bp), primer pair 2 (794bp) and primer pair 3 (1085bp).

(B; D-D") isl2b:*loxP-STOP-loxP*:TeNT-Lc:EGFP recombines into the genome of AB x Tup(LF) wild-type fish. The position of amplification within the transgene of each primer pair are indicated in **B**. The size of the products are as follows: PCR using primer pair 4 (675bp), primer pair 5 (647bp), primer pair 6 (970bp) primer pair 7 (887bp) and primer pair 8 (895bp).

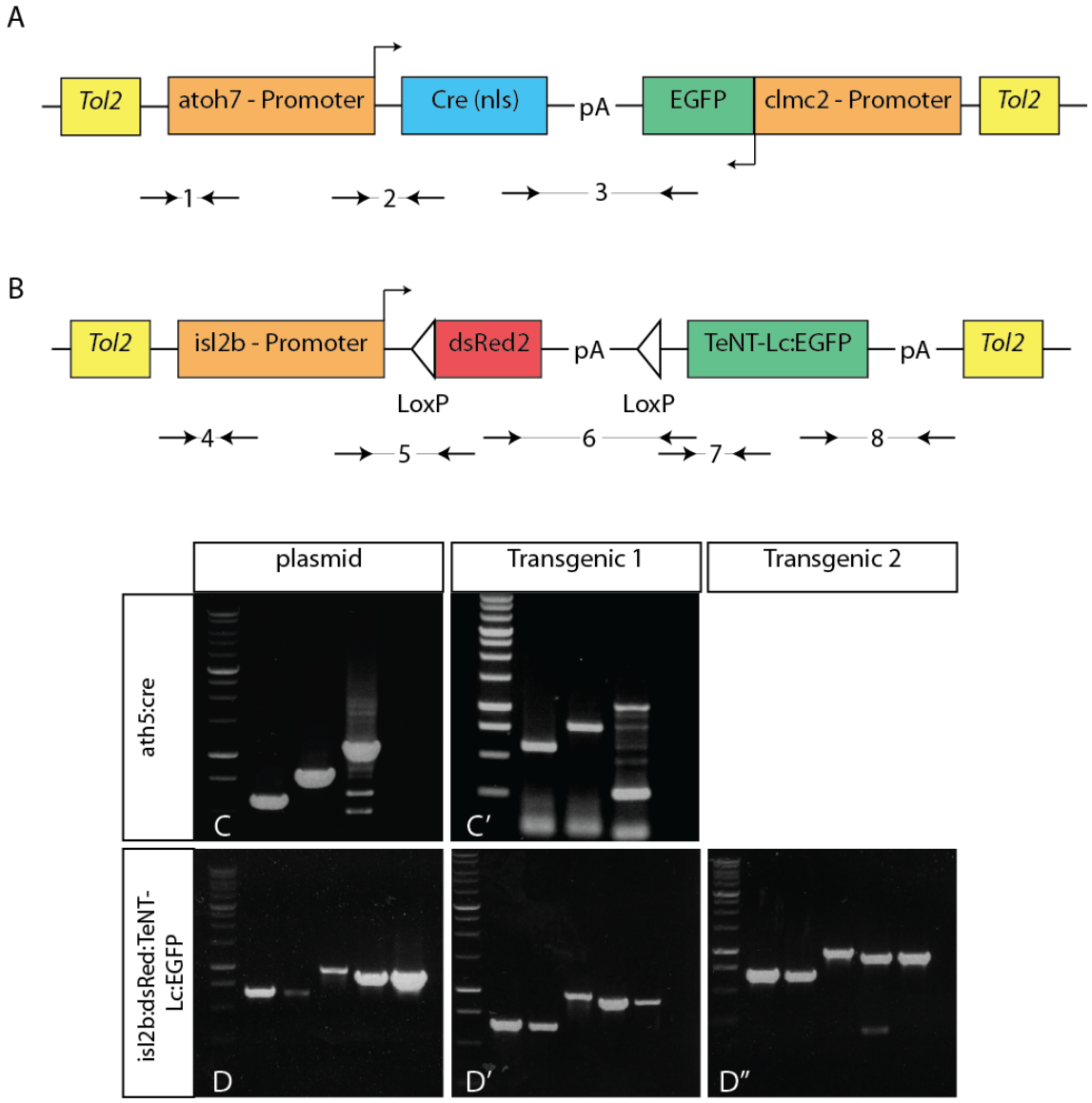
A
Tol2
atoh7 - Promoter
Cre (nls)
pA
EGFP
clmc2 - Promoter
Tol2
1
2
3
B
Tol2
isl2b - Promoter
dsRed2
pA
TeNT-Lc:EGFP
pA
Tol2
LoxP
LoxP
4
5
6
7
8
plasmid
Transgenic 1
Transgenic 2
ath5:cre
C
C′
isl2b:dsRed:TeNT-Lc:EGFP
D
D′
D″

transposase mRNA to generate 77 and 466 larvae with expression from the atoh7:cre^{nls} and isl2b:dsRed:TeNT-Lc:EGFP transgenes respectively. We grew up the larvae to adulthood and screened fish for transmission into the F1 generation.

For *Tg(atoh7:cre^{nls})*, we crossed injected adult fish to the AB wild-type line and screened for EGFP expression in the embryonic heart. Out of the fish screened, we identified one adult with *clmc:EGFP* expressing progeny, suggestive of germline recombination.

For *Tg(isl2b:loxP-dsRed-STOP-loxP:TeNT-Lc:EGFP)* we crossed injected adult fish to the AB wild-type line and screened for dsRed expression in embryos. Out of the fish screened, we identified two adults with dsRed positive progeny.

We outcrossed the F1 generation to AB wild-type fish. To verify that the two transgenes had correctly inserted into the genome and each part was present rather than just the dsRed or EGFP section, we performed PCR on finclips, using PCR primers to amplify sections within the atoh7:cre^{nls} and isl2b:dsRed:TeNT-Lc:EGFP transgenes. We confirmed that the Tg(atoh7:cre^{nls}) transgenic had the atoh7 promoter upstream of cre^{nls}, followed by the 3' end of EGFP (*Figure 1.C-C'*). We also confirmed that both the *Tg(isl2b:loxP-dsRed-STOP-loxP:TeNT-Lc:EGFP)* F1 transgenics from the two founder fish had the isl2b promoter upstream of dsRed, followed by TeNT-Lc:EGFP-pA (*Figure 1.D-D''*). These results indicate that stable insertions were successfully generated and the transgenic lines transmit through the germline. We next decided to test the activity of the Cre recombinase in our *Tg(atoh7:cre^{nls})* line.

2.4 *atoh7:cre^{nls}* transgenic larvae do no induce Cre-mediated excision of loxP cassettes

To test the enzymatic activity of Cre recombinase in the *Tg(atoh7:cre^{nls})* line, we crossed it to *Tg(-3.5ubi:loxP-GFP-loxP-mCherry)*, also termed *Tg(ubi:Switch)* (Mossimann et al., 2011). *Tg(ubi:switch)* fish express GFP under the control of a 3.5kb Ubiquitin promoter fragment in all cell types, including the retina (*Figure 2.A*). In the absence of Cre recombinase, these fish do not express mCherry (*Figure 2.A'*), but when we crossed them to *Tg(hsp:cre)* fish, which contain the *cre-recombinase* gene under the control of a heatshock promoter (Feng et al., 2007; Le et al., 2007), and heatshocked

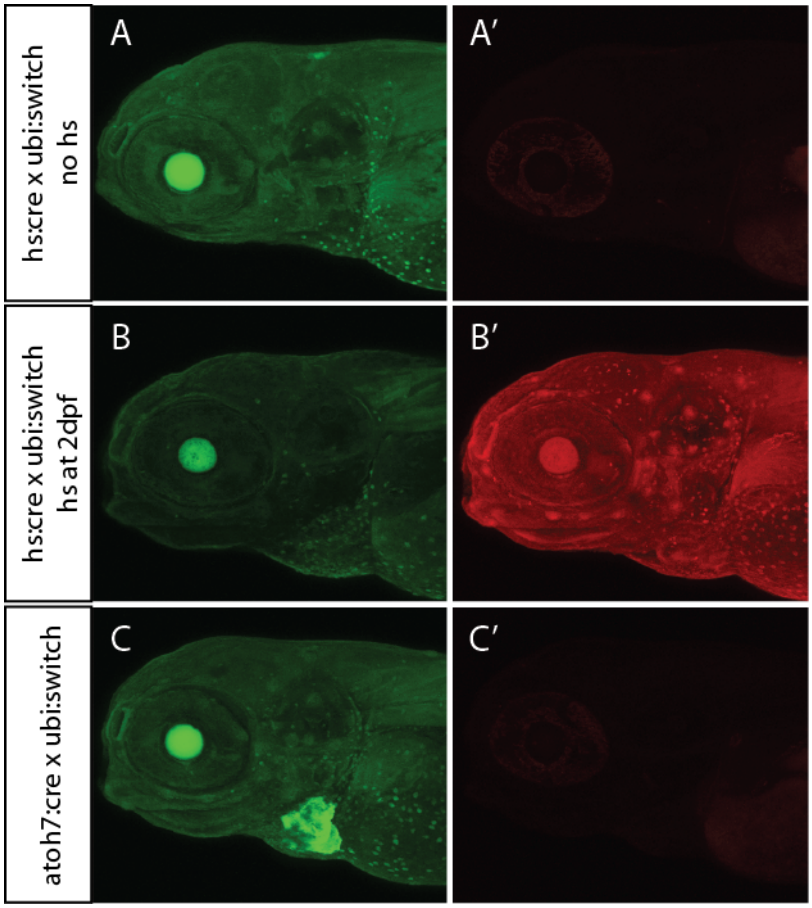

Figure 2. *atoh7:cre* transgenic larvae do not induce excision of *LoxP* cassettes

Images depict the anterior region of live *hs:cre; ubi:switch* **(A-B')** and *atoh7:cre; ubi:switch* **(C-C')** double positive zebrafish larvae at 5dpf.

(A-B') EGFP fluoresence indicates default ubi:switch expression, which is present in hs:cre; ubi:switch non-heatshocked larvae **(A-A').** Upon heatshock, mCherry expression reveals Cre-mediated loxP recombination in the ubi:switch transgene

(C-C') atoh7:cre; ubi:switch larvae (with *cmlc2:EGFP* confirming the presence of the *atoh7:cre* transgene) do not express mCherry, indicating that the *atoh7:cre* transgene does not induce loxP site recombination.

larvae at 2dpf for 40 minutes at 39°C, we observed widespread mCherry expression (*Figure 2.B-B'*).

When we crossed *Tg(atoh7:cre^{nls})* to *Tg(ubi:switch)*, we found that double positive larvae did not express mCherry in the RGCs (*Figure 2.C-C'*). This indicates that our *Tg(atoh7:cre^{nls})* line does not induce excision of loxP cassettes and therefore we cannot specifically silence neurotransmission in RGCs. This may be because there are mutations in the atoh7:cre^{nls} sequence that prevent a functional Cre enzyme from being expressed, or the sequence(s) surrounding the atoh7:cre^{nls} prevents Cre expression in retinal ganglion cells.

We next decided to analyse our two *Tg(isl2b:loxP-dsRed-STOP-loxP:TeNT-Lc:EGFP)* lines, because although we cannot specifically target RGC synapses, we should still be able to silence neurotransmission in RGCs alongside photoreceptors, trigeminal ganglia, Rohon-Beards cells, Dorsal Root Ganglia and the mesencephalic nuclei.

2.5 *isl2b:loxP-dsRed-STOP-loxP:TeNT-Lc:EGFP* transgenic larvae express dsRed in the retinal ganglion cells

To characterize the expression of the two *Tg(isl2b:loxP-dsRed-STOP-loxP:TeNT-Lc:EGFP)* lines, we stained fixed larvae at 5dpf with an antibody against dsRed and the nuclear marker DAPI (*Figure 3.A-D'*). The first line, (transgenic 1), displays an expression pattern restricted to RGCs and cranial ganglia derived neurons (*Figure 3.A-B'*). The second line, (transgenic 2), shows a wider expression pattern that is not only restricted to RGCs and cranial ganglia derived neurons, but also in the habenulae, olfactory bulb, olfactory pit and telencephalon (*Figure 3.C-D'*). This is likely due to different insertion sites of the transgene causing a wider expression pattern for transgenic 2. Nevertheless, both transgenes express dsRed in the RGCs, therefore we crossed both of the lines to various Cre recombinase expressing transgenic lines.

When we crossed both *Tg(isl2b:loxP-dsRed-STOP-loxP:TeNT-Lc:EGFP)* lines to *Tg(hsp:cre)* and heatshocked at 24hpf, 32hpf, 48hpf or 72hpf for 40 minutes at 39°C, we could not detect any EGFP expression (data not shown).

We also could not detect any EGFP expression when we crossed both *Tg(isl2b:loxP-dsRed-STOP-loxP:TeNT-Lc:EGFP)* lines to *Tg(ubi:cre^{ert2})* and treated larvae with

Figure 3. ***isl2b:loxP-dsRed-STOP-loxP:TeNT-Lc:EGFP*** **transgenic larvae express dsRed in the retinal ganglion cells**

Dorsal **(A-A'; C-C')** and lateral **(B-B'; D-D')** images of two stable *isl2b:loxP-dsRed-STOP-loxP:TeNT-Lc:EGFP* transgenic lines. dsRed expression is in red and brain morphology is visualised with the nuclear marker DAPI (blue).

(A-B') *isl2b:loxP-dsRed-STOP-loxP:TeNT-Lc:EGFP* transgenic 1 larvae express dsRed in retinal ganglion cells and cranial ganglia derived neurons

(C-D') *isl2b:loxP-dsRed-STOP-loxP:TeNT-Lc:EGFP* transgenic 2 larvae express dsRed in retinal ganglion cells, habenulae, olfactory bulb, olfactory pit, telencephalon and cranial ganglia derived neurons

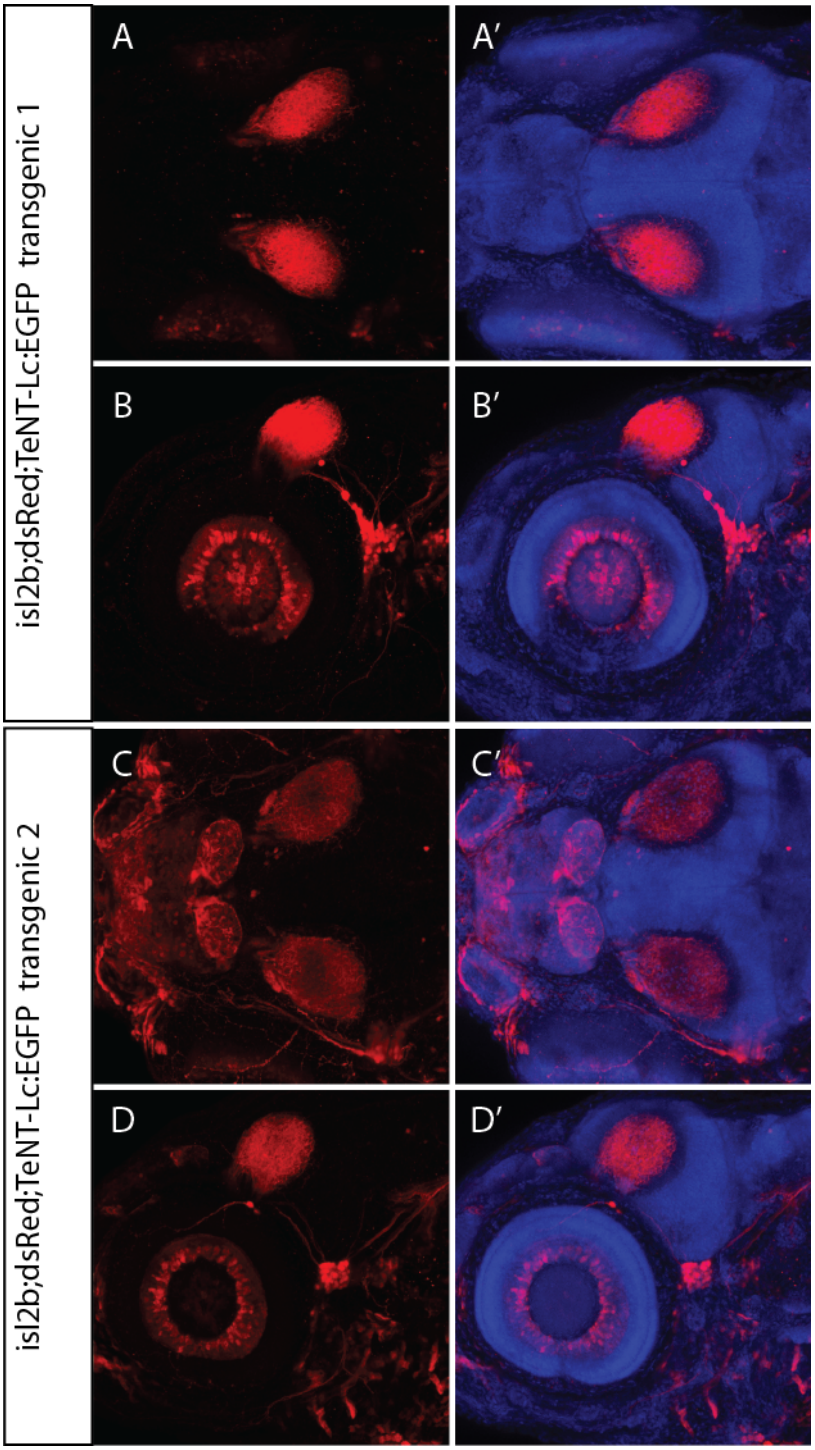
isl2b;dsRed;TeNT-Lc:EGFP transgenic 1
isl2b;dsRed;TeNT-Lc:EGFP transgenic 2
A
A′
B
B′
C
C′
D
D′

4- hydroxy-tamoxifen (4-OHT), or when we crossed both *Tg(isl2b:loxP-dsRed-STOP-loxP:TeNT-Lc:EGFP)* lines to *Tg(atoh7:cre^{nls})* (Data not shown).

We finally injected *Tg(isl2b:loxP-dsRed-STOP-loxP:TeNT-Lc:EGFP)* larvae from both lines with Cre^{nls} mRNA (provided by Masa Tada, UCL), but again could not detect any EGFP expression (Data not shown).

These results show that dsRed is expressed in RGCs in both *Tg(isl2b:loxP-dsRed-STOP-loxP:TeNT-Lc:EGFP)* lines. However, using a number of approaches, we have not been able to excise the loxP-dsRed-STOP-loxP cassette and activate TeNT-Lc:EGFP expression in RGCs. This suggests that there are either mutations in the loxP sequences that prevent recognition by Cre recombinase, or the integration site(s) prevents Cre-mediated excision of the loxP-dsRed-STOP-loxP cassette.

2.6 Summary and Discussion

In an attempt to silence neurotransmission and dissect the relationship between RGC innervation and growth of the optic tectum, we created *Tg(atoh7:cre^{nls})* and *Tg(isl2b:loxP-dsRed-STOP-loxP:TeNT-Lc:EGFP)* transgenic zebrafish. We have shown that both constructs recombined into the zebrafish genome and we identified EGFP expression in the heart of of *Tg(atoh7:cre)* F1 larvae and dsRed expression in RGCs and cranial ganglia of *Tg(isl2b:loxP-dsRed-STOP-loxP:TeNT-Lc:EGFP)* F1 larvae. Unfortunately our results show that Tg(atoh7:cre^{nls}) and both of the *Tg(isl2b:loxP-dsRed-STOP-loxP:TeNT-Lc:EGFP)* lines we created do not work as expected.

We have shown that the *Tg(atoh7:cre)* line does not generate excision of LoxP sites in *Tg(ubi:switch)* larvae. This is surprising, given that *Tg(ubi:switch)* larvae report Cre-recombinase activity when crossed to a *Tg(hsp:cre)* line. It is likely that the lack of Cre-recombinase activity in the *Tg(atoh7:cre)* line is due to either the integration site silencing expression from the *atoh7* promoter, or transgene-sequence mutations prevent a functional Cre-recombinase from being expressed.

In principle, we should be able to see red-to-green expression in *Tg(isl2b:loxP-dsRed-STOP-loxP:TeNT-Lc:EGFP)* larvae when Cre-recombinase is expressed in overlapping regions with dsRed. Although we identified dsRed expression in *Tg(isl2b:loxP-dsRed-STOP-loxP:TeNT-Lc:EGFP)* larvae, we did not detect any EGFP expression in larvae

injected with *cre* mRNA or in resultant larvae from crosses of *Tg(isl2b:loxP-dsRed-STOP-loxP:TeNT-Lc:EGFP)* to *Tg(hsp:Cre)* or *Tg(ubi:Cre^{ert2})*. These results suggest that the *LoxP-dsRed2-LoxP* cassette cannot be excised in either of the two *Tg(isl2b:loxP-dsRed-STOP-loxP:TeNT-Lc:EGFP)* integration lines that we created.

This is unexpected given that the same *LoxP-dsRed2-STOP-LoxP* cassette showed efficient excision in the presence of *cre* RNA, when used downstream of a *rag2* or *CMV* promoter (Langenau et al., 2005). It is possible that there are mutations in the LoxP sites of the *LoxP-dsRed2-LoxP* cassette, thus preventing recognition and excision of dsRed2. Another possibility is that *LoxP-dsRed2-STOP-LoxP* is excised in regions where Cre-recombinase is expressed, but sequences in the transgene prevent read-through and expression of TeNT-Lc:EGFP. However, we do not see reduced dsRed expression in larvae, which would suggest this is the case. A third possibility is that in both lines, the integration site surrounding the *isl2b:loxP-dsRed-STOP-loxP:TeNT-Lc:EGFP* transgenes prevents Cre-recombinase mediated excision of LoxP flanked sequences. This could easily be resolved by isolation of genomic DNA and sequencing to look at the surrounding genomic landscape.

Chapter 6. Discussion

1.1 Retinal input regulates proliferation in the optic tectum

In this Thesis, I have used the *atoh7* mutant *lakritz* and unilateral eye enucleations to show that retinal input regulates proliferation in the zebrafish optic tectum. Incubations with the thymidine analogue EdU revealed that fewer cells progress through the S phase of the cell cycle in wild-types with an eye surgically removed at 5pdf. However, when we performed unilateral eye enucleation between 24hpf and 32hpf, we did not observe a change in tectal cell proliferation. Comparison of proliferation in the optic tectum of larvae enculeated before and after retinal axons reach the tectum suggests that an initial period of innervation by the retina is required for tectal growth to be influenced by retinal input. However in the *lakrtiz* mutant optic tectum there is significantly reduced proliferation at 9dpf despite the retina never producing retinal ganglion cells.

A possible reason for the discrepancies could be because we only studied larvae up to 14dpf, and surgical enucleation between 24hpf and 32hpf could more severely affect the rate of larval development, as the eye is harder to remove and thus the surgical procedure is more severe than eye removal at 5dpf. Therefore we would need to extend our study into older larvae.

A second possibility is the lakritz mutants, which completely lack retinal input to the tectum, grow at a different rate to their wild-type siblings and we inadvertently compared larvae with mutants at a slightly different age, where tectal cell proliferation is reduced. This would mean that innervation prior to eye removal is indeed required for growth of the tectum to be affected by the absence of retinal input.

Our results disagree with findings from Schmatolla (1972) and Schmatolla and Erdman (1973) who used zebrafish to show that no change occurs to the number of proliferating cells in the non-innervated tectum, despite a clear increase in cell number in the innervated tectum. Instead, our results strengthen evidence of a reduced rate of tectal cell proliferation after eye removal in frogs (Eichler, 1971) and goldfish (Raymond et al., 1983). It was thought that the discrepancies between reports arose because of the different species used (Raymond et al., 1983), however our results provide evidence that regulation of tectal growth in zebrafish is similar to the regulation in frogs and goldfish.

1.2 Regulation of the cell cycle

How is a reduction in proliferating tectal cells achieved? The cell cycle is controlled by a number of cell cycle regulators, which are in turn regulated by transcriptional changes and/or post-translational modifications (Jensen et al., 2006). Indeed our initial observations report no change to the transcription of *cmyc, ccnD1* or *p57*, which suggests that either it is other cell cycle regulators that are controlled at the transcriptional level or the cell cycle is regulated by post-translational modifications. Dissection of the activation of cell cycle components will help to address this.

A second possibility is that cell cycle kinetics have been altered, resulting in a slower rate of progression through the cell cycle in the absence of retinal input. With a slower cell cycle, fewer cells progress through S phase and fewer cells exit the cell cycle over a given time period.

A third possibility is that there are fewer stem cells present in the non-innervated optic tectum. This would mean that fewer transit amplifying cells are produced over the lifetime of the fish and thus there are fewer proliferating cells in the non-innervated optic tectum.

Finally a fourth possibility is that the ratio of asymmetric to symmetric stem-cell divisions has been altered, resulting in a smaller contribution to the population of transit amplifying cells and therefore fewer total proliferating cells in the non-innervated optic tecutm.

1.3 Retinal input influences cell survival in the optic tectum

Control of tissue growth involves the regulation of both proliferation and programmed cell death (reviewed by Hipfner and Cohen, 2004). We found no significant change in cell death when the eye was removed between 24hpf and 32hpf, and a significant increase in cell death in the non-innervated tectum when the eye was removed at 5dpf. This observation could be because stable retinotectal synapses start to form between 3dpf and 7dpf, (Meyer and Smith, 2006) and it may be that their disruption affects the survival of the postsynaptic tectal cells. If this were true we would expect that after 9dpf, cell survival in the non-innervated tectum increases to the same level found in the innervated tectum, as the cells that had formed synapses with RGCs die.

A second possibility is that, as mentioned in discussion section 1.1, eye removal between 24hpf and 32hpf more severely affects the rate of larval development than eye removal at 5dpf. If this were true, we would expect to find increased apoptosis in all non-innervated tecta after 9dpf, as lack of retinal innervation starts to impact tectal cell survival.

1.4 Surgical eye removal affects proliferation and cell survival in innervated and non-innervated tecta

We noticed that when an eye was removed either between 24hpf and 32hpf or at 5dpf, proliferation and/or cell survival in both the innervated and non-innervated tecta sometimes varied to their respective tecta in larvae with two eyes. The differences identified between one-eyed and two-eyed larvae were not consistent and varied between the time-points studied. As both tecta are sometimes affected in one-eyed larvae, it could mean that the entire larval growth rate is different to the growth rate in the wild-type siblings. This could be due to an impairment in the larval ability to capture prey. To assess whether the growth rate of non-innervated larvae is dissimilar to their wild-type siblings it will be worth comparing the larval lengths at various time points.

A second possibility is that when the eye was surgically removed, the remaining eye and optic tract were adversely affected, which had a secondary affect on the innervated tectum.

A third possibility is that intra-tectal connections are affected by the lack of retinal input to one tectum, and this results in the innervated tectum being dissimilar to its respective tectum in wild-type larvae.

These observations highlight the importance of comparing not just the innervated and non-innervated tecta but also the left and right tecta in larvae with two eyes, as the innervated tectum may not be an ideal control.

1.5 Migration of cells from the ventricular surface of the optic tectum

Our observation on the migration of EdU-retaining cells away from the ventricular surface of the optic tectum supports the suggestion that proliferating cells and/or their progeny survive in non-innervated tecta and contribute to the growth of the optic tectum.

Although we stained transverse sections for the neuronal marker Elavl3 and noticed EdU^+ cells in $Elavl3^+$ regions, we cannot be certain whether proliferating cells exit the cell cycle and differentiate, because our staining did not have sufficient resolution to detect co-labelled cells. Given that extrinsic and intrinsic cues can alter the decision to generate either neuronal or glial progentiors (Tomita et al., 2000; Nieto et al., 2001), it will be interesting to expand our experiment and ask whether removal of retinal input changes the fate of proliferating cells and also whether the specification between the different types of tectal neuron is altered. Additionally, we did not investigate whether there are fewer differentiated cells in the non-innervated tectum and whether there is a decreased rate of tectal cell differentation after eye removal. We infer from a lower rate of tectal proliferation and no change to cellular survival that the non-innervated optic tectum contains fewer differentiated cells.

1.6 A marker of glutamatergic neurons is decreased when retinal innervation into the optic tectum is removed

As there at least fifteen cell types in the optic tectum, based on morphological classification (Meek and Schellart, 1978) and a diversity of neurons identified using molecular and genetic markers (Scott and Baier, 2009; Robles et al., 2011), we hypothesized that abrogation of retinal input into the optic tectum may change the composition and/or distribution of differentiated cell types in the tectum. In support of our hypothesis, analysis of the glutamatergic marker, *slc17a6b*, suggests that there are fewer glutamatergic neurons in the tectum lacking retinal afferents. However, it is also possible that the change in *slc17a6b* expression indicates a lower activity of glutamatergic neurons rather than a reduction in gluatamateric cell number.

It is interesting that we did not also detect a change in the expression of GABAergic neuron markers. Perhaps this is because GABAergic neurons are involved with processing input primarily from other tectal afferents, or that GABAergic neurons are involved in the processing of retinal input sufficiently downstream to not be affected?

We have also shown that there is no change in the distribution of parvalbumin and calretinin immunoreactive interneurons in the tecta of unilaterally eye enucleated larvae. This supports our result on the lack of change to the distribution of the GABAergic neuronal population, because parvalbumin and calretinin are mainly expressed in

GABAergic interneurons and some pyramidal neurons in the mammalian neocortex (reviewed by DeFelipe, 1997).

The optic tectum receives inputs primarily from the retina, but also from multiple telencephalic, diencephalic, mesencephalic and rhombencephalic nuclei, including but not restricted to the torus semicircularis, torus longitudinalis, nucleus pretectalis and nucleus isthmi (Meek, 1983). Anterograde and retrograde tracing techniques have determined that different tectal afferents project to dissimilar tectal lamina. It would be interesting to investigate the laminar distribution of tectal dendritic arbors after removal of retinal input and whether there is also a sensory compensation for the lack of retinal input.

1.7 Wnt pathway activity is downregulated when retinal innervation into the optic tectum is removed

One initial hypothesis was that Sonic-Hedgehog (Shh), released from RGCs, could regulate tectal cell proliferation either directly or indirectly. This was based on a number of reports in *Drosophila* and rodents that Hedgehog is transported along the optic nerve and in *Drosophila* mediates lamina neuronal differentiation (Huang and Kunes, 1996; Wallace and Raff, 1999). Despite expression of *shh* in RGCs, we did not detect obvious changes in the tectal expression of Hedgehog pathway targets *gli1, gli2, ptc1* or *ptc2*. This led us to conclude that Shh protein secretion from RGC axons terminals is not critical in the regulation of tectal cell proliferation.

We observed a decrease in *axin2* expression in the non-innervated tectum at 9dpf. This suggests that Wnt pathway activity in the optic tectum is decreased upon removal of retinal innervation, because *axin2* is a direct target of the Wnt pathway (Jho et al., 2002). We also detected reduced *lef1* expression in tecta lacking retinal innervation when an eye was removed between 24hpf and 32hpf, but not when an eye was removed at 5dpf. qRT-PCR analysis using RNA extracted from fixed, dissected brains confirmed that *axin2* expression is decreased in the non-innervated midbrain and tectal *lef1* expression is not affected following enucleation.

Since *axin2* transcription is mediated through β-catenin (Jho et al., 2002), a better readout for Wnt pathway activity would be to investigate the nuclear localization levels of β-catenin.

Our results using the *Tg(TOP:dGFP)* line do not fit easily with our finding of reduced Wnt pathway activity. It is possible that the number of cells with active Wnt signalling in the optic tectum doesn't change, rather the level of Wnt activity within them does, which we would not be able to detect using the *Tg(TOP:dGFP)* transgenic reporter line. Another reason could be that the responsiveness and sensitivity of the *Tg(TOP:dGFP)* line is insufficient to detect a difference in Wnt activity in the optic tectum. As previously reported, there are differences between Wnt reporter lines in both mice and zebrafish (Al Alam et al., 2011; Moro et al., 2012), and therefore each line does not report all sites of Wnt activation. Another zebrafish Wnt reporter line, *Tg(7xTCF-Xla.Siam:GFP)*^{ia4}, utilizes seven Tcf/Lef binding sites and reports a wider range of Wnt reporter expressing domains than detected in *Tg(TOP:dGFP)* embryos (Moro et al., 2012). Investigations into the effect of eye removal in the *Tg(7xTCF-Xla.Siam:GFP)*^{ia4} line may report differences in Wnt activity that we could not detect with the *Tg(TOP:dGFP)* line.

Is the Wnt pathway involved in retinal regulation of tectal cell proliferation? Although our observations suggest that Wnt pathway activity could be downregulated in the optic tectum upon absence of innervation, we cannot be sure as to whether the Wnt pathway is involved in the regulation of proliferation. An equally possible scenario is that decreased Wnt pathway activity simply correlates with a reduction in tectal cell proliferation. To better understand this, we would need to identify the source of Wnt signalling and use knock-down and overexpression approaches to dissect the role of the Wnt pathway in the optic tectum. In chicks and mice, *wnt3* is expressed in the dorso-ventral axis of the optic tectum and superior colliculus respectively (Schmitt et al., 2006) and previous work in our lab identified *wnt3* expression in the zebrafish optic tectum (M. Varga). Because Wnt proteins tend to act as close-range signals, (Sato et al., 2011; Strand and Micchelli, 2011) the close proximity of *wnt3* expression to the dorsal midline (M. Varga, data not shown) denotes this Wnt as a candidate for future analysis. It is also possible that other Wnt proteins are present in the optic tectum or are released from RGC axons.

1.8 *in vitro* analysis of differential gene expression between innervated and non-innervated midbrains

We do not doubt that other genes are also differentially expressed in non-innervated tecta. That we did not detect differential expression of *axin2* in our RNAseq analysis emphasizes the limitations of the approach we used. The first problem we encountered was that RNA extracted from unfixed whole larvae or separated head samples did not detect differential gene expression of *axin2* when analysed with qRT-PCR (data not shown). We believe this is because we were looking for subtle differences in gene expression, which were masked by expression across the whole organism or across the head. In order to increase the signal from genes differentially expressed in the non-innervated tectum, we decided to isolate RNA from dissected brain samples. A second problem we encountered was that there is currently no promoter with which to drive marker expression specifically in the optic tectum to enable isolation of tectal cells by Fluorescence Activated Cell Sorting (FACS).

We decided to manually separate innervated and non-innervated midbrains by separation down the midline in fixed tissue. The problem with this approach is that manual separation introduces slight variation in the position of separation between each pair of midbrains. Genes expressed closest to the midline will probably be the most susceptible to the human error involved. Furthermore, fixation is required prior to manual separation, which generates cross-links between proteins and nucleic acids and also causes some RNA degradation.

It is also worth noting that RNA was extracted not just from the optic tectum, but also neural regions ventral and caudal to the optic tectum. This is emphasized by the detection of *cabp5b* in the pretectum and *oxt* in the preoptic nuclei. Therefore it is necessary to confirm any results *in vivo,* not only to verify that the gene is differentially expressed but also to assess the pattern of expression and whether expression in the optic tectum is truly affected.

1.9 How does RGC input regulate the growth of the optic tectum in zebrafish?

Although we have not been able to silence RGC neuronal activity, analysis of RGCs that fail to transmit across neuronal synapses will likely lead to insights into the nature of the mechanism by which RGC innervation influences growth of the optic tectum.

One potential mechanism would involve the release of neurotransmitters from RGC presynaptic membranes. In the mammalian hippocampus GABA release controls the turnover of neural stem cells (Song et al., 2012; Song et al., 2013; Giachino et al., 2014) and promotes neuronal differentiation and synaptic integration (Tozuka et al., 2005; Ge et al., 2006; Jagasia et al., 2009). It has also been reported that glutamate excitation increases the fraction of proliferating cells that differentiate into neurons (Deisseroth et al., 2004), and perhaps a similar mechanism involving the release of glutamate from RGCs occurs in the optic tectum.

A second mechanism for how RGC innervation could influence growth of the optic tectum would involve secretion of growth factors from RGC axons. Studies have shown that Bone Morphogenetic Proteins, Sonic Hedgehog and Wnts can be involved in regulating neurogenesis (Ahn and Joyner, 2005; Lie et al., 2005; Ables et al., 2010; Mira et al., 2010) and one or more of these growth factors may be released from RGC axons and regulate tectal cell proliferation and/or differentiation. However, a transcriptional profile of zebrafish RGCs is currently not available which would be useful in identification of candidate growth factors for this mechanism. Also, we have shown that despite a role for RGC-derived Hh in the regulation of lamina neurogenesis in *Drosophila*, the transcription of Hedgehog pathway targets in the non-innervated zebrafish optic tectum is unchanged, which suggests that RGC-derived Sonic Hedgehog does not play a major role in the retinal regulation of growth of the optic tectum.

Given that proliferating cells located at the caudo-medial edge of the tectum are thought to have neuroepithelial characteristics, it is very unlikely that they extend processes into the synaptic laminae, which would allow RGC axons to directly contact them and thus directly control proliferation. A much more likely situation is that control of proliferation is indirect, with signalling achieved through tectal neurons and interneurons, which respond to the release of neurotransmitters or growth factors from RGC axons.

1.10 The zebrafish optic tectum as a tool for studying neural stem cells

The zebrafish optic tectum provides an important and underused resource for studying the biology of neural stem cells. Not only is the tectal stem cell niche located superficially, but the tissue also grows over the lifetime of the fish, with new cells

integrated into the tissue architecture. That the tectum incorporates these new tectal cells and new RGC input from the retina has allowed us to study how proliferation in one tissue can be moderated by a defined, external input. As more genetic and molecular tools emerge, and the cellular components of tectal circuitry are better understood, we will be able to further dissect the role of RGC innervation in the control of proliferation and differentiation in the optic tectum.

2. Future Directions

2.1 How does retinal innervation regulate the number of cells proceeding through the cell cycle?

Resolving how a reduction in proliferating cells is achieved in the non-innervated optic tectum will possibly shed light on the signalling pathways involved in regulating this process. We have shown that fewer cells are in S phase in denervated tecta but we have not resolved if other aspects of cell cycle progression are affected. Incubations with S-phase markers and subsequent staining for various cell cycle phases will ascertain whether cell cycle kinetics are affected. For example, one report used long incubations with the S-phase markers IdU and CldU, to investigate cycling patterns in the Medaka Optic tectum (Alunni et al., 2010). Another tool for investigating cell cycle kinetics is Fluorescent ubiquitin mediated cell cycle-indicator (FUCCI), which distinguishes S, G2 or M phase cells with GFP and G1 cells with a red fluorescent protein (Sakaue-Sawano et al., 2008). By performing such experiments, we may be able to obtain a better picture of the mechanistic basis for how retinal input controls proliferation and differentiation of tectal cells.

Are stem cell divisions affected in the de-innervated optic tectum? Long incubations with an S-phase marker will permit further investigations into the population of slowly-dividing cells at the periphery of the optic tectum. In addition, ‘pulse-chase’ experiments, using S-phase incubations followed by an intervening period before staining samples for differentiation markers will resolve questions regarding the fate of dividing cells. Is there a decreased rate of tectal cell differentiation? Is the proportion of dividing cells that go on to become neurons altered in the de-innervated tectum? Unfortunately due to the small catalogue of differentiation markers, these questions may

not be fully addressed until tools are developed to distinguish between the majority of tectal neuron classes.

Further understanding is also required about the survival of cells in tecta without retinal innervation. Investigations into the distribution of TUNEL cells in unilaterally eye enucleated larvae at older stages than presented here would resolve whether the significant increase in apoptotic cells identified after eye removal at 5dpf is due to the death of tectal cells that momentarily formed synapses with RGC axons.

2.2 Is the Wnt pathway involved in retinal regulation of tectal cell proliferation?

Further dissection of Wnt pathway activity in tecta without retinal innervation is required to assess whether tectal Wnt activity is reduced in the absence of retinal input. The *Tg(7xTCF-Xla.Siam:GFP)*^{ia4} Wnt reporter line will be useful to verify whether the number of Wnt responsive cells in the non-innervated tectum is changed. It will also be possible to use a number of genetic tools for inhibition or overactivation of the pathway, to assess whether altering Wnt pathway activity in the optic tectum can modify the number of proliferating cells in the tissue. In addition, it should be possible to alter either the activity of the canonical or noncanonical Wnt pathways, which will help to identify which Wnt pathway is responsible for the regulation of proliferation in the optic tectum.

Where is the source of Wnt signalling? Is Wnt3a, which is expressed near the tectal cell margin, responsible for decreased *axin2* expression in the absence of retinal innervation into the tectum? If this is not the case, might Wnt proteins be released from RGC axons? Investigations into the expression and secretion of Wnt3a may help to address this. If expression of *wnt3a* is affected by the removal of retinal input, and Wnt3a knock down leads to reduced proliferation in the optic tectum, it would suggest that Wnts are involved in retinal regulation of tectal cell proliferation.

2.3 Is calcium signalling involved in retinal regulation of tectal cell proliferation?

Although we did not find significantly altered expression of genes involved in the calcium signalling pathway in the non-innervated tectum, it would still be interesting to investigate the role of this pathway in the control of growth of the optic tectum. Previous studies in Xenopus have used PKC membrane localisation and

Ca^{2+}/calmodullin-dependent protein kinase II (CamKII) activity as readouts for Wnt-Ca^{2+} pathway activity (Sheldahl et al., 1999; Kühl et al., 2000), and both methods could be used for this study. It will also be worth investigating whether inhibition or activation of PKC and CamKII can alter proliferation in the optic tectum and therefore address whether this pathway is involved in the control of growth in the tectum.

Along with investigations into the expression of PKC, it will be worth looking at the expression of metabotropic glutamate receptor 5 (mGluR5), a G protein-coupled receptor that activates PKC through the release of intracellular Ca^{2+} and along with mGluR3, has been implicated in the regulation of stem cell proliferation and differentiation (Conn and Pin, 1997; Melchiorri et al, 2007).

2.4 Does neuronal activity promote growth of the optic tectum?

Does decreased *slc17a6b* expression in de-innervated tecta reflect the presence of fewer glutamatergic neurons? Antibodies against glutamate, as well as other neurotransmitters will be required to confirm this and to identify whether other neurotransmitter pathways are affected by the removal of retinal input. In addition, it will be interesting to analyse tectal cell proliferation in the presence of NMDA agonists and AMPA antagonists, which alter signalling through glutamate receptors.

How does RGC input regulate growth? We started to address this question with the construction of *Tg(atoh7:cre)* and *Tg(isl2b:dsRed:TeNT-Lc:EGFP)* but we were unable to use the transgenic lines to silence RGC neuronal activity. Perhaps injections of the Cre-recombinase protein into the retina of *Tg(isl2b:dsRed:TeNT-Lc:EGFP),* larvae will lead to the expression of *TeNT-Lc:EGFP* through provision of higher levels of Cre to the RGCs. This study focused on a method to express TeNT-Lc in RGCs, but it is also possible to investigate the effect of RGC neuronal activity on the optic tectum through the use of retinal tetrodotoxin (TTX) injections (Stuermer et al., 1990) and the zebrafish *macho* mutant in which RGC are unable to generate action potentials (Gnuegge et al., 2001). Both these methods have their caveats: tetrodotoxin will become distributed throughout the embryo, causing paralysis and *macho* mutant larvae are also paralysed and do not survive past 7-8 dpf. To prevent indirect affects on the optic tectum caused by paralysis of tectal neurons and other tectal afferents and to analyse the tecta of larvae

at 9dpf and beyond, it would be necessary to do either cellular or whole eye transplants from *macho* mutant embryos into wild-types.

3. Summary

Overall, the results presented in this thesis show that retinal innervation regulates tectal cell proliferation. In the absence of retinal input, either in the *lakritz* mutant or in surgically eye-enucleated larvae, tectal cell proliferation is reduced. We have shown that retinal innervation also affects cell survival and that proliferating cells migrate away from the ventricular surface, towards regions of differentiated cells Our data also suggests that retinal innervation regulates the distribution of differentiated cells in the optic tectum, as tectal expression of the glutamatergic marker, *slc17a6b,* is decreased after unilateral eye removal. However, we still do not know how retinal ganglion cell innervation regulates tectal cell proliferation and differentiation and there are many questions still to be addressed.

To determine which genes and signalling pathways are involved in input-dependent growth of the tectum, we investigated differential gene expression in the non-innervated tectum compared to the innervated tectum. We have shown that expression of the Wnt pathway component *axin2* is downregulated in the non-innervated tectum. This suggests that Wnt signalling may be involved in the retinal regulation of optic tectum proliferation and/or differentiation, but detailed examination of this pathway will be required to resolve its role in controlling these processes.

Appendix

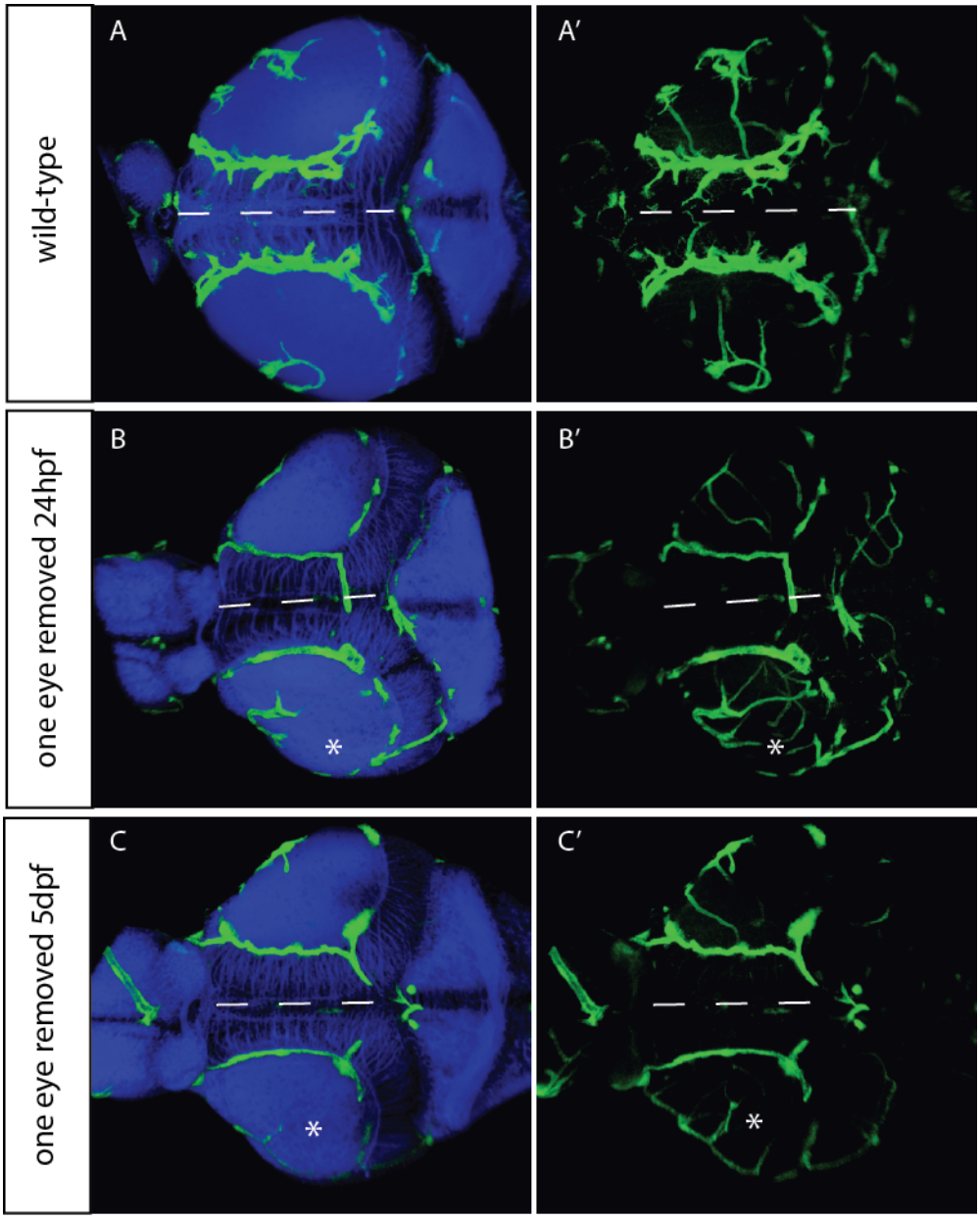

Figure 1. Absence of retinal input to the tectum does not alter the vascular network

(A-C') 3D reconstructions of dorsal views of 9dpf dissected brains from *Tg(fli:GFP)* wild-type larvae **(A-A'),** larvae with the left eye surgically removed between 24 and 32hpf **(B-B')** and larvae with the left eye surgically removed at 5dpf **(C-C').** Brain morphology is visualised with ant-acetylated tubulin (blue).

(A-C') Both tecta in wild-type and one-eyed larvae display a similar vascular network (Innervated tecta in one-eyed larvae are marked with an asterisk).

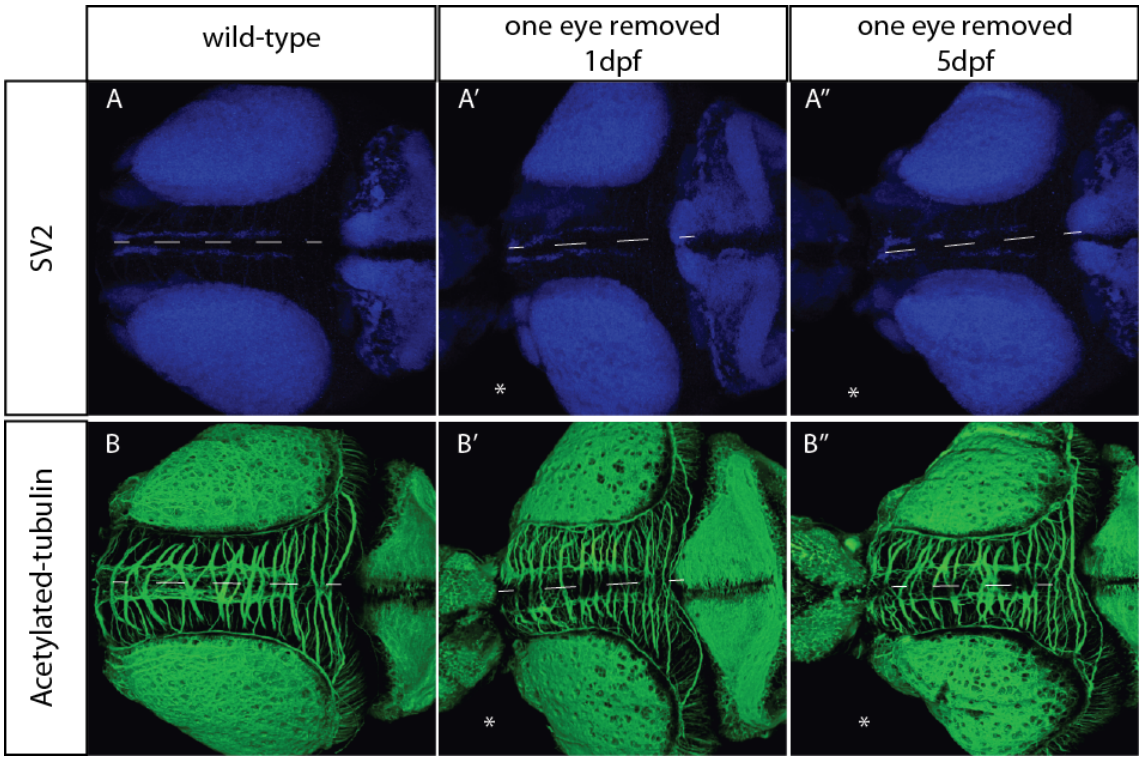

Figure 2. Absence of retinal input to the tectum does not affect the tectal architecture

(A-B') 3D reconstructions of dorsal views of 9dpf dissected brains from wild-type larvae **(A-B),** larvae with the left eye surgically removed between 24 and 32hpf **(A'-B')** and larvae with the left eye surgically removed at 5dpf **(A"-B").** Neuropil regions are visualised with the synaptic vesicle protein, SV2 (**A-A",** blue) and axons tracts are visualised with ant-acetylated tubulin (**B-B"**green).

(A-B") Both tecta in wild-type and one-eyed larvae display similar neuropil regions and axons tracts (Innervated tecta in one-eyed larvae are marked with an asterisk).

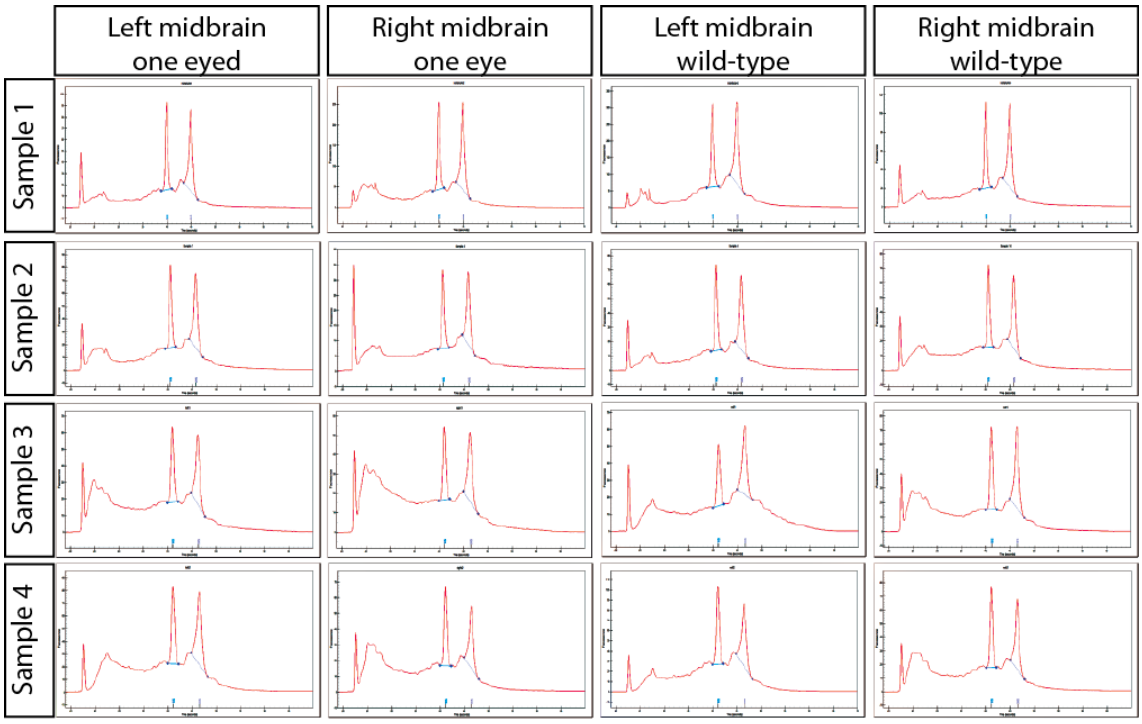

Sample		RQI	260/280
Sample 1	Left midbrain, one eye	8.5	2.14
	Right midbrain, one eye	8.5	2.09
	Left midbrain, wild-type	8.7	2.09
	Right midbrain, wild-type	8.3	2.10
Sample 2	Left midbrain, one eye	8.2	2.09
	Right midbrain, one eye	7.8	2.07
	Left midbrain, wild-type	8.2	2.11
	Right midbrain, wild-type	7.8	2.09
Sample 3	Left midbrain, one eye	7.6	2.08
	Right midbrain, one eye	7.6	2.05
	Left midbrain, wild-type	8.0	2.05
	Right midbrain, wild-type	7.8	2.12
Sample 4	Left midbrain, one eye	7.8	2.01
	Right midbrain, one eye	7.6	2.03
	Left midbrain, wild-type	7.8	2.03
	Right midbrain, wild-type	7.8	2.02

Figure 3. RNA electrophoretograms and OD260/280 values for the RNA samples obtained from dissected larval midbrains at 9dpf

RNA electrophoretograms for the all the RNA samples used for RNAseq and qRT-PCR analysis. Samples were analysed on a Biorad Experion RNA Highsens Analysis machine, and RQI values are shown in the table. Also shown are the OD260/280 absorption ratios for each sample

Reference List

Ables, J.L., Decarolis, N.A., Johnson, M.A., Rivera, P.D., Gao, Z., Cooper, D.C., Radtke, F., Hsieh, J., and Eisch, A.J. (2010). Notch1 is required for maintenance of the reservoir of adult hippocampal stem cells. J Neurosci *30*, 10484-10492.

Abraham, W.C., and Williams, J.M. (2003). Properties and mechanisms of LTP maintenance. Neuroscientist *9*, 463-474.

Ahmad, I., Tang, L., and Pham, H. (2000). Identification of neural progenitors in the adult mammalian eye. Biochem Biophys Res Commun *270*, 517-521.

Ahn, S., and Joyner, A.L. (2005). In vivo analysis of quiescent adult neural stem cells responding to Sonic hedgehog. Nature *437*, 894-897.

Al Alam, D., Green, M., Tabatabai Irani, R., Parsa, S., Danopoulos, S., Sala, F.G., Branch, J., El Agha, E., Tiozzo, C., Voswinckel, R.*, et al.* (2011). Contrasting expression of canonical Wnt signaling reporters TOPGAL, BATGAL and Axin2(LacZ) during murine lung development and repair. PLoS One *6*, e23139.

Altar, C.A., Laeng, P., Jurata, L.W., Brockman, J.A., Lemire, A., Bullard, J., Bukhman, Y.V., Young, T.A., Charles, V., and Palfreyman, M.G. (2004). Electroconvulsive seizures regulate gene expression of distinct neurotrophic signaling pathways. J Neurosci *24*, 2667-2677.

Alunni, A., Hermel, J.M., Heuze, A., Bourrat, F., Jamen, F., and Joly, J.S. (2010). Evidence for neural stem cells in the medaka optic tectum proliferation zones. Dev Neurobiol *70*, 693-713.

Artavanis-Tsakonas, S., Rand, M.D., and Lake, R.J. (1999). Notch signaling: cell fate control and signal integration in development. Science *284*, 770-776.

Austin, C.P., Feldman, D.E., Ida, J.A., Jr., and Cepko, C.L. (1995). Vertebrate retinal ganglion cells are selected from competent progenitors by the action of Notch. Development *121*, 3637-3650.

Babb, S.G., Kotradi, S.M., Shah, B., Chiappini-Williamson, C., Bell, L.N., Schmeiser, G., Chen, E., Liu, Q., and Marrs, J.A. (2005). Zebrafish R-cadherin (Cdh4) controls visual system development and differentiation. Dev Dyn *233*, 930-945.

Baker, N.E. (2001). Cell proliferation, survival, and death in the Drosophila eye. Semin Cell Dev Biol *12*, 499-507.

Barlow, H.B., Hill, R.M., and Levick, W.R. (1964). Retinal Ganglion Cells Responding Selectively to Direction and Speed of Image Motion in the Rabbit. J Physiol *173*, 377-407.

Ben Fredj, N., Hammond, S., Otsuna, H., Chien, C.B., Burrone, J., and Meyer, M.P. (2010). Synaptic activity and activity-dependent competition regulates axon arbor maturation, growth arrest, and territory in the retinotectal projection. J Neurosci *30*, 10939-10951.

Bianco, I.H., Kampff, A.R., and Engert, F. (2011). Prey capture behavior evoked by simple visual stimuli in larval zebrafish. Front Syst Neurosci *5*, 101.

Bilotta, J. (2000). Effects of abnormal lighting on the development of zebrafish visual behavior. Behav Brain Res *116*, 81-87.

Blankenberg, D., Von Kuster, G., Coraor, N., Ananda, G., Lazarus, R., Mangan, M., Nekrutenko, A., and Taylor, J. (2010). Galaxy: a web-based genome analysis tool for experimentalists. Curr Protoc Mol Biol *Chapter 19*, Unit 19 10 11-21.

Borday, C., Cabochette, P., Parain, K., Mazurier, N., Janssens, S., Tran, H.T., Sekkali, B., Bronchain, O., Vleminckx, K., Locker, M.*, et al.* (2012). Antagonistic cross-regulation between Wnt and Hedgehog signalling pathways controls post-embryonic retinal proliferation. Development *139*, 3499-3509.

Boucher, S.E., and Hitchcock, P.F. (1998). Insulin-related growth factors stimulate proliferation of retinal progenitors in the goldfish. J Comp Neurol *394*, 386-394.

Braisted, J.E., McLaughlin, T., Wang, H.U., Friedman, G.C., Anderson, D.J., and O'Leary D, D. (1997). Graded and lamina-specific distributions of ligands of EphB receptor tyrosine kinases in the developing retinotectal system. Dev Biol *191*, 14-28.

Burrill, J.D., and Easter, S.S., Jr. (1994). Development of the retinofugal projections in the embryonic and larval zebrafish (Brachydanio rerio). J Comp Neurol *346*, 583-600.

Centanin, L., Ander, J.J., Hoeckendorf, B., Lust, K., Kellner, T., Kraemer, I., Urbany, C., Hasel, E., Harris, W.A., Simons, B.D.*, et al.* (2014). Exclusive multipotency and preferential asymmetric divisions in post-embryonic neural stem cells of the fish retina. Development.

Centanin, L., Hoeckendorf, B., and Wittbrodt, J. (2011). Fate restriction and multipotency in retinal stem cells. Cell Stem Cell *9*, 553-562.

Cerveny, K.L., Cavodeassi, F., Turner, K.J., de Jong-Curtain, T.A., Heath, J.K., and Wilson, S.W. (2010). The zebrafish flotte lotte mutant reveals that the local retinal environment promotes the differentiation of proliferating precursors emerging from their stem cell niche. Development *137*, 2107-2115.

Cerveny, K.L., Varga, M., and Wilson, S.W. (2012). Continued growth and circuit building in the anamniote visual system. Dev Neurobiol *72*, 328-345.

Chapouton, P., Skupien, P., Hesl, B., Coolen, M., Moore, J.C., Madelaine, R., Kremmer, E., Faus-Kessler, T., Blader, P., Lawson, N.D.*, et al.* (2010). Notch activity levels

control the balance between quiescence and recruitment of adult neural stem cells. J Neurosci *30*, 7961-7974.

Cicero, S.A., Johnson, D., Reyntjens, S., Frase, S., Connell, S., Chow, L.M., Baker, S.J., Sorrentino, B.P., and Dyer, M.A. (2009). Cells previously identified as retinal stem cells are pigmented ciliary epithelial cells. Proc Natl Acad Sci U S A *106*, 6685-6690.

Clapham, D.E. (2007). Calcium signaling. Cell *131*, 1047-1058.

Coffman, C.R., Skoglund, P., Harris, W.A., and Kintner, C.R. (1993). Expression of an extracellular deletion of Xotch diverts cell fate in Xenopus embryos. Cell *73*, 659-671.

Concordet, J.P., Lewis, K.E., Moore, J.W., Goodrich, L.V., Johnson, R.L., Scott, M.P., and Ingham, P.W. (1996). Spatial regulation of a zebrafish patched homologue reflects the roles of sonic hedgehog and protein kinase A in neural tube and somite patterning. Development *122*, 2835-2846.

Conn, P.J., and Pin, J.P. (1997). Pharmacology and functions of metabotropic glutamate receptors. Annu Rev Pharmacol Toxicol *37*, 205-237.

Crooks, J., and Kolb, H. (1992). Localization of GABA, glycine, glutamate and tyrosine hydroxylase in the human retina. J Comp Neurol *315*, 287-302.

Currie, J., and Cowan, W.M. (1974). Some observations on the early development of the optic tectum in the frog (Rana pipiens), with special reference to the effects of early eye removal on mitotic activity in the larval tectum. J Comp Neurol *156*, 123-141.

Dakubo, G.D., Wang, Y.P., Mazerolle, C., Campsall, K., McMahon, A.P., and Wallace, V.A. (2003). Retinal ganglion cell-derived sonic hedgehog signaling is required for optic disc and stalk neuroepithelial cell development. Development *130*, 2967-2980.

Dang, C.V. (2012). MYC on the path to cancer. Cell *149*, 22-35.

de Oliveira-Carlos, V., Ganz, J., Hans, S., Kaslin, J., and Brand, M. (2013). Notch receptor expression in neurogenic regions of the adult zebrafish brain. PLoS One *8*, e73384.

DeFelipe, J. (1997). Types of neurons, synaptic connections and chemical characteristics of cells immunoreactive for calbindin-D28K, parvalbumin and calretinin in the neocortex. J Chem Neuroanat *14*, 1-19.

Deisseroth, K., Singla, S., Toda, H., Monje, M., Palmer, T.D., and Malenka, R.C. (2004). Excitation-neurogenesis coupling in adult neural stem/progenitor cells. Neuron *42*, 535-552.

Del Bene, F., Wyart, C., Robles, E., Tran, A., Looger, L., Scott, E.K., Isacoff, E.Y., and Baier, H. (2010). Filtering of visual information in the tectum by an identified neural circuit. Science *330*, 669-673.

Denayer, T., Locker, M., Borday, C., Deroo, T., Janssens, S., Hecht, A., van Roy, F., Perron, M., and Vleminckx, K. (2008). Canonical Wnt signaling controls proliferation of retinal stem/progenitor cells in postembryonic Xenopus eyes. Stem Cells *26*, 2063-2074.

Di Donato, V., Auer, T.O., Duroure, K., and Del Bene, F. (2013). Characterization of the calcium binding protein family in zebrafish. PLoS One *8*, e53299.

Dorsky, R.I., Chang, W.S., Rapaport, D.H., and Harris, W.A. (1997). Regulation of neuronal diversity in the Xenopus retina by Delta signalling. Nature *385*, 67-70.

Dorsky, R.I., Sheldahl, L.C., and Moon, R.T. (2002). A transgenic Lef1/beta-catenin-dependent reporter is expressed in spatially restricted domains throughout zebrafish development. Dev Biol *241*, 229-237.

Drescher, U., Bonhoeffer, F., and Muller, B.K. (1997). The Eph family in retinal axon guidance. Curr Opin Neurobiol *7*, 75-80.

Dyer, M.A., and Cepko, C.L. (2000). p57(Kip2) regulates progenitor cell proliferation and amacrine interneuron development in the mouse retina. Development *127*, 3593-3605.

Easter, S.S., Jr., and Nicola, G.N. (1996). The development of vision in the zebrafish (Danio rerio). Dev Biol *180*, 646-663.

Easter, S.S., Jr., and Stuermer, C.A. (1984). An evaluation of the hypothesis of shifting terminals in goldfish optic tectum. J Neurosci *4*, 1052-1063.

Eichler, V.B. (1971). Neurogenesis in the optic tectum of larval Rana pipiens following unilateral enucleation. J Comp Neurol *141*, 375-395.

Eilers, M., and Eisenman, R.N. (2008). Myc's broad reach. Genes Dev *22*, 2755-2766.

Enroth-Cugell, C., and Robson, J.G. (1966). The contrast sensitivity of retinal ganglion cells of the cat. J Physiol *187*, 517-552.

Ewert, J.P. (1987). Neuroethology of releasing mechanisms: Prey-catching in toads. Behavioral and Brain Sciences *10*, 337-368.

Ewert, J.P., Buxbaum-Conradi, H., Dreisvogt, F., Glagow, M., Merkel-Harff, C., Rottgen, A., Schurg-Pfeiffer, E., and Schwippert, W.W. (2001). Neural modulation of visuomotor functions underlying prey-catching behaviour in anurans: perception, attention, motor performance, learning. Comp Biochem Physiol A Mol Integr Physiol *128*, 417-461.

Feng, H., Langenau, D.M., Madge, J.A., Quinkertz, A., Gutierrez, A., Neuberg, D.S., Kanki, J.P., and Look, A.T. (2007). Heat-shock induction of T-cell

lymphoma/leukaemia in conditional Cre/lox-regulated transgenic zebrafish. Br J Haematol *138*, 169-175.

Fischer, A.J., Omar, G., Walton, N.A., Verrill, T.A., and Unson, C.G. (2005). Glucagon-expressing neurons within the retina regulate the proliferation of neural progenitors in the circumferential marginal zone of the avian eye. J Neurosci *25*, 10157-10166.

Fischer, A.J., and Reh, T.A. (2000). Identification of a proliferating marginal zone of retinal progenitors in postnatal chickens. Dev Biol *220*, 197-210.

Gabriel, J.P., Trivedi, C.A., Maurer, C.M., Ryu, S., and Bollmann, J.H. (2012). Layer-specific targeting of direction-selective neurons in the zebrafish optic tectum. Neuron *76*, 1147-1160.

Gabriel, R., Straznicky, C., and Wye-Dvorak, J. (1992). GABA-like immunoreactive neurons in the retina of Bufo marinus: evidence for the presence of GABA-containing ganglion cells. Brain Res *571*, 175-179.

Gaze, R.M., Keating, M.J., Ostberg, A., and Chung, S.H. (1979). The relationship between retinal and tectal growth in larval Xenopus: implications for the development of the retino-tectal projection. J Embryol Exp Morphol *53*, 103-143.

Ge, S., Goh, E.L., Sailor, K.A., Kitabatake, Y., Ming, G.L., and Song, H. (2006). GABA regulates synaptic integration of newly generated neurons in the adult brain. Nature *439*, 589-593.

Giachino, C., Barz, M., Tchorz, J.S., Tome, M., Gassmann, M., Bischofberger, J., Bettler, B., and Taylor, V. (2014). GABA suppresses neurogenesis in the adult hippocampus through GABAB receptors. Development *141*, 83-90.

Giardine, B., Riemer, C., Hardison, R.C., Burhans, R., Elnitski, L., Shah, P., Zhang, Y., Blankenberg, D., Albert, I., Taylor, J.*, et al.* (2005). Galaxy: a platform for interactive large-scale genome analysis. Genome Res *15*, 1451-1455.

Gnuegge, L., Schmid, S., and Neuhauss, S.C. (2001). Analysis of the activity-deprived zebrafish mutant macho reveals an essential requirement of neuronal activity for the development of a fine-grained visuotopic map. J Neurosci *21*, 3542-3548.

Goecks, J., Nekrutenko, A., and Taylor, J. (2010). Galaxy: a comprehensive approach for supporting accessible, reproducible, and transparent computational research in the life sciences. Genome Biol *11*, R86.

Gosse, N.J., Nevin, L.M., and Baier, H. (2008). Retinotopic order in the absence of axon competition. Nature *452*, 892-895.

Grant, S., and Keating, M.J. (1989). Changing patterns of binocular visual connections in the intertectal system during development of the frog, Xenopus laevis. II.

Abnormalities following early visual deprivation. Exp Brain Res *75*, 117-132.

Greenberg, M.E., Ziff, E.B., and Greene, L.A. (1986). Stimulation of neuronal acetylcholine receptors induces rapid gene transcription. Science *234*, 80-83.

Hairston, N.G., Jr., Li, K.T., and Easter, S.S., Jr. (1982). Fish vision and the detection of planktonic prey. Science *218*, 1240-1242.

Harrison, R.G. (1929). Correlation in the development and growth of the eye studied by means of heteroplastic transplantation. W Roux Archiv fur Entwicklungsmechanik der Organismen *120*, 1-55.

Hartline, H.K. (1938). The response of single optic nerve fibers of the vertebrate eye to illumination of the retina. Am J Physiol *121*, 400-415.

Herbomel, P., Thisse, B., and Thisse, C. (2001). Zebrafish early macrophages colonize cephalic mesenchyme and developing brain, retina, and epidermis through a M-CSF receptor-dependent invasive process. Dev Biol *238*, 274-288.

Herget, U., Wolf, A., Wullimann, M.F., and Ryu, S. (2014). Molecular neuroanatomy and chemoarchitecture of the neurosecretory preoptic-hypothalamic area in zebrafish larvae. J Comp Neurol *522*, 1542-1564.

Higashijima, S., Mandel, G., and Fetcho, J.R. (2004). Distribution of prospective glutamatergic, glycinergic, and GABAergic neurons in embryonic and larval zebrafish. J Comp Neurol *480*, 1-18.

Hipfner, D.R., and Cohen, S.M. (2004). Connecting proliferation and apoptosis in development and disease. Nat Rev Mol Cell Biol *5*, 805-815.

Hitchcock, P.F., and Easter, S.S., Jr. (1986). Retinal ganglion cells in goldfish: a qualitative classification into four morphological types, and a quantitative study of the development of one of them. J Neurosci *6*, 1037-1050.

Hitoshi, S., Alexson, T., Tropepe, V., Donoviel, D., Elia, A.J., Nye, J.S., Conlon, R.A., Mak, T.W., Bernstein, A., and van der Kooy, D. (2002). Notch pathway molecules are essential for the maintenance, but not the generation, of mammalian neural stem cells. Genes Dev *16*, 846-858.

Hofbauer, A., and Drager, U.C. (1985). Depth segregation of retinal ganglion cells projecting to mouse superior colliculus. J Comp Neurol *234*, 465-474.

Holt, C.E., and Harris, W.A. (1983). Order in the initial retinotectal map in Xenopus: a new technique for labelling growing nerve fibres. Nature *301*, 150-152.

Hoskins, S.G., and Grobstein, P. (1985). Development of the ipsilateral retinothalamic projection in the frog Xenopus laevis. II. Ingrowth of optic nerve fibers and production of ipsilaterally projecting retinal ganglion cells. J Neurosci *5*, 920-929.

Hovanes, K., Li, T.W., Munguia, J.E., Truong, T., Milovanovic, T., Lawrence Marsh, J., Holcombe, R.F., and Waterman, M.L. (2001). Beta-catenin-sensitive isoforms of lymphoid enhancer factor-1 are selectively expressed in colon cancer. Nat Genet *28*, 53-57.

Hua, J.Y., Smear, M.C., Baier, H., and Smith, S.J. (2005). Regulation of axon growth in vivo by activity-based competition. Nature *434*, 1022-1026.

Huang, Z., and Kunes, S. (1996). Hedgehog, transmitted along retinal axons, triggers neurogenesis in the developing visual centers of the Drosophila brain. Cell *86*, 411-422.

Huang, Z., and Kunes, S. (1998). Signals transmitted along retinal axons in Drosophila: Hedgehog signal reception and the cell circuitry of lamina cartridge assembly. Development *125*, 3753-3764.

Huang, Z., Shilo, B.Z., and Kunes, S. (1998). A retinal axon fascicle uses spitz, an EGF receptor ligand, to construct a synaptic cartridge in the brain of Drosophila. Cell *95*, 693-703.

Hughes, A. (1971). Topographical relationships between the anatomy and physiology of the rabbit visual system. Doc Ophthalmol *30*, 33-159.

Hwang, W.Y., Fu, Y., Reyon, D., Maeder, M.L., Tsai, S.Q., Sander, J.D., Peterson, R.T., Yeh, J.R., and Joung, J.K. (2013). Efficient genome editing in zebrafish using a CRISPR-Cas system. Nat Biotechnol *31*, 227-229.

Inoue, A., and Sanes, J.R. (1997). Lamina-specific connectivity in the brain: regulation by N-cadherin, neurotrophins, and glycoconjugates. Science *276*, 1428-1431.

Isbell, L. (2006). Snakes as agents of evolutionary change in primate brains. J Human Evol *51*, 1-35.

Ito, Y., Tanaka, H., Okamoto, H., and Ohshima, T. (2010). Characterization of neural stem cells and their progeny in the adult zebrafish optic tectum. Dev Biol *342*, 26-38.

Jacobson, M. (1976). Histogenesis of retina in the clawed frog with implications for the pattern of development of retinotectal connections. Brain Res *103*, 541-545.

Jacobson, M. (1977). Mapping the developing retinotectal projection in frog tadpoles by a double label autoradiographic techinque. Brain Res *127*, 55-67.

Jagasia, R., Steib, K., Englberger, E., Herold, S., Faus-Kessler, T., Saxe, M., Gage, F.H., Song, H., and Lie, D.C. (2009). GABA-cAMP response element-binding protein signaling regulates maturation and survival of newly generated neurons in the adult hippocampus. J Neurosci *29*, 7966-7977.

Jensen, L.J., Jensen, T.S., de Lichtenberg, U., Brunak, S., and Bork, P. (2006). Co-

evolution of transcriptional and post-translational cell-cycle regulation. Nature *443*, 594-597.

Jho, E.H., Zhang, T., Domon, C., Joo, C.K., Freund, J.N., and Costantini, F. (2002). Wnt/beta-catenin/Tcf signaling induces the transcription of Axin2, a negative regulator of the signaling pathway. Mol Cell Biol *22*, 1172-1183.

Johns, P.R. (1977). Growth of the adult goldfish eye. III. Source of the new retinal cells. J Comp Neurol *176*, 343-357.

Johns, P.R., and Easter, S.S., Jr. (1977). Growth of the adult goldfish eye. II. Increase in retinal cell number. J Comp Neurol *176*, 331-341.

Jojich, L., and Pourcho, R.G. (1996). Glutamate immunoreactivity in the cat retina: a quantitative study. Vis Neurosci *13*, 117-133.

Jung, S.H., Kim, H.S., Ryu, J.H., Gwak, J.W., Bae, Y.K., Kim, C.H., and Yeo, S.Y. (2012). Her4-positive population in the tectum opticum is proliferating neural precursors in the adult zebrafish brain. Mol Cells *33*, 627-632.

Karlstrom, R.O., Talbot, W.S., and Schier, A.F. (1999). Comparative synteny cloning of zebrafish you-too: mutations in the Hedgehog target gli2 affect ventral forebrain patterning. Genes Dev *13*, 388-393.

Karlstrom, R.O., Trowe, T., Klostermann, S., Baier, H., Brand, M., Crawford, A.D., Grunewald, B., Haffter, P., Hoffmann, H., Meyer, S.U*., et al.* (1996). Zebrafish mutations affecting retinotectal axon pathfinding. Development *123*, 427-438.

Karlstrom, R.O., Tyurina, O.V., Kawakami, A., Nishioka, N., Talbot, W.S., Sasaki, H., and Schier, A.F. (2003). Genetic analysis of zebrafish gli1 and gli2 reveals divergent requirements for gli genes in vertebrate development. Development *130*, 1549-1564.

Kawakami, K. (2007). Tol2: a versatile gene transfer vector in vertebrates. Genome Biol *8 Suppl 1*, S7.

Kay, J.N., Finger-Baier, K.C., Roeser, T., Staub, W., and Baier, H. (2001). Retinal ganglion cell genesis requires lakritz, a Zebrafish atonal Homolog. Neuron *30*, 725-736.

Kengaku, M., Capdevila, J., Rodriguez-Esteban, C., De La Pena, J., Johnson, R.L., Izpisua Belmonte, J.C., and Tabin, C.J. (1998). Distinct WNT pathways regulating AER formation and dorsoventral polarity in the chick limb bud. Science *280*, 1274-1277.

Kim, D., Pertea, G., Trapnell, C., Pimentel, H., Kelley, R., and Salzberg, S.L. (2013). TopHat2: accurate alignment of transcriptomes in the presence of insertions, deletions and gene fusions. Genome Biol *14*, R36.

Kinoshita, M., Ueda, R., Kojima, S., Sato, K., Watanabe, M., Urano, A., and Ito, E. (2002). Multiple-site optical recording for characterization of functional synaptic

organization of the optic tectum of rainbow trout. Eur J Neurosci *16*, 868-876.

Kollros, J. (1953). The development of the optic lobes in the frog. I. The effects of unilateral enucleation in embryonic stages. J Exp Zool *123*, 153-187.
Kollros, J.J. (1982). Peripheral control of midbrain mitotic activity in the frog. J Comp Neurol *205*, 171-178.

Kubota, R., Hokoc, J.N., Moshiri, A., McGuire, C., and Reh, T.A. (2002). A comparative study of neurogenesis in the retinal ciliary marginal zone of homeothermic vertebrates. Brain Res Dev Brain Res *134*, 31-41.

Kuffler, S.W. (1952). Neurons in the retina; organization, inhibition and excitation problems. Cold Spring Harb Symp Quant Biol *17*, 281-292.

Langenau, D.M., Feng, H., Berghmans, S., Kanki, J.P., Kutok, J.L., and Look, A.T. (2005). Cre/lox-regulated transgenic zebrafish model with conditional myc-induced T cell acute lymphoblastic leukemia. Proc Natl Acad Sci U S A *102*, 6068-6073.

Larsell, O. (1931). The effect of experimental excision of one eye on the development of the optic lobe and opticus layer in larvae of the tree-frog (Hyla regilla). II. The effect on cell size and differentiation of cell processes. J Exp Zool *58*, 1-20.

Lawson, N.D., and Weinstein, B.M. (2002). In vivo imaging of embryonic vascular development using transgenic zebrafish. Dev Biol *248*, 307-318.

Le, H.G., Dowling, J.E., and Cameron, D.J. (2012). Early retinoic acid deprivation in developing zebrafish results in microphthalmia. Vis Neurosci *29*, 219-228.

Le, X., Langenau, D.M., Keefe, M.D., Kutok, J.L., Neuberg, D.S., and Zon, L.I. (2007). Heat shock-inducible Cre/Lox approaches to induce diverse types of tumors and hyperplasia in transgenic zebrafish. Proc Natl Acad Sci U S A *104*, 9410-9415.

Lee, J.E., Wu, S.F., Goering, L.M., and Dorsky, R.I. (2006). Canonical Wnt signaling through Lef1 is required for hypothalamic neurogenesis. Development *133*, 4451-4461.

Lee, S., and Stevens, C.F. (2007). General design principle for scalable neural circuits in a vertebrate retina. Proc Natl Acad Sci U S A *104*, 12931-12935.

Lewis, K.E., Concordet, J.P., and Ingham, P.W. (1999). Characterisation of a second patched gene in the zebrafish Danio rerio and the differential response of patched genes to Hedgehog signalling. Dev Biol *208*, 14-29.

Li, Z., and Fite, K.V. (1998). Distribution of GABA-like immunoreactive neurons and fibers in the central visual nuclei and retina of frog, Rana pipiens. Vis Neurosci *15*, 995-1006.

Lie, D.C., Colamarino, S.A., Song, H.J., Desire, L., Mira, H., Consiglio, A., Lein, E.S., Jessberger, S., Lansford, H., Dearie, A.R.*, et al.* (2005). Wnt signalling regulates adult

hippocampal neurogenesis. Nature *437*, 1370-1375.

Lim, B.K., Cho, S.J., Sumbre, G., and Poo, M.M. (2010). Region-specific contribution of ephrin-B and Wnt signaling to receptive field plasticity in developing optic tectum. Neuron *65*, 899-911.

Liu, C., and Nathans, J. (2008). An essential role for frizzled 5 in mammalian ocular development. Development *135*, 3567-3576.

Liu, H., Lu, M., and Guthrie, K.M. (2013). Anterograde trafficking of neurotrophin-3 in the adult olfactory system in vivo. Exp Neurol *241*, 125-137.

Locker, M., Agathocleous, M., Amato, M.A., Parain, K., Harris, W.A., and Perron, M. (2006). Hedgehog signaling and the retina: insights into the mechanisms controlling the proliferative properties of neural precursors. Genes Dev *20*, 3036-3048.

Lowe, A.S., Nikolaou, N., Hunter, P.R., Thompson, I.D., and Meyer, M.P. (2013). A systems-based dissection of retinal inputs to the zebrafish tectum reveals different rules for different functional classes during development. J Neurosci *33*, 13946-13956.

Malumbres, M., and Barbacid, M. (2009). Cell cycle, CDKs and cancer: a changing paradigm. Nat Rev Cancer *9*, 153-166.

Mann, F., Ray, S., Harris, W., and Holt, C. (2002). Topographic mapping in dorsoventral axis of the Xenopus retinotectal system depends on signaling through ephrin-B ligands. Neuron *35*, 461-473.

Masai, I., Yamaguchi, M., Tonou-Fujimori, N., Komori, A., and Okamoto, H. (2005). The hedgehog-PKA pathway regulates two distinct steps of the differentiation of retinal ganglion cells: the cell-cycle exit of retinoblasts and their neuronal maturation. Development *132*, 1539-1553.

Masland, R.H. (2001). Neuronal diversity in the retina. Curr Opin Neurobiol *11*, 431-436.

McMurray, V.M. (1954). The development of the optic lobes in Xenopus laevis. The effect of repeated crushing of the optic nerve. J Exp Zool *125*, 247-263.

Meek, J. (1983). Functional anatomy of the tectum mesencephali of the goldfish. An explorative analysis of the functional implications of the laminar structural organization of the tectum. Brain Res *287*, 247-297.

Meek, J., and Schellart, N.A. (1978). A Golgi study of goldfish optic tectum. J Comp Neurol *182*, 89-122.

Melchiorri, D., Cappuccio, I., Ciceroni, C., Spinsanti, P., Mosillo, P., Sarichelou, I., Sale, P., and Nicoletti, F. (2007). Metabotropic glutamate receptors in stem/progenitor cells. Neuropharmacology *53*, 473-480.

Menna, E., Cenni, M.C., Naska, S., and Maffei, L. (2003). The anterogradely transported BDNF promotes retinal axon remodeling during eye specific segregation within the LGN. Mol Cell Neurosci *24*, 972-983.

Meyer, M.P., and Smith, S.J. (2006). Evidence from in vivo imaging that synaptogenesis guides the growth and branching of axonal arbors by two distinct mechanisms. J Neurosci *26*, 3604-3614.

Meyer, R.L. (1978). Evidence from thymidine labeling for continuing growth of retina and tectum in juvenile goldfish. Exp Neurol *59*, 99-111.

Meyer, R.L. (1983). Tetrodotoxin inhibits the formation of refined retinotopography in goldfish. Brain Res *282*, 293-298.

Mira, H., Andreu, Z., Suh, H., Lie, D.C., Jessberger, S., Consiglio, A., San Emeterio, J., Hortiguela, R., Marques-Torrejon, M.A., Nakashima, K.*, et al.* (2010). Signaling through BMPR-IA regulates quiescence and long-term activity of neural stem cells in the adult hippocampus. Cell Stem Cell *7*, 78-89.

Moe, M.C., Kolberg, R.S., Sandberg, C., Vik-Mo, E., Olstorn, H., Varghese, M., Langmoen, I.A., and Nicolaissen, B. (2009). A comparison of epithelial and neural properties in progenitor cells derived from the adult human ciliary body and brain. Exp Eye Res *88*, 30-38.

Mooney, R., Penn, A.A., Gallego, R., and Shatz, C.J. (1996). Thalamic relay of spontaneous retinal activity prior to vision. Neuron *17*, 863-874.

Morgan, J.I., and Curran, T. (1986). Role of ion flux in the control of c-fos expression. Nature *322*, 552-555.

Moro, E., Ozhan-Kizil, G., Mongera, A., Beis, D., Wierzbicki, C., Young, R.M., Bournele, D., Domenichini, A., Valdivia, L.E., Lum, L.*, et al.* (2012). In vivo Wnt signaling tracing through a transgenic biosensor fish reveals novel activity domains. Dev Biol *366*, 327-340.

Morris, V.B., Wylie, C.C., and Miles, V.J. (1976). The growth of the chick retina after hatching. Anat Rec *184*, 111-113.

Mosimann, C., Kaufman, C.K., Li, P., Pugach, E.K., Tamplin, O.J., and Zon, L.I. (2011). Ubiquitous transgene expression and Cre-based recombination driven by the ubiquitin promoter in zebrafish. Development *138*, 169-177.

Nakamura, H., and O'Leary, D.D. (1989). Inaccuracies in initial growth and arborization of chick retinotectal axons followed by course corrections and axon remodeling to develop topographic order. J Neurosci *9*, 3776-3795.

Neuhauss, S.C., Biehlmaier, O., Seeliger, M.W., Das, T., Kohler, K., Harris, W.A., and

Baier, H. (1999). Genetic disorders of vision revealed by a behavioral screen of 400 essential loci in zebrafish. J Neurosci *19*, 8603-8615.

Neumann, C.J., and Nuesslein-Volhard, C. (2000). Patterning of the zebrafish retina by a wave of sonic hedgehog activity. Science *289*, 2137-2139.

Nevin, L.M., Robles, E., Baier, H., and Scott, E.K. (2010). Focusing on optic tectum circuitry through the lens of genetics. BMC Biol *8*, 126.

Nicol, X., Voyatzis, S., Muzerelle, A., Narboux-Neme, N., Sudhof, T.C., Miles, R., and Gaspar, P. (2007). cAMP oscillations and retinal activity are permissive for ephrin signaling during the establishment of the retinotopic map. Nat Neurosci *10*, 340-347.

Niell, C.M., Meyer, M.P., and Smith, S.J. (2004). In vivo imaging of synapse formation on a growing dendritic arbor. Nat Neurosci *7*, 254-260.

Nieto, M., Schuurmans, C., Britz, O., and Guillemot, F. (2001). Neural bHLH genes control the neuronal versus glial fate decision in cortical progenitors. Neuron *29*, 401-413.

Nikolaou, N., Lowe, A.S., Walker, A.S., Abbas, F., Hunter, P.R., Thompson, I.D., and Meyer, M.P. (2012). Parametric functional maps of visual inputs to the tectum. Neuron *76*, 317-324.

O'Rourke, N.A., Cline, H.T., and Fraser, S.E. (1994). Rapid remodeling of retinal arbors in the tectum with and without blockade of synaptic transmission. Neuron *12*, 921-934.

Ohtsuka, T., Sakamoto, M., Guillemot, F., and Kageyama, R. (2001). Roles of the basic helix-loop-helix genes Hes1 and Hes5 in expansion of neural stem cells of the developing brain. J Biol Chem *276*, 30467-30474.

Ota, S., Ishitani, S., Shimizu, N., Matsumoto, K., Itoh, M., and Ishitani, T. (2012). NLK positively regulates Wnt/beta-catenin signalling by phosphorylating LEF1 in neural progenitor cells. EMBO J *31*, 1904-1915.

Otteson, D.C., Cirenza, P.F., and Hitchcock, P.F. (2002). Persistent neurogenesis in the teleost retina: evidence for regulation by the growth-hormone/insulin-like growth factor-I axis. Mech Dev *117*, 137-149.

Park, H.C., Kim, C.H., Bae, Y.K., Yeo, S.Y., Kim, S.H., Hong, S.K., Shin, J., Yoo, K.W., Hibi, M., Hirano, T.*, et al.* (2000). Analysis of upstream elements in the HuC promoter leads to the establishment of transgenic zebrafish with fluorescent neurons. Dev Biol *227*, 279-293.

Perron, M., Kanekar, S., Vetter, M.L., and Harris, W.A. (1998). The genetic sequence of retinal development in the ciliary margin of the Xenopus eye. Dev Biol *199*, 185-200.

Perry, V.H., and Cowey, A. (1984). Retinal ganglion cells that project to the superior

colliculus and pretectum in the macaque monkey. Neuroscience *12*, 1125-1137.

Pittman, A.J., Law, M.Y., and Chien, C.B. (2008). Pathfinding in a large vertebrate axon tract: isotypic interactions guide retinotectal axons at multiple choice points. Development *135*, 2865-2871.

Pollack, J.G., and Hickey, T.L. (1979). The distribution of retino-collicular axon terminals in rhesus monkey. J Comp Neurol *185*, 587-602.

Prestige, M.C., and Willshaw, D.J. (1975). On a role for competition in the formation of patterned neural connexions. Proc R Soc Lond B Biol Sci *190*, 77-98.

Provis, J.M., Dubis, A.M., Maddess, T., and Carroll, J. (2013). Adaptation of the central retina for high acuity vision: cones, the fovea and the avascular zone. Prog Retin Eye Res *35*, 63-81.

Pujic, Z., Omori, Y., Tsujikawa, M., Thisse, B., Thisse, C., and Malicki, J. (2006). Reverse genetic analysis of neurogenesis in the zebrafish retina. Dev Biol *293*, 330-347.

Rahmann, H. (1968). [Autoradiographic studies on the DNA metabolism (mitosis frequency) in the CNS of Brachydanio rerio Ham. Buch. (Cyprinidae, Pisces)]. J Hirnforsch *10*, 279-284.

Raymond, P.A. (1986). Movement of retinal terminals in goldfish optic tectum predicted by analysis of neuronal proliferation. J Neurosci *6*, 2479-2488.

Raymond, P.A., Barthel, L.K., Bernardos, R.L., and Perkowski, J.J. (2006). Molecular characterization of retinal stem cells and their niches in adult zebrafish. BMC Dev Biol *6*, 36.

Raymond, P.A., and Easter, S.S., Jr. (1983). Postembryonic growth of the optic tectum in goldfish. I. Location of germinal cells and numbers of neurons produced. J Neurosci *3*, 1077-1091.

Raymond, P.A., Easter, S.S., Jr., Burnham, J.A., and Powers, M.K. (1983). Postembryonic growth of the optic tectum in goldfish. II. Modulation of cell proliferation by retinal fiber input. J Neurosci *3*, 1092-1099.

Raymond, P.A., and Rivlin, P.K. (1987). Germinal cells in the goldfish retina that produce rod photoreceptors. Dev Biol *122*, 120-138.

Ready, D.F., Hanson, T.E., and Benzer, S. (1976). Development of the Drosophila retina, a neurocrystalline lattice. Dev Biol *53*, 217-240.

Recher, G., Jouralet, J., Brombin, A., Heuze, A., Mugniery, E., Hermel, J.M., Desnoulez, S., Savy, T., Herbomel, P., Bourrat, F.*, et al.* (2013). Zebrafish midbrain slow-amplifying progenitors exhibit high levels of transcripts for nucleotide and ribosome biogenesis. Development *140*, 4860-4869.

Reh, T.A., and Constantine-Paton, M. (1984). Retinal ganglion cell terminals change their projection sites during larval development of Rana pipiens. J Neurosci *4*, 442-457.

Ring, H., Mendu, S.K., Shirazi-Fard, S., Birnir, B., and Hallbook, F. (2012). GABA maintains the proliferation of progenitors in the developing chick ciliary marginal zone and non-pigmented ciliary epithelium. PLoS One *7*, e36874.

Robles, E., Filosa, A., and Baier, H. (2013). Precise lamination of retinal axons generates multiple parallel input pathways in the tectum. J Neurosci *33*, 5027-5039.

Robles, E., Smith, S.J., and Baier, H. (2011). Characterization of genetically targeted neuron types in the zebrafish optic tectum. Front Neural Circuits *5*, 1.

Rockhill, R.L., Daly, F.J., MacNeil, M.A., Brown, S.P., and Masland, R.H. (2002). The diversity of ganglion cells in a mammalian retina. J Neurosci *22*, 3831-3843.

Rodrigues, M.A., Gomes, D.A., Leite, M.F., Grant, W., Zhang, L., Lam, W., Cheng, Y.C., Bennett, A.M., and Nathanson, M.H. (2007). Nucleoplasmic calcium is required for cell proliferation. J Biol Chem *282*, 17061-17068.

Rubel, E.W., Hyson, R.L., and Durham, D. (1990). Afferent regulation of neurons in the brain stem auditory system. J Neurobiol *21*, 169-196.

Sakaue-Sawano, A., Kurokawa, H., Morimura, T., Hanyu, A., Hama, H., Osawa, H., Kashiwagi, S., Fukami, K., Miyata, T., Miyoshi, H*., et al.* (2008). Visualizing spatiotemporal dynamics of multicellular cell-cycle progression. Cell *132*, 487-498.

Sanes, J.R., and Yamagata, M. (1999). Formation of lamina-specific synaptic connections. Curr Opin Neurobiol *9*, 79-87.

Sanes, J.R., and Zipursky, S.L. (2010). Design principles of insect and vertebrate visual systems. Neuron *66*, 15-36.

Sato, T., Hamaoka, T., Aizawa, H., Hosoya, T., and Okamoto, H. (2007). Genetic single-cell mosaic analysis implicates ephrinB2 reverse signaling in projections from the posterior tectum to the hindbrain in zebrafish. J Neurosci *27*, 5271-5279.

Sato, T., van Es, J.H., Snippert, H.J., Stange, D.E., Vries, R.G., van den Born, M., Barker, N., Shroyer, N.F., van de Wetering, M., and Clevers, H. (2011). Paneth cells constitute the niche for Lgr5 stem cells in intestinal crypts. Nature *469*, 415-418.

Sauer, B. (1993). Manipulation of transgenes by site-specific recombination: use of Cre recombinase. Methods Enzymol *225*, 890-900.

Schindelin, J., Arganda-Carreras, I., Frise, E., Kaynig, V., Longair, M., Pietzsch, T., Preibisch, S., Rueden, C., Saalfeld, S., Schmid, B*., et al.* (2012). Fiji: an open-source platform for biological-image analysis. Nat Methods *9*, 676-682.

Schmatolla, E. (1972). Dependence of tectal neuron differentiation on optic innervation in teleost fish. J Embryol Exp Morphol *27*, 555-576.

Schmatolla, E., and Erdmann, G. (1973). Influence of retino-tectal innervation on cell proliferation and cell migration in the embryonic teleost tectum. J Embryol Exp Morphol *29*, 697-712.

Schmitt, A.M., Shi, J., Wolf, A.M., Lu, C.C., King, L.A., and Zou, Y. (2006). Wnt-Ryk signalling mediates medial-lateral retinotectal topographic mapping. Nature *439*, 31-37.

Schwaller, B. (2010). Cytosolic Ca2+ buffers. Cold Spring Harb Perspect Biol *2*, a004051.

Scott, E.K., and Baier, H. (2009). The cellular architecture of the larval zebrafish tectum, as revealed by gal4 enhancer trap lines. Front Neural Circuits *3*, 13.

Scott, T.M., and Lazar, G. (1976). An investigation into the hypothesis of shifting neuronal relationships during development. J Anat *121*, 485-496.

Selleck, S.B., and Steller, H. (1991). The influence of retinal innervation on neurogenesis in the first optic ganglion of Drosophila. Neuron *6*, 83-99.

Sheldahl, L.C., Park, M., Malbon, C.C., and Moon, R.T. (1999). Protein kinase C is differentially stimulated by Wnt and Frizzled homologs in a G-protein-dependent manner. Curr Biol *9*, 695-698.

Sherr, C.J., and Roberts, J.M. (1999). CDK inhibitors: positive and negative regulators of G1-phase progression. Genes Dev *13*, 1501-1512.

Simon, D.K., and O'Leary, D.D. (1992). Development of topographic order in the mammalian retinocollicular projection. J Neurosci *12*, 1212-1232.

Smear, M.C., Tao, H.W., Staub, W., Orger, M.B., Gosse, N.J., Liu, Y., Takahashi, K., Poo, M.M., and Baier, H. (2007). Vesicular glutamate transport at a central synapse limits the acuity of visual perception in zebrafish. Neuron *53*, 65-77.

Song, J., Sun, J., Moss, J., Wen, Z., Sun, G.J., Hsu, D., Zhong, C., Davoudi, H., Christian, K.M., Toni, N.*, et al.* (2013). Parvalbumin interneurons mediate neuronal circuitry-neurogenesis coupling in the adult hippocampus. Nat Neurosci *16*, 1728-1730.

Song, J., Zhong, C., Bonaguidi, M.A., Sun, G.J., Hsu, D., Gu, Y., Meletis, K., Huang, Z.J., Ge, S., Enikolopov, G.*, et al.* (2012). Neuronal circuitry mechanism regulating adult quiescent neural stem-cell fate decision. Nature *489*, 150-154.

Sperry, R.W. (1963). Chemoaffinity in the Orderly Growth of Nerve Fiber Patterns and Connections. Proc Natl Acad Sci U S A *50*, 703-710.

Spitzer, N.C. (2006). Electrical activity in early neuronal development. Nature *444*, 707-712.

Stephens, W.Z., Senecal, M., Nguyen, M., and Piotrowski, T. (2010). Loss of adenomatous polyposis coli (apc) results in an expanded ciliary marginal zone in the zebrafish eye. Dev Dyn *239*, 2066-2077.

Stout, R.P., and Graziadei, P.P. (1980). Influence of the olfactory placode on the development of the brain in Xenopus laevis (Daudin). I. Axonal growth and connections of the transplanted olfactory placode. Neuroscience *5*, 2175-2186.

Strand, M., and Micchelli, C.A. (2011). Quiescent gastric stem cells maintain the adult Drosophila stomach. Proc Natl Acad Sci U S A *108*, 17696-17701.

Straznicky, K., and Gaze, R.M. (1971). The growth of the retina in Xenopus laevis: an autoradiographic study. J Embryol Exp Morphol *26*, 67-79.

Straznicky, K., and Gaze, R.M. (1972). The development of the tectum in Xenopus laevis: an autoradiographic study. J Embryol Exp Morphol *28*, 87-115.

Stuermer, C.A. (1988). Retinotopic organization of the developing retinotectal projection in the zebrafish embryo. J Neurosci *8*, 4513-4530.

Stuermer, C.A., Rohrer, B., and Munz, H. (1990). Development of the retinotectal projection in zebrafish embryos under TTX-induced neural-impulse blockade. J Neurosci *10*, 3615-3626.

Sun, H., and Crossland, W.J. (2000). Quantitative assessment of localization and colocalization of glutamate, aspartate, glycine, and GABA immunoreactivity in the chick retina. Anat Rec *260*, 158-179.

Takeda, M., Takamiya, A., Jiao, J.W., Cho, K.S., Trevino, S.G., Matsuda, T., and Chen, D.F. (2008). alpha-Aminoadipate induces progenitor cell properties of Muller glia in adult mice. Invest Ophthalmol Vis Sci *49*, 1142-1150.

Tessmar-Raible, K., Raible, F., Christodoulou, F., Guy, K., Rembold, M., Hausen, H., and Arendt, D. (2007). Conserved sensory-neurosecretory cell types in annelid and fish forebrain: insights into hypothalamus evolution. Cell *129*, 1389-1400.

Thoenen, H. (1995). Neurotrophins and neuronal plasticity. Science *270*, 593-598.

Tigges, J., and Tigges, M. (1981). Distribution of retinofugal and corticofugal axon terminals in the superior colliculus of squirrel monkey. Invest Ophthalmol Vis Sci *20*, 149-158.

Tomita, K., Moriyoshi, K., Nakanishi, S., Guillemot, F., and Kageyama, R. (2000). Mammalian achaete-scute and atonal homologs regulate neuronal versus glial fate determination in the central nervous system. EMBO J *19*, 5460-5472.

Tozuka, Y., Fukuda, S., Namba, T., Seki, T., and Hisatsune, T. (2005). GABAergic excitation promotes neuronal differentiation in adult hippocampal progenitor cells. Neuron *47*, 803-815.

Trapnell, C., Williams, B.A., Pertea, G., Mortazavi, A., Kwan, G., van Baren, M.J., Salzberg, S.L., Wold, B.J., and Pachter, L. (2010). Transcript assembly and quantification by RNA-Seq reveals unannotated transcripts and isoform switching during cell differentiation. Nat Biotechnol *28*, 511-515.

Tropepe, V., Coles, B.L., Chiasson, B.J., Horsford, D.J., Elia, A.J., McInnes, R.R., and van der Kooy, D. (2000). Retinal stem cells in the adult mammalian eye. Science *287*, 2032-2036.

Udin, S.B., and Fisher, M.D. (1985). The development of the nucleus isthmi in Xenopus laevis. I. Cell genesis and the formation of connections with the tectum. J Comp Neurol *232*, 25-35.

Ullen, F., Deliagina, T.G., Orlovsky, G.N., and Grillner, S. (1997). Visual pathways for postural control and negative phototaxis in lamprey. J Neurophysiol *78*, 960-976.

Volgyi, B., Chheda, S., and Bloomfield, S.A. (2009). Tracer coupling patterns of the ganglion cell subtypes in the mouse retina. J Comp Neurol *512*, 664-687.

von Bartheld, C.S., Byers, M.R., Williams, R., and Bothwell, M. (1996). Anterograde transport of neurotrophins and axodendritic transfer in the developing visual system. Nature *379*, 830-833.

Wallace, V.A., and Raff, M.C. (1999). A role for Sonic hedgehog in axon-to-astrocyte signalling in the rodent optic nerve. Development *126*, 2901-2909.

Wassle, H., and Illing, R.B. (1980). The retinal projection to the superior colliculus in the cat: a quantitative study with HRP. J Comp Neurol *190*, 333-356.

Wehman, A.M., Staub, W., Meyers, J.R., Raymond, P.A., and Baier, H. (2005). Genetic dissection of the zebrafish retinal stem-cell compartment. Dev Biol *281*, 53-65.

Weidinger, G., Thorpe, C.J., Wuennenberg-Stapleton, K., Ngai, J., and Moon, R.T. (2005). The Sp1-related transcription factors sp5 and sp5-like act downstream of Wnt/beta-catenin signaling in mesoderm and neuroectoderm patterning. Curr Biol *15*, 489-500.

Westerfield, M. (1993). The Zebrafish Book; A Guide for the Laboratory Use of Zebrafish (Brachydanio rerio), 2nd edn (Eugene, University of Oregon Press).

White, E.L. (1948). An experimental study of the relationship between the size of the eye and the size of the optic tectum in the brain of the developing teleost, Fundulus heteroclitus. J Exp Zool *108*, 439-469.

Wiesel, T.N., and Hubel, D.H. (1963a). Effects of Visual Deprivation on Morphology and Physiology of Cells in the Cats Lateral Geniculate Body. J Neurophysiol *26*, 978-993.

Wiesel, T.N., and Hubel, D.H. (1963b). Single-Cell Responses in Striate Cortex of Kittens Deprived of Vision in One Eye. J Neurophysiol *26*, 1003-1017.

Xiao, T., and Baier, H. (2007). Lamina-specific axonal projections in the zebrafish tectum require the type IV collagen Dragnet. Nat Neurosci *10*, 1529-1537.

Xiao, T., Roeser, T., Staub, W., and Baier, H. (2005). A GFP-based genetic screen reveals mutations that disrupt the architecture of the zebrafish retinotectal projection. Development *132*, 2955-2967.

Yamaguchi, M., Tonou-Fujimori, N., Komori, A., Maeda, R., Nojima, Y., Li, H., Okamoto, H., and Masai, I. (2005). Histone deacetylase 1 regulates retinal neurogenesis in zebrafish by suppressing Wnt and Notch signaling pathways. Development *132*, 3027-3043.

Yeo, S.Y., and Chitnis, A.B. (2007). Jagged-mediated Notch signaling maintains proliferating neural progenitors and regulates cell diversity in the ventral spinal cord. Proc Natl Acad Sci U S A *104*, 5913-5918.

Young, S.Z., Taylor, M.M., and Bordey, A. (2011). Neurotransmitters couple brain activity to subventricular zone neurogenesis. Eur J Neurosci *33*, 1123-1132.

Zeutzius, I., Probst, W., and Rahmann, H. (1984). Influence of dark-rearing on the ontogenetic development of Sarotherodon mossambicus (Cichlidae, Teleostei): II. Effects on allometrical growth relations and differentiation of the optic tectum. Exp Biol *43*, 87-96.

Zu, Y., Tong, X., Wang, Z., Liu, D., Pan, R., Li, Z., Hu, Y., Luo, Z., Huang, P., Wu, Q., *et al.* (2013). TALEN-mediated precise genome modification by homologous recombination in zebrafish. Nat Methods *10*, 329-331.